THE DEVELOPMENT OF A SUSTAINABLE CATALYTIC REDUCTIVE AMINATION PROCESS

SOFÍA MARÍN MALLO

A dissertation submitted for the degree of Master of Philosophy

Heriot-Watt University

School of Engineering and Physical Sciences

June 2015

Abstract

The development of more sustainable catalytic reductive amination processes for the generation of high value amines represents a high priority challenge. An alternative cleaner route for the selective production of an amino acid (Tert-butylglycine, TBG) from a α-keto-carboxylic acid (Trimethylpyruvic acid TMP) under mild reaction conditions has been investigated. TMP was reacted with aqueous NH_3 and hydrogen gas under atmospheric pressure at 343 K over commercial Pd/C, Pt/C, Rh/C and Pd/Al_2O_3 catalysts. Catalyst characterization in terms of temperature programmed reduction (TPR), H_2 chemisorption, X-ray diffraction (XRD), transmission electron microscopy (TEM), BET area/pore volume and pH point of zero charge (pH_{pzc}) measurements is provided and correlated with catalytic activity and selectivity. Mass transport contributions during reaction in a three phase slurry reactor were evaluated experimentally by varying (i) hydrogen flow rate, (ii) stirring speed, (iii) catalyst concentration and (iv) temperature. Reaction conditions wherein chemical control prevailed were established. Reductive amination rate was pressure invariant over the 1-20 bar range. Process optimisation revealed that the rate was sensitive to solution pH and NH_3/TMP ratio. An increase in pH (with NaOH addition) above the pK_a of ammonia was shown to elevate reaction rate. The basic character of the aminating agent also influenced rate as demonstrated by a comparison of activity using ammonium hydroxide, ammonium acetate and ammonium nitrate. Catalyst reuse was examined where a decline in activity was observed and is linked to pore occlusion and metal sintering. Solvent (water, 1-propanol, 1-butanol and aqueous mixtures of 1-propanol/1-butanol) effects were established where, in absence of mass transport limitations, reaction in pure 1-butanol delivered higher rate, a response that is attributed to combined TMP solubility and ammonia solvation. With the goal of probing reaction mechanism, the amination of two additional α-keto-carboxylic acids (pyruvic acid and phenylpyruvic acid) were screened where steric hindrance due to the substituent resulted in lower reaction rate.

Dedication

To my family

Acknowledgements

I want to give my most sincere thanks to Professor Mark A. Keane for presenting me to a very interesting project. My gratitude goes to him for his patience and encouragement, providing the mentoring and skilful guidance throughout my research. Without his restless advice, dedication and discussions, I would not have been able to solve the different scientific challenges that came by my way.

I would also like to say thank you to Dr. Humphrey Yiu for his unfailingly support since he joined to supervise this work. I am really very grateful for his continuous corrections, comments and inspiring questions which I have found to be invaluable for this work.

My laboratory colleages at Ingenza Ltd, Dr. Fraser Brown and Dr. Reuben Carr, also deserve recognition for all the continuous help they have given to me. I was privileged to carry out part of this research at Ingenza laboratories and borrow its equipments. I would also like to acknowledge the assistance of the Heriot-Watt University staff, especially to Alan Boyd for his assistance with NMR analysis, Marian K. Millar for her assistance with XRD measurements, Cameron Smith, Ronald Millar, Curtis L. Abbott, Eileen M. McEvoy, Craig Bell, Christina Graham, George Smith and Aftab Aziz for helping with the acquisition of experimental and office facilities. Also thanks to the Electricians Workshop of Heriot-Watt University for its assistance in repairing electrical items and the Chemistry Department at St. Andrews University for conducting TEM analysis.

This research was possible by the financial support from the Scottish Funding Council through the Spirit programme. I also owe this work to the several students I had the opportunity to research with for their help and support: Santiago Gomez-Quero, Fernando Cardenas-Lizana, Noemie Perret, Xiaodong Wang and Yufen Hao, while they were researching at Heriot-Watt laboratories. There are quite a few people in the Chemical Engineering department that I would like to thank: Cameron Brown, Alexander Foster, Ricardo Caldeira, Luis Cebamanos, Panagiotis Angelikopoulos, Fatemeh Mohsenpour, Manhal Alnasser, Oyegbe Ibhanesebhor and Dalila Capao. My deepest thanks to my family, who has made all of this worthwhile, and to them I dedicate my thesis.

Declaration Statement

Table of Contents

Abstract ii
Dedication iii
Acknowledgements iv
Declaration Statement v
Table of Contents vi
List of Tables viii
List of Figures ix
Nomenclature xi
List of Posters by the Candidate xiv

Chapter 1
Introduction and Scope of the Research 1
1.1 Sustainability in Chemical Processes 1
1.2 Sustainability in Amine Production 4
1.3 Thesis Scope and Organisation 5
1.4 References 5

Chapter 2
Experimental Procedures 9
2.1 Materials 9
2.2 Catalyst Characterisation 10
2.3 Catalytic Reaction 13
2.4 Product Analysis 15
2.5 Catalyst reuse 18
2.6 References 19

Chapter 3
Development of a Sustainable Catalytic Reductive Amination Process: Conversion of Trimethylpyruvic acid (TMP) to Tertbutylglycine (TBG) 20
3.1 Introduction 20
3.2 Results and Discussion 28
3.2.1 Catalyst Characterisation 28
3.2.2 Catalytic Activity and Selectivity 32
3.2.3 Transport limitations 34
3.2.4 Effect of agitation speed 35
3.2.5 Effect of hydrogen flow rate 35
3.2.6 Effect of catalyst mass: TMP/Pd mol ratio 36
3.2.7 Effect of reaction temperature 39
3.2.8 Process parameters 40
3.2.8.1 Effect of NH_3/TMP mol ratio and pH 40
3.2.8.2 Effect of Amination Reagent 42
3.3 Catalyst Reuse 43
3.4 Conclusions 44
3.5 References 45

Chapter 4
Role of the Catalyst (Metal and Support) in the Conversion of Trimethylpyruvic Acid (TMP) to Tertbutylglycine (TBG)..... 52
4.1 Introduction 52
4.2 Results and Discussion 54
4.2.1 Catalyst Characterization 54
4.2.2 Catalytic Activity and Selectivity 58
4.2.3 Effect of pH on initial rate 63
4.2.4 Effect of solvent on initial rate 65
4.3 Conclusions 67
4.4 References 68

Chapter 5
Further Developments, Conclusion and Future Work..... 75
5.1 Further Developments 75
5.1.1 Effect of Substrate Substitution 75
5.2 Conclusions 78
5.3 Future Work 79
5.3.1 Catalyst Deactivation 79
5.3.2 Effect of base addition 80
5.3.3 Effect of Catalyst Support 80
5.3.4 Effect of the Reductant 81
5.4 References 81

List of Tables

Table 1.1: Tools for environmental assessment. 3

Table 2.1: HPLC reversed phase gradient conditions for the analysis of TBG using OPA/BME at a flow rate of 1 cm^3 min^{-1}. 18

Table 3.1: Compilation of published studies of reductive amination using carbon supported metal catalysts. 24
Table 3.2: Physico-chemical characteristics of the 5% w/w Pd/C catalyst. 29
Table 3.3: Variation of reaction selectivity (to TBG and HTBA) as a function of reaction temperature: TMP/Pd = 600; NH_3/TMP = 2.5; stirring speed = 1100 rpm. 40
Table 3.4: Variation of pH (t = 0-50 min) and reaction selectivity (to TBG and HTBA) as a function of NH_3/TMP mol ratio: TMP/Pd = 600; T = 343 K; stirring speed = 1100 rpm. 42
Table 3.5: Initial rate of TBG production (r_o) obtained using different amination reagents (t = 0-50 min): TMP/Pd = 600; NH_3/TMP = 1 .5; T = 343 K; stirring speed = 1100 rpm. 43
Table 3.6: Initial activity decrease (%) and associated catalyst characteristics for reuse with and without treatment: TMP/Pd = 600; NH_3/TMP = 2.5; T = 343 K; stirring speed = 1100 rpm. 44

Table 4.1: BET surface area, hydrogen chemisorption capacity, specific metal surface area, metal particle diameter and pH point of zero charge (pH_{pzc}). 56
Table 4.2: Palladium dispersion, H_{abs}:Pd mol ratio (from TPR analysis), hydride decomposition temperature and H_{ads}:Pd mol ratio from chemisorption measurements. 57
Table 4.3: Initial specific rate of TBG production (r'_o) and variation of pH (t = 0-50 min) for reaction over carbon and alumina supported Pd, Pt and Rh: initial pH = 10.6; TMP/catalyst = 600; stirring speed = 1100 rpm; NH_3/TMP = 2.5; T = 343 K. 62
Table 4.4: Initial and final pH values during reaction at variable and fixed pH; the datum points are identified in Figure 4.5. 64

Table 5.1: Reductive amination of α-keto-carboxylic acids with aqueous ammonia over 5% carbon supported Rh: TMP/Rh = 600; stirring speed = 1100 rpm; NH_3/TMP = 2.5; T = 298 K; t = 50 min. 78

List of Figures

Figure 2.1: Representative H_2 chemisorption pulses generated for 5% w/w Pd/C (Degussa) activated at 423 K. 11
Figure 2.2: Representative BET surface area measure for 5% w/w Pd/C (Degussa) recovered after a second reaction: TMP/Pd = 600; NH_3/TMP = 2.5; T = 343 K; stirring speed = 1100 rpm. 12
Figure 2.3: (a) Schematic representation of the catalytic reactor system. (b) Image of the three phase liquid phase reactor. 15
Figure 2.4: The derivatisation reaction of TBG prior analysis by HPLC. 16
Figure 2.5: Representative chromatogram of a sample taken at the end of the reaction (t = 50 min); NH_3/TMP = 2.5; TMP/Pd = 600; solvent = 14% v/v water-propanol; T = 343 K. Chromatographic conditions are as given in Table 2.1. 17
Figure 2.6: Calibration plot for TBG. 17
Figure 2.7: The 400 MHz proton spectrum of a sample at the end of the reaction (t = 50 min): NH_3/TMP = 0.5; TMP/Pd = 600; T = 343 K. HTBA and TMP appear as singlets centred at 0.95 and 1.2 ppm, respectively; signal due to TBG should appear as a singlet centred at 1.08 ppm... 18

Figure 3.1: Reaction scheme for reductive amination: R = tert-butyl; (1) = TMP; (6) = TBG; (7) = 2-hydroxy-3,3-dimethylbutyric acid (HTBA). 23
Figure 3.2: Temperature-programmed reduction (TPR) profile (to 423 K) for Pd/C. 30
Figure 3.3: XRD pattern for Pd/C: peak assignment based on JCPDS-ICDD standards for (●) PdO (Card No. 75-584) and (▼) Pd (Card No. 06-0581). 30
Figure 3.4: a) Representative (I) high and (II) low magnification TEM images and b) Pd particle size distribution for Pd/C. 31
Figure 3.5: pH profiles associated with the pH of point of zero charge (pH_{pzc}) determined for 0.025 g (■), 0.050 g (▲) and 0.075 g (●) Pd/C. 32
Figure 3.6: Temporal variation of TBG production where (■) TMP/Pd = 50 ($r_o = 6.8\times10^{-2}$ mol dm^{-3} min^{-1} g_{Pd}^{-1}), (●) TMP/Pd = 300 ($r_o = 24\times10^{-2}$ mol dm^{-3} min^{-1} g_{Pd}^{-1}) and (▲) TMP/Pd = 900 ($r_o = 34\times10^{-2}$ mol dm^{-3} min^{-1} g_{Pd}^{-1}); stirring speed = 1100 rpm; NH_3/TMP = 2.5; T = 343 K. 34
Figure 3.7: a) Initial rate of TBG production (r_o) as a function of stirring speed (NH_3/TMP = 2.2; TMP/Pd = 670; T = 343 K) and b) hydrogen flow rate (NH_3/TMP = 2.2; TMP/Pd = 670; T = 343 K; stirring speed = 1100 rpm). 37
Figure 3.8: a) Initial rate of TBG production (r_o) as a function of TMP/Pd (NH_3/TMP = 2.5; T = 343 K; stirring speed = 1100 rpm) and b) reaction temperature as an Arrhenius plot (NH_3/TMP = 2.5; TMP/Pd = 600; stirring speed = 1100 rpm). 38
Figure 3.9: Initial rate of TBG production (r_o) as a function of NH_3/TMP mol ratio where pH varies with time (●) or is adjusted to 8.4 with acetic acid (▲): TMP/Pd = 600; T = 343 K; stirring speed = 1100 rpm. 42

Figure 4.1: TPR profiles generated for 5% w/w Pd/C (Degussa, I), 5% w/w Pd/C (Sigma-Aldrich, II), 5% w/w Pt/C (Sigma-Aldrich, III), 5% w/w Rh/C (Sigma-Aldrich, IV), 1% w/w Pd/C (Sigma-Aldrich, V) and 1% w/w Pd/Al_2O_3 (Sigma-Aldrich, VI). 56
Figure 4.2: pH profiles associated with the pH of point of zero charge (pH_{pzc}) determination for 0.025 g (■), 0.075 g (▲) and 1.125 g (●) of 5% w/w Rh/C. 58
Figure 4.3: Formation of the imine from carbinolamine (see Figure 3.1). 61
Figure 4.4: Temporal variation of moles TBG produced over (■) Rh/C 5% w/w ($r'_o = 3.6\times10^{-5}$ mol dm^{-3} min^{-1} m_{Rh}^{-2}), (●) Pd/C 5% w/w (Sigma-Aldrich, $r'_o = 3.2\times10^{-5}$ mol dm^{-3} min^{-1} m_{Pd}^{-2}) and (▲) Pd/C 5% w/w (Degussa, $r'_o = 1.5\times10^{-5}$ mol dm^{-3} min^{-1} m_{Pd}^{-2}); TMP/catalyst = 600; stirring speed = 1100 rpm; NH_3/TMP = 2.5; T = 343 K. 62
Figure 4.5: Initial rate of TBG production (r'_o) as a function of NH_3/TMP mol ratio where pH varies with time (●), pH is adjusted to 11.2 with NaOH (■), adjusted to 8.4 (▲) and adjusted to 4.7 with CH_3COOH (♦); TMP/Rh = 600; T = 343 K; stirring speed = 1100 rpm. 65

Figure 4.6: Initial rate of TBG production (r'_o) as a function of dielectric constant (ε) for reaction in 2-25% v/v water+1-propanol (▼), 14% v/v water+1-butanol (♦) mixtures and single component 1-propanol (■), 1-butanol (●) and water (×): NH_3/TMP = 2.5; TMP/Rh = 600; T = 343 K; stirring speed = 1100 rpm. 67

Nomenclature

List of Symbols

A_{cal}	Calibration area in H_2 chemisorption measurement
A_i	Peak area of a peak in H_2 chemisorption measurement
β	Peak width at half the maximum intensity in XRD analysis
D	Metal dispersion
d	Metal particle size (nm)
$\bar{d}_n$	Number weighted average diameter (nm)
ΔE_a	Apparent activation energy (kJ mol^{-1})
ε	Dielectric constant
ε_m	Dielectric constant of a water + organic solvent mixture
$\varepsilon_{organic}$	Dielectric constant of the organic solvent
ε_{water}	Dielectric constant of water
H_{abs}:Pd	Hydrogen absorbed to Pd mol ratio ($\mu mol_H\ \mu mol_{Pd}^{-1}$)
H_{ads}:Pd	Hydrogen adsorbed to Pd mol ratio ($\mu mol_H\ \mu mol_{Pd}^{-1}$)
φ	Particle Shape Constant
k	Shape factor
λ	Incident radiation wavelength (Å)
n	Number of pulses in H_2 chemisorption measurement
N_C	Total H_2 chemisorbed per unit mass of catalyst
n_i	Number of particles of diameter d_i
N_S	Number of surface metal atoms per unit mass of catalyst
N_T	Total number of metal atoms per unit mass of catalyst
P	Pressure (bar)
pH_{pzc}	pH point of zero charge
pK_a	Acid dissociation constant
R	Universal gas constant (J mol^{-1} K^{-1})
r_o	Initial reaction rate (mol dm^{-3} min^{-1} g_{Pd}^{-1})
r'_o	Specific initial reaction rate (mol dm^{-3} min^{-1} m_{metal}^{-2})
S_M	Specific metal atom surface (m^2 g^{-1})
T	Temperature (K)
θ	Diffraction angle corresponding to the main plane of the metal

V	Volume of H_2 chemisorbed (cm^3)
V_{inj}	Volume of H_2 per injection (cm^3)
V_M	Specific metal atom volume ($m^3\ g^{-1}$)
X_M	Chemisorption stoichiometry
x_{water}	Molar fraction of water in the solvent mixture

List of Acronyms

AIDS	Acquired immunodeficiency syndrome
BET	Brunauer-Emmet-Teller
BJH	Barrett-Joyner-Halenda
BME	2-beta-mercapto ethanol
CBA	Cost-Benefit Analysis
DAD	Diode Array Detector
EIA	Environmental Impact Analysis
EPA	Environment Protection Agency
ERA	Environmental Risk Assessment
IR	Infrared analysis
JCPDS-ICDD	Joint Committee on Powder Diffraction Standards-International Centre for Diffraction Data
HTBA	2-hydroxy-3,3-dimethylbutyric acid
HPLC	High Pressure Liquid Chromatography
IOA	Input-Output Analysis
LCA	Life Cycle Assessment
LCC	Life Cycle Costing
MFA	Materials Flow Accounting
MIPS	Material input per unit service
NMR	Nuclear Magnetic Resonance
OPA	*o*-Phthaldialdehyde
OSHA	Occupational Safety and Health Administration
PMT	Potentiometric Mass Titration
PS-Pd-NHC	Polymer Supported Pd *N*-Heterocyclic Carbine
RP	Reverse Phase
rpm	Revolutions per Minute
TBG	Tert-butylglycine
TCD	Thermal Conductivity Detector

TEM	Transmission Electron Microscopy
TMP	Trimethylpyruvic acid
TMPNa	Trimethylpyruvic sodium salt
TPO	Temperature Programmed Oxidation
TPR	Temperature Programmed Reduction
TSCA	Toxic Substances Control Act
UNCED	United Nations Conference on Environment and Development
WCED	World Commission on Environment and Development
WSSD	World Summit on Sustainable Development
XPS	X-ray Photoelectron Spectroscopy
XRD	Powder X-ray Diffraction

List of Posters by the Candidate

1) "Development of a Sustainable Catalytic Reductive Amination Process: Conversion of a Keto-acid to an Amino Acid", Scotchem Spirit Conference; St. Andrews University, May 2011.

2) "Development of a Sustainable Catalytic Reductive Amination Process", EPS Poster Event for PG Research Students; Chemical Engineering Department (Heriot-Watt University), October 2009.

Chapter 1

Introduction and Scope of the Research

This Chapter provides some general insights into the sustainability of chemical processes, focusing on the application of heterogeneous catalysis in reductive amination. The organisation and approach applied to this research project are outlined.

1.1 Sustainability in Chemical Processes

Mismanagement of industrial activities in past decades have contributed to serious contemporary environmental problems such as global warming, air pollution, water contamination and depletion of non-renewable resources [1, 2]. Because of this, sustainability in process design is now an important and key challenge that faces the chemical sector [3]. The accepted definition of sustainable development was established in 1989 by the World Commission on Environment and Development (WCED), *i.e.* the 'Bruntland commission', as "the development that meets the needs of the present without compromising the ability of future generations to meet their own needs" [4]. This concept is built on three basic factors: social responsibility; environmental protection; economic viability [5]. The directives approved at the United Nations Conference on Environment and Development (UNCED) in Rio de Janeiro in 1992, notably "Agenda 21", included both national and local action to ensure sustainable development [6, 7]. However, it was recognised that the social terms were difficult to quantify and sustainable development largely focused on the environmental factor. A more practical approach to sustainability was given in the World Summit on Sustainable Development (WSSD) in Johannesburg in 2002 with an emphasis on a limited number of areas [8]. The Bruntland commission has also laid the groundwork for other initiatives such as the Kyoto Protocol on climate change (1997) [9] and more recently the United Nations Climate Change Conference COP 15 in Copenhagen (2009) [10].

Green and sustainable chemistry are terms used to describe similar ideas. Green chemistry uses efficient synthetic routes with a reduced environmental impact. While green chemistry addresses both environmental and economic viability, the sustainable term also considers the social impact factor in business decisions [11]. The introduction of the social factor must be taken with care as it can justify environmentally

unsustainable decisions. For instance, if the introduction of an infrastructure that improves the quality of a community requires a higher supply of energy, then this improvement fails [12]. Certain principles and guidelines provided by some authors and institutions can be used as a reference to design processes that achieve sustainability. In 1998 Anastas and Warner [13] published a list of twelve principles of green chemistry applicable in the design, manufacture and use of chemical products: (i) waste prevention; (ii) maximum incorporation of all materials used into the final product (atom economy); (iii) less hazardous chemical processes; (iv) design of less toxic compounds; (v) safer solvents and auxiliaries; (vi) energy efficiency (synthesis conducted at ambient temperature and pressure); (vii) use of renewable feedstock, (viii) minimisation of derivatisation steps that can increase waste; (ix) use of selective catalytic reagents; (x) design of chemicals for innocuous degradation; (xi) in-process analysis prior to the formation of hazardous substances; (xii) safer chemistry for accident prevention. Environmental protection can facilitate economic viability [14]. The research presented in this thesis has been conducted to address as many of these green chemistry principles as possible. The work has focused on sustainability in the reductive amination of carboxylic acids. This has required an assessment of the role of solution pH and ammonia: organic reactant ratio in determining reaction rate and selectivity in order to ensure atom efficiency and circumvent by-product/waste formation. Hydrogen flow rate, agitation speed and catalyst loading in the reactor were varied to determine conditions where the reaction was operated under catalytic control, free from mass transfer limitations. Feasibility of catalyst reuse/recycle has also been considered as an important sustainability factor. In accordance with the critical ninth principle, conditions were established where the supported metal catalysts employed delivered 100% selectivity to the target amino acid product. Furthermore, the reaction has been conducted at atmospheric pressure and at low temperatures (down to ambient), achieving energy efficiency. Water and primary alcohols have been used as safe and viable reaction media. The samples taken from the reaction were analysed by high performance liquid chromatography in real time, avoiding the formation of possible by-products by decomposition. Finally, the process generated a valuable product that is not considered either toxic by the U.S. EPA Toxic Substances Control Act (TSCA) inventory or hazardous by the OSHA Hazard Communication Standard.

A number of "tools" are now in place, and summarized in **Table 1.1**, to enable a quantitative assessment of environmental impact. Catalysis is recognised as a critical component in green and sustainable chemistry that serves to lower energy requirements

and waste production by facilitating selectivity under milder reaction conditions [15, 16]. Innovation in catalyst preparation (homogeneous, heterogeneous and enzymatic) can realise more sustainable processes for the chemical industry. Efforts directed at sustainability have focused on decreasing impacts from both upstream (choice of sustainable raw materials and energy sources) and downstream (reduction of waste disposal, maximising recycle) of the chain, down-sizing and integrating processes (catalysts for multi-steps reactions) [17]. Over the past two decades there has been an expansion of environmental catalytic processes, largely driven by the tightening regulations on emissions such as NO_x, SO_x and CO [18]. It is now established that sustainability considerations must be built into process design from the very outset [19].

Table 1.1: Tools for environmental assessment.

Tool	**Main characteristics**	**Reference**
Life Cycle Assessment (LCA)	Assessment of a system from raw material extraction to disposal or recycling.	[20, 21]
Material input per unit service (MIPS)	Assessment of the life-cycle-wide material input: reduction in raw materials usage lowers environmental impact).	[22]
Environmental Risk Assessment (ERA)	Prediction of potential risks to human health/environment.	[23]
Materials Flow Accounting (MFA)	Measurement of flow and stock of materials to reduce both costs and environmental impact.	[24]
Input-Output Analysis (IOA)	Analysis of system nodes (industrial entity) and flows (material, energy).	[25]
Environmental Impact Analysis (EIA)	Identification of the positive or negative impacts of a process considering environmental, social and economic effects.	[26]
Eco-design	Integration of environmental aspects into product process development.	[27]
Life Cycle Costing (LCC)	Summation of all the costs associated with a product from acquisition to disposal.	[28]
Cost-Benefit Analysis (CBA)	Comparison of benefits and costs of a process to determine feasibility.	[29]

1.2 Sustainability in Amine Production

The synthesis of amines is a key step in the pharmaceutical and agrochemical industries [30-32]. Amines can be obtained by hydrogenation of nitro compounds, amides, nitriles, alkylazides as well as by reductive amination [33]. Although a range of catalytic methods have been established for amine synthesis, the search for new environmentally friendly procedures is challenging due to the associated undesired toxic by-products and harsh reaction conditions. The application of heterogeneous catalysts has the advantage of easy product/catalyst separation and waste reduction relative to homogeneous catalysis [34]. A significant source of unsustainability in the hydrogenation of nitro-compounds arises from the generation of waste streams due to reaction of other reducible groups (*e.g.* nitrile, amide, halide, alkene, azide, benzyl, ether) associated with the nitro-reactant [35, 36]. Homogeneous and heterogeneous reduction of nitro-compounds using CO/H_2O as reductant/hydrogen transfer allows the use of water-based solvents under mild conditions (room temperature and atmospheric pressure) [36, 37]. Reduction of nitro compounds has also drawn on the use of iron (II) salt/iron phthalocyanine [38] as catalyst with hydrazine hydrate as the hydrogen source in a water/ethanol solvent mixture. Selective reduction of amides is an important route to generate amines [34, 39]. Homogeneous reduction of amides is frequently carried out with hydride reagents and has several disadvantages including reduction of substituent groups other than the carbonyl function, the generation of by-products such as metal hydroxides, laborious product purification and the requirement for elevated pressure and temperature [40-43]. Use of hydrogen as reductant necessitates elevated pressures (50-350 bar) and temperatures (403-673 K) [44, 45]. Recently, reduction of tertiary amides with zinc acetate and a triethoxysilane as the hydrogen source was achieved at room temperature and atmospheric pressure [46]. Amination of alcohols and halides with homogeneous catalysts represents another route to amines where alcohols are preferred reactants due to lower toxicity and higher reactivity [30, 47]. Nitriles can also be reduced using metal hydrides (aluminium hydride and sodium borohydride) but this results in the generation of secondary amines and imines, requires hazardous solvents, exothermic work-up and maintenance of anhydrous conditions [48, 49]. Reductive amination of ketones and aldehydes is viewed as a more sustainable approach to the synthesis of structurally diverse amines as it can be carried out under mild conditions with high selectivity and yields [43, 50]. Reductive amination procedures use either hydride reducing agents or hydrogenation catalysts. Processes based on hydrides have the drawback of appreciable associated toxicity with

contamination of the target product(s), generation of cyanide salts and operability at high reaction temperatures [51-54]. In this thesis, reductive amination employing solid supported metal catalysts has been examined with a full evaluation of process sustainability and consideration of the dependence of performance (rate and selectivity) on catalyst structure.

1.3 Thesis Scope and Organisation

The goal of this project was to apply the principles of sustainable chemistry to optimise a reductive amination process, *i.e.* the liquid phase conversion of trimethylpyruvic acid (TMP) to tert-butyl glycine (TBG). A range of alumina and activated carbon supported transition metals have been tested to achieve selective TBG formation under mild reaction conditions (P = 1 atm and T = 293-343 K). The experimental procedures employed in this work are described in **Chapter 2**. Fundamental features of TMP reductive amination over a commercial Pd/carbon catalyst are examined in **Chapter 3**, notably the reaction conditions required to eliminate possible mass transport limitations and ensure kinetic control. The roles of temperature, pH, solvent, NH_3/TMP and NH_3/catalyst ratios are considered and the feasibility of catalyst reuse is addressed. The performance of a range of supported metals is presented in **Chapter 4**, correlating the catalytic response with critical catalyst structural characteristics. The results of a preliminary analysis of the reaction with additional organic acid reactants are given in **Chapter 5**, with recommendations for further study that can take this work forward. The results contained in this thesis represent a contribution to enhanced sustainable amine production.

1.4 References

[1.1] A. J. McMichael, Climate Change and Human Health Risks and Responses, Global Climate Change and Health: An Old Story Writ Large, World Health Organization, Geneva, pp. 1-17 (2003)

[1.2] J. L. Innes, A. H. Haron, Air Pollution and Forestry in Rapidly Industrializing Countries, Air Pollution and Forestry in Rapidly Industrializing Countries: an Introduction, CAB International Cambridge, pp. 1-14 (2000)

[1.3] M. R. Othman, J.-U. Repke, G. Wozny, Y. Huang; Ind. Eng. Chem. Res., 49, 7870-7881 (2010)

[1.4] J. H. Hulse, Sustainable Development at Risk Ignoring the Past, From Pearson to Johannesburg, Cambridge University Press India, New Delhi, pp. 74-78 (2007)

[1.5] B. R. Bakshi, J. Fiksel; AIChE J., 49, 1350-1358 (2003)

[1.6] F. Langeweg; Sci. Tot. Environ., 218, 227-238 (1998)

[1.7] J. H. Spangenberg, S. Pfahl, K. Deller; Ecol. Indic., 2, 61-77 (2002)

[1.8] D. L. Carr, E. S. Norman; Geoforum, 39, 358-371 (2008)

[1.9] A. S. Dagoumas, G. K. Papagiannis, P. S. Dokopoulos; Energy Pol., 34, 26-39 (2006)

[1.10] S. Sawyer; Renew. En. Focus, 9, 28-29 (2009)

[1.11] M. A. Abraham; Environ. Progress, 24, 10-11 (2005)

[1.12] J. Garcia-Serna, L. Perez-Barrigon, M. J. Cocero; Chem. Eng. J., 133, 7-30 (2007)

[1.13] R. Apodaca, W. Xiao; Org. Lett., 3, 1745-1748 (2001)

[1.14] D. Y. Murzin, R. Leino; Chem. Eng. Res. Des., 86, 1002-1010 (2008)

[1.15] G. Centi, S. Perathoner; Catal. Today, 138, 69-76 (2008)

[1.16] M. M. Kirchhoff; Res. Cons. Recyc., 44, 237-243 (2005)

[1.17] A. Azapagic, A. Millington, A. Collett; Chem. Eng. Res. Des., 84, 439-452 (2006)

[1.18] G. Centi, P. Ciambelli, S. Perathoner, P. Russo; Catal. Today, 75, 3-15 (2002)

[1.19] A. Lapkin, L. Joyce, B. Crittenden; Environ. Sci. Technol., 38, 5815-5823 (2004)

[1.20] A. Björklund; Environ. Impact Assess. Rev., 32, 82-87 (2012)

[1.21] J. A. Assies; J. Hazard. Mater., 61, 23-29 (1998)

[1.22] J. Dewulf, H. Van Langenhoven; Res. Conserv. Recyc., 38, 161-174 (2003)

[1.23] J. Beyer, L. P. Myhre, R. C. Sundt, S. Meier, K. E. Tollefsen; Mar. Environ. Res., 71, 2-9 (2012)

[1.24] H. Haberl, M. Fischer-Kowalski, F. Krausmann, H. Weisz, V. Winiwarter; Land Use Pol., 21, 199-213 (2004)

[1.25] C. Piluso, Y. Huang, H. H. Lou; Ind. Eng. Chem. Res., 47, 1955-1066 (2008)

[1.26] K. Vizayakumar, P. K. J. Mohapatra; J. Environ. Manag., 34, 79-103 (1992)

[1.27] S. Byggeth, E. Hochschorner; J. Cleaner Prod., 14, 1420-1430 (2006)

[1.28] L. Luo, E. Van der Boet, G. Huppes; Renew. Sust. En. Rev., 13, 1613-1619 (2009)

[1.29] J. M. Gowdy, R. B. Howarth; Ecol. Econ., 63, 637-638 (2007)

[1.30] G. W. Lamb, F. A. Al Badran, J. M. J. Williams, S. T. Kolaczkowski; Chem. Eng. Res. Des., 88, 1533-1540 (2010)

[1.31] J. Bowman, L. Tang, C. E. Silverman; J. Pharm. Biom. Anal., 23, 663-669 (2000)

[1.32] J. W. Bae, Y. J. Cho, S. H. Lee, C. M. Yoon; Tetrahedron Lett., 41, 175-177 (2000)

[1.33] J. Mc Murry, Fundamentals of Organic Chemistry, Amines, Brooks/Cole, Belmont, pp. 411-415 (2011)

[1.34] S. Hanada, E. Tsutsumi, Y. Motoyama, H. Nagashima; J. Am. Chem. Soc., 131, 15032-15040 (2009)

[1.35] C. Yu, B. Liu, L. Hu; J. Org. Chem., 66, 919-924 (2001)

[1.36] R. S. Downing, P. J. Hunkeler, H. van Bekkum; Catal. Today, 37, 121-136 (1997)

[1.37] L. He, L.-C. Wang, H. Sun, J. Ni, Y. Cao, H.-Y. He, K.-N. Fan; Angew. Chem. Int. Ed., 48, 9538-9541 (2009)

[1.38] U. Sharma, P. K. Verma, N. Kumar, V. Kumar, M. Bala, B. Singh; Chem. Eur. J., 17, 5903-5907 (2011)

[1.39] G. Barbe, A. B. Charette; J. Am. Chem. Soc., 130, 18-19 (2008)

[1.40] G. B. Fisher, J. C. Fuller, J. Harrison, S. G. Alvarez, E. Burkhardt, C. T. Goralski, B. Singaram; J. Org. Chem., 59, 6378-6385 (1994)

[1.41] N. Sakai, K. Fujii, T. Konakahara; Tetrahedron Lett., 49, 6873-6875 (2008)

[1.42] A. C. Fernandes, C. C. Romao; J. Mol. Catal. A: Chem., 272, 60-63 (2007)

[1.43] D. C. Constable, P. J. Dunn, J. D. Hayler; Green Chem., 9, 411-420 (2007)

[1.44] J. M. Woodley; Trends Biotechnol., 26, 321-327 (2008)

[1.45] G. Beamson, A. J. Papworth, C. Philipps, A. M. Smith, R. Whyman; J. Catal., 269, 93-102 (2010)

[1.46] S. Das, D. Addis, S. Zhou, K. Junge, M. Beller; J. Am. Chem. Soc., 132, 1770-1771 (2010)

[1.47] O. Navarro, N. Marion, J. Mei, S. P. Nolan; Chem. Eur. J., 12, 5142-5148 (2006)

[1.48] S. Enthaler, D. Addis, K. Junge, G. Erre, M. Beller; Chem. Eur. J., 14, 9491-9494 (2008)

[1.49] S. Laval, W. Dayoub, A. Favre-Reguillon, M. Berthod, P. Demonchaux, G. Mignani, M. Lemaire; Tetrahedron Lett., 50, 7005-7007 (2009)

[1.50] R. Arora; J. Microwave Power Electromag. En., 45, 94-102 (2011)

[1.51] A. Robichaud, A. N. Ajjou; Tetrahedron Lett., 47, 3633-3636 (2006)

[1.52] G. B. Giovenzana, D. Imperio, A. Penoni, G. Palmisano; Beilstein J. Org. Chem., 7, 1095-1099 (2011)

[1.53] E. Byun, B. Hong, K. A. De Castro, M. Lim, H. Rhee; J. Org. Chem., 72, 9815-9817 (2007)

[1.54] N. Azizi, E. Akbari, A. K. Amiri, M. R. Saidi; Tetrahedron Lett., 49, 6682-6684 (2008)

Chapter 2

Experimental Procedures

This Chapter presents details of the experimental systems and techniques used to characterise the catalysts. A three-phase glass slurry reactor has been used to conduct the catalytic reactions. The catalysts have been characterized by temperature programmed reduction (TPR), H_2 chemisorption, BET surface area (N_2 adsorption), pore volume, pH point of zero charge, transmission electron microscopy (TEM) and x-ray diffraction (XRD) measurements.

2.1 Materials

Trimethylpyruvic acid (TMP) was supplied by Taizhou Orient Special Chemical Co Ltd. TMP purity was determined by NMR and HPLC against a standard TMP sample of known concentration prepared by Ingenza Ltd. An Agilent Autosystem 1200 HPLC unit with a variable wavelength DAD (diode array detector), a binary gradient pump, a variable volume autosampler, a degasser and a RP (reverse phase) C18 column 5 mm, 150 mm × 4.6 mm (Grace) was used for analysis; measurements were made at λ = 308 nm. The ^{1}HNMR spectra were recorded using a Bruker DPX400 spectrometer at 400 MHz. Samples for NMR measurement (in 5 mm o.d. tubes at 298 K) were prepared in H_2O containing *ca.* 10% D_2O to provide a deuterium lock signal. The TMP purity was 63-65% w/w based on HPLC and NMR measurements. The trimethylpyruvic sodium salt (TMPNa) was prepared to increase the purity of TMP up to 88% w/w. This was carried out by dissolving 10 g TMP in 50 cm^3 distilled water and 5 M NaOH was dropwise added until pH reached 7. Water was then removed by rotary evaporation with the addition of toluene. The solid was then recrystallised by heating the solution to 373 K. The solid was finally cooled to room temperature, filtered and dried in a dessicator for 24 h under vacuum. The HPLC analysis used two mobile phases (A, B) to adjust the chromatographic separation and retention. The mobile phase A was prepared by mixing 61.5 cm^3 1M K_2HPO_4 and 38.5 cm^3 1M KH_2PO_4 in 1×10^3 cm^3 water, diluting to 5 mM with distilled water and filtering through a 0.2 μm Nalgene filter. The mobile phase B was acetonitrile (HPLC grade). The derivatisation method used to measure TBG by HPLC required a 0.4 M potassium borate buffer, which was prepared by dropwise addition of 10 M potassium hydroxide (until pH = 10) to 50 cm^3

boric acid (2.5 g), making up the final volume to 100 cm^3 with distilled water. A 5% w/w Pd/C catalyst (55% w/w water) was supplied by Degussa. In addition, 5% w/w Pd/C, 5% w/w Pt/C, 5% w/w Rh/C, 1% w/w Pd/C and 1% w/w Pd/Al_2O_3 were purchased from Sigma-Aldrich. Ammonium hydroxide (35% aqueous NH_3, 18.1 M) was obtained from Fisher. *o*-Phthaldialdehyde (OPA, 98%) was supplied by Alfa Aesar. Methanol (anhydrous, 99.8%), 2-beta-mercapto ethanol (BME, ≥99%), tertbutylglycine (TBG, 98%), potassium hydroxide (≥85%), acetic acid (≥99.7%), KH_2PO_4 (99.99%) and K_2HPO_4 (99.99%) were supplied by Sigma-Aldrich. Boric acid (99.99%), acetonitrile (HPLC grade, 99.9%) and sodium hydroxide (98.5%) were provided by Fisher Scientific. All gases (H_2 and He) used were ultra pure (≥99.995%) and supplied by BOC.

2.2 Catalyst Characterisation

Catalyst characterisation by BET surface area, temperature programmed reduction (TPR) and H_2 chemisorption was carried out using the commercial CHEMBET 3000 (Quantachrome Instruments) unit. The samples were first outgassed at 423 K for 1 h under flowing N_2 at 30 cm^3 min^{-1}. A known mass (*ca*. 0.1 g) of catalyst was loaded into a U-tube (100 × 3.76 mm i.d.) and subjected to TPR at 10 K min^{-1} to 423 K in flowing 5% v/v H_2/N_2 at 15 cm^3 min^{-1} controlled using a Brooks mass flow controller. The effluent gas was directed through a liquid N_2 trap and the H_2 consumption/release was monitored by a thermal conductivity detector (TCD) with data acquisition/manipulation using the TPR Win^{TM} software. The sample was then purged with a flow of N_2 (65 cm^3 min^{-1}) for 90 min, cooled to room temperature and subjected to H_2 chemisorption using a pulse (0.05 cm^3) titration procedure [1]. The peaks shown in **Figure 2.1** represent the downstream hydrogen in each pulse. Hydrogen pulse introduction was repeated until the signal area was constant (peak 9 in **Figure 2.1**), indicating surface saturation. The final peak area was taken as the value for calibration (A_{cal}). The volume of hydrogen chemisorbed (V) was obtained according to:

$$V = (n\ x\ A_{cal} - \sum_{i=1}^{n} A_i)\ x\ \frac{V_{inj}}{A_{cal}} \qquad \textbf{(2.1)}$$

where n is the total number of pulses, A_i is the area of the peak and V_{inj} is the volume of hydrogen per injection. Metal dispersion (D) was calculated from the H_2 chemisorption measurement using the following relationships [2]:

$$D = \frac{N_S}{N_T} = \frac{X_M x\, N_C}{N_T} \quad \textbf{(2.2)}$$

where N_S is the number of surface metal atoms per unit mass of catalyst, N_T is the total number of metal atoms, X_M is the chemisorption stoichiometry (H:metal = 1:1 [3, 4]) and N_C is the total H_2 chemisorbed. Metal particle size (d) was then calculated using the following equation:

$$d = \frac{\varphi\, x\, V_M}{D\, x\, S_M} \quad \textbf{(2.3)}$$

where φ is a constant that takes in account the particle shape (= 6 for spheres), V_M and S_M are the specific metal atom volume and area, respectively.

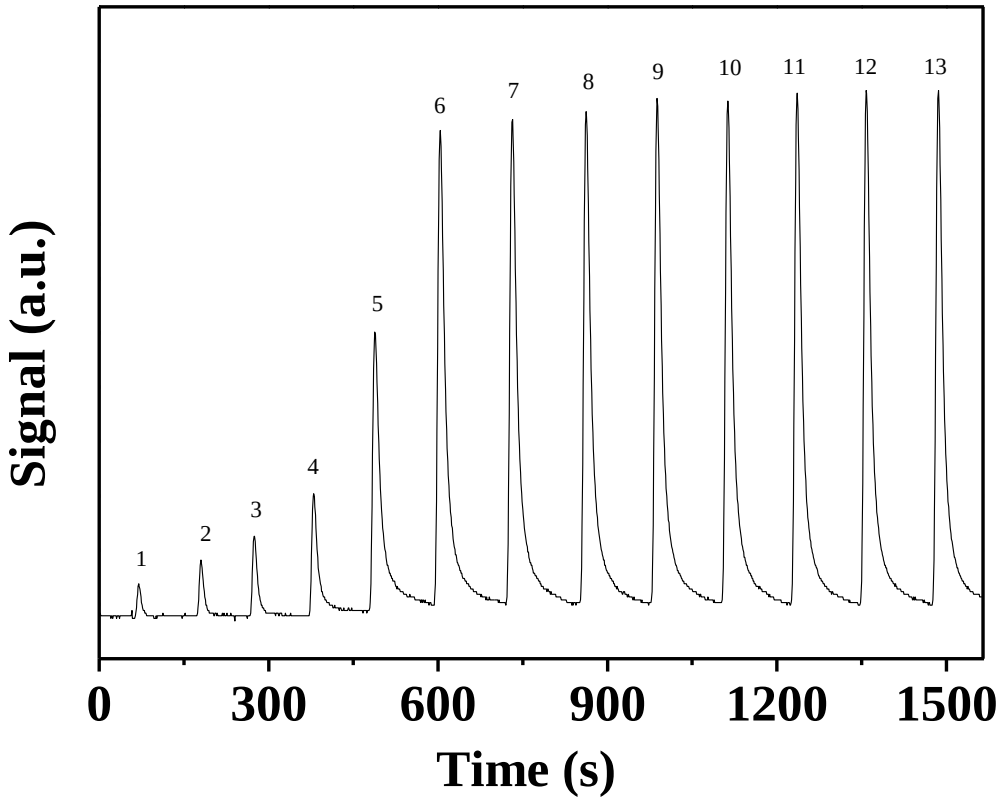

Figure 2.1: Representative H_2 chemisorption pulses generated for 5% w/w Pd/C (Degussa) activated at 423 K.

BET surface area was recorded in a 30% v/v N_2/He flow, using two cycles of N_2 adsorption-desorption to determine total surface area using the standard single-point BET method, which is based on a single partial pressure of N_2 (= 0.3 atm) [5, 6]. The sample cell was immersed in liquid nitrogen and the sample contacted with the N_2/He flow to generate the adsorption response (Peak 1 in **Figure 2.2**). The sample cell was then immersed in water at room temperature and the desorbed N_2 resulted in Peak 2

shown in **Figure 2.2**. Known volumes of N_2 were then injected to determine calibration (Peaks 3-4 in **Figure 2.2**). Hydrogen chemisorption and BET area measurements were reproducible to within ±4%. BET surface area was also measured using the commercial Micromeritics Flowsorb II unit to generate values that were in good agreement (±5%) with those obtained with the Quantachrome measurements.

Nitrogen adsorption-desorption isotherms were determined at 77 K on the automated Micromeritics Gemini 2390P system over the relative pressure range $0.004 \leq P_0 \leq 0.85$. The average pore size, cumulative pore volume and pore size distribution were obtained using the BJH model from the adsorption isotherm [7]; catalysts were outgassed at 423 K under flowing N_2 for 2 h prior to analysis.

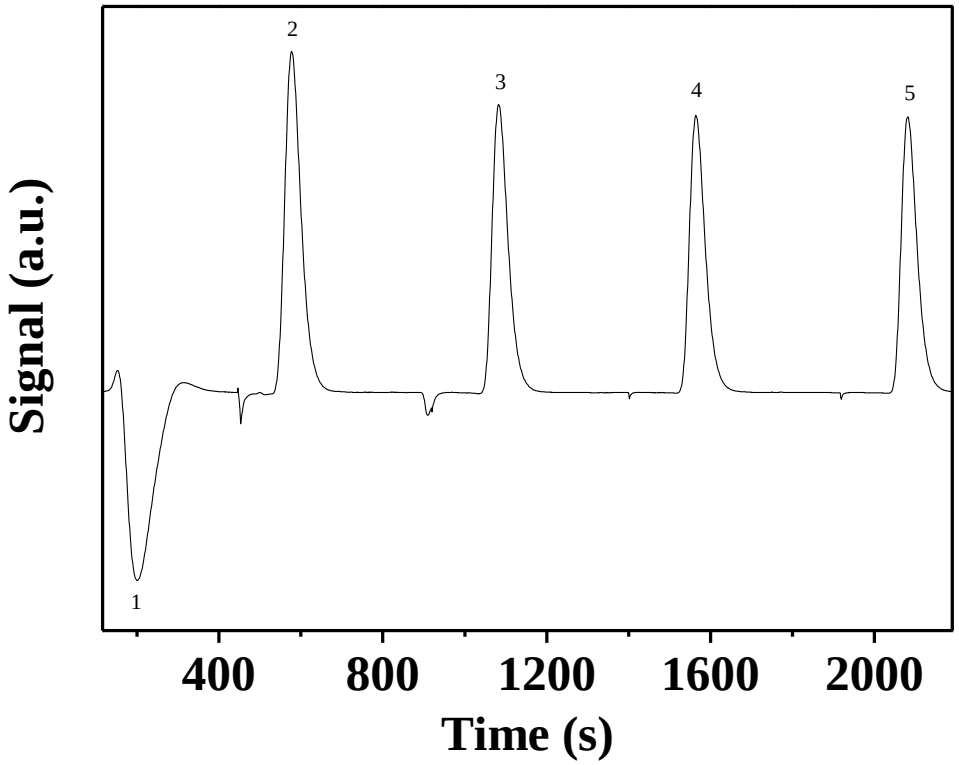

Figure 2.2: Representative BET surface area measure for 5% w/w Pd/C (Degussa) recovered after a second reaction: TMP/Pd = 600; NH_3/TMP = 2.5; *T* = 343 K; stirring speed = 1100 rpm.

The pH associated with the point of zero charge (pH_{pzc}) was determined using the potentiometric mass titration (PMT) technique [8]. In a typical measurement, three different masses (0.025-1.050 g) of catalyst were suspended in 50 cm^3 0.1 M NaCl with a known amount of HCl (0.1 M). Titration of the samples was performed under continuous agitation in a He atmosphere with NaOH (0.1 M) as titrant at 2 cm^3 h^{-1}. The temporal pH response was recorded with a pH meter (Hanna Instruments) equipped with a crystal-body electrode, coupled to a data logging and collection system (Pico

Technology Ltd.); calibration was performed with standard buffer solutions (Fisher, pH 4.0 and 7.0).

Palladium particle size and morphology were determined by transmission electron microscopy (TEM). TEM analysis was conducted on a JEOL JEM 2011 TEM unit with a UTW energy-dispersive X-ray detector (Oxford Instruments) operated at an accelerating voltage of 200 keV and using Gatan Digital Micrograph 3.4 for data acquisition/manipulation. The sample was dispersed in acetone and deposited on a holey-carbon/Cu grid (300 Mesh). A total of 300 individual Pd particles were counted and the mean Pd particle sizes are quoted as the number average diameter ($\bar{d}_n$) [9]:

$$\bar{d}_n = \frac{\sum_i n_i d_i}{\sum_i n_i} \qquad \textbf{(2.4)}$$

where n_i is the number of particles of diameter d_i.

X-ray diffraction (XRD) analysis was conducted using a Bruker-Siemens D500 incident X-ray diffractometer with Cu Kα radiation. The sample was scanned at a rate of 0.02º step^{-1} over the range $5º \leq 2\theta \leq 90º$. The diffractogram was compared with the JCPDS-ICDD reference for Pd (Card No. 05-681). Palladium mean particle size (d) was evaluated by standard line broadening using the standard Scherrer expression [10]:

$$d = \frac{k\ x\ \lambda}{\beta x\ cos\ \theta} \qquad \textbf{(2.5)}$$

where k = 0.89 is the shape factor (for spherical particles), λ is the incident radiation wavelength (1.541 Å), β is the peak width at half the maximum intensity and θ is the diffraction angle corresponding to the main plane of the metal.

2.3 Catalytic Reaction

The catalytic reactions were carried out using a modified commercial stirred glass reactor i.d. = 60 mm (Ken Kimble Reactors Ltd.). A schematic that illustrates the catalytic reactor system and an image showing the experimental setup are given in **Figures 2.3a** and **2.3b**, respectively. The reactor was equipped with a H_2 supply at a constant (Brooks mass flow controller) volumetric flow rate (5-150 cm^3 min^{-1}). A vertically mounted four blade glass impeller provided agitation at stirring speeds in the range 100-1100 rpm. A recirculator (Julabo HD-4) was used to stabilise the reaction temperature at T = 293-343 ± 0.5 K with water as coolant. A 100 cm^3 aqueous solution of TMP and aqueous ammonia (NH_3/TMP mole ratio = 0.5-15) was introduced to the

reactor with the catalyst (TMP/metal mole ratio = 50-3500). The solution was heated to the reaction temperature (293-343 K) and a sample of the reaction mixture (0.5 cm^3) was taken using a syringe fitted with in-line filters (Sartorius 0.45 mm pore size) and analysed by HPLC. The reactor was flushed with He (50 cm^3 min^{-1}) for 3 min followed by H_2 (50 cm^3 min^{-1}) for 3 min and a continuous flow of H_2 was then introduced (time *t* = 0 for reaction). Samples were withdrawn every 10 min for up to 50 min and analysed by HPLC. Temporal changes to solution pH was measured using a pH meter (Hanna Instruments) equipped with a crystal-body electrode, coupled to a data logging and collection system (Pico Technology Ltd.); calibration was performed with standard buffer solutions (Fisher pH 7.0 and 10.0). As control, experiments carried out under He did not result in any measurable conversion. Measurement of initial reductive amination rate was based on sample analysis for up to 50 min where NH_3 loss from the reactor was less than 0.1% v/v. The effect of solution pH was also studied by varying the starting NH_3/TMP mole ratio in the range 0.5-15 and fixing pH at 11.2, 8.4 and 4.7 by adding sodium hydroxide or acetic acid. Reactions were repeated and generated a product composition that was reproducible to within ± 4%. The reaction was also conducted at elevated pressures (from 1-20 atm) in a 1000 cm^3 Zipperclave Reactor Model 401C-0417 (Autoclave Engineers); hydrogen consumption (mol h^{-1}) was recorded using the Sentinel software. The initial rate measured at 1 atm agreed with that obtained using the slurry reactor (to within ± 5%) at the same reaction temperature, NH_3/TMP and Pd/TMP mole ratios.

(a)

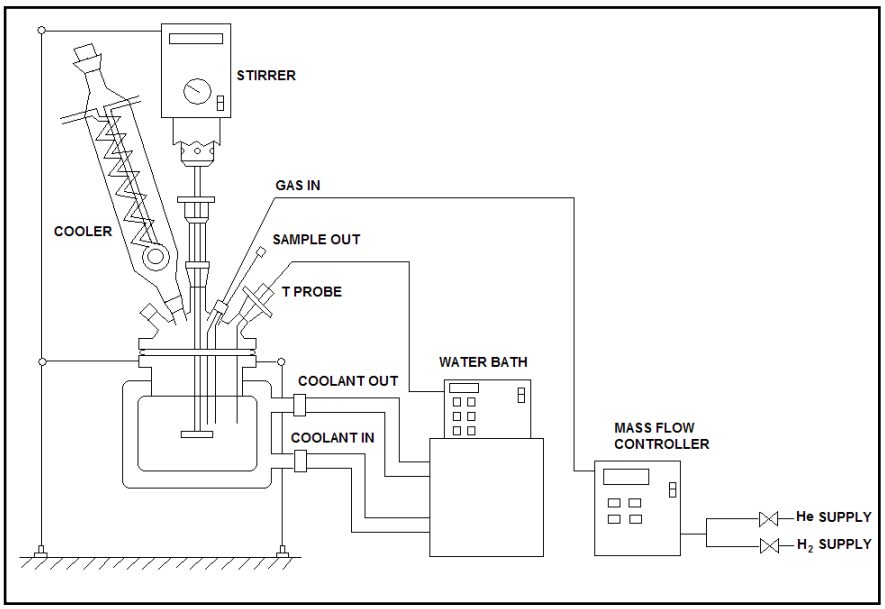

(b)

Figure 2.3: (a) Schematic representation of the catalytic reactor system. (b) Image of the three phase liquid phase reactor.

2.4 Product Analysis

Tertbutylglycine (TBG) in the diluted reaction mixture samples (1:10 dilution) was derivatised by reaction with *o*-phthaldialdehyde (OPA) in the presence of 2-beta-mercapto ethanol (BME) [11] (see **Figure 2.4**) followed by separation on a RP C18 column. The autosampler allowed the automated in-needle derivatisation (without transfer to an additional vial) by holding the sample taken from the reactor for 4 minutes with 6×10^{-3} cm^3 0.4 M potassium borate buffer (pH = 10.0) and 6×10^{-3} cm^3 derivatisation mixture at a fixed flow rate (= 1 cm^3 min^{-1}). After derivatisation, an

amount equivalent to 2×10^{-3} cm^3 was injected into the HPLC unit. The derivatisation mixture was prepared by mixing 0.05 g of OPA, 0.05 cm^3 of BME and 0.5 cm^3 methanol in a 5 cm^3 volumetric flask, agitating until full dissolution, making up to a final volume of 5 cm^3 with 0.4 M potassium borate buffer. Mobile phase A was 5 mM potassium phosphate buffer (pH = 7.5) while mobile phase B was acetonitrile. Separation was achieved at a flow rate of 1 cm^3 min^{-1} with a gradient programme that increased in a first 4 min step eluent B from 5 to 25%, followed by a second 2 min step that raised eluent B to 80%. Eluent B was maintained for 2 min at 80% B and equilibration at 5% B was performed over a total analysis time of 12 min (**Table 2.1**). Data acquisition and manipulation was carried out using the Chemstation LC Rev B.01.01 (164) 2001-2004 Agilent software, where quantitative analysis was based on relative peak area. A representative chromatogram is provided in **Figure 2.5**. A set of injections of TBG in the range 0.1-100 mM was conducted made to convert peak area to concentration; the resultant calibration plot is shown in **Figure 2.6**.

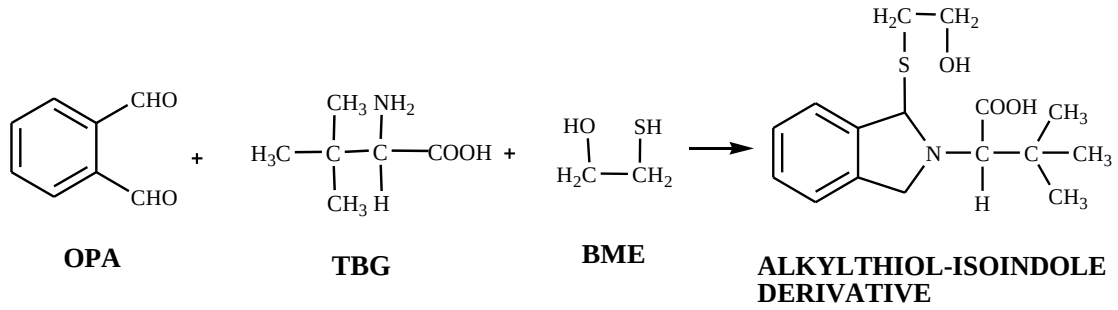

Figure 2.4: The derivatisation reaction of TBG prior analysis by HPLC.

In parallel, reaction selectivity to 2-hydroxy-3,3-dimethylbutyric acid (HTBA) was measured from ^{1}H-NMR analysis in H_2O with *ca.* 10% D_2O added as described above. Tetramethylsilane was used as a reference. A representative NMR analysis is illustrated in **Figure 2.7**.

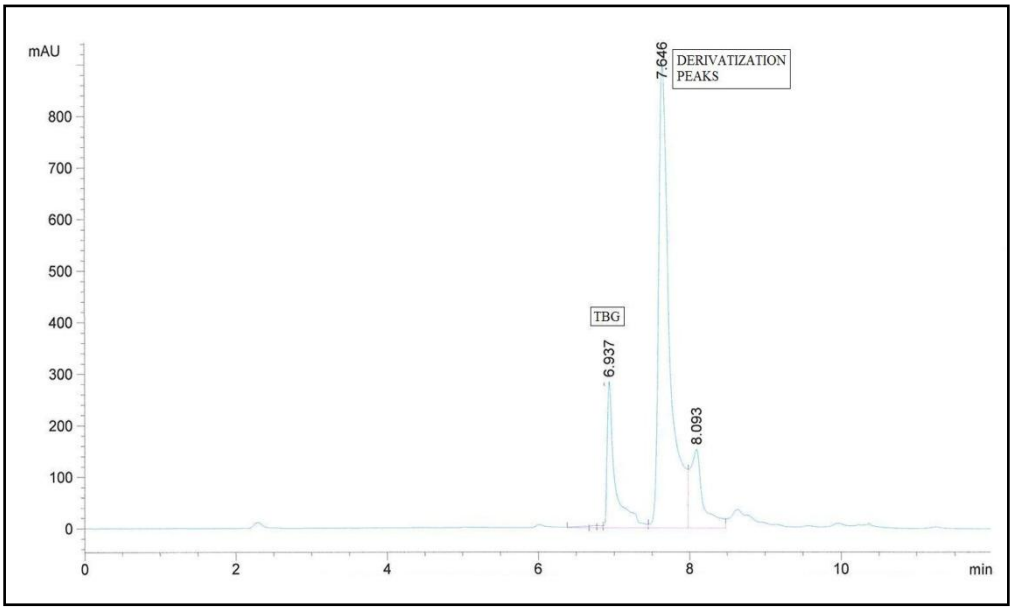

Figure 2.5: Representative chromatogram of a sample taken at the end of the reaction (*t* = 50 min); NH_3/TMP = 2.5; TMP/Pd = 600; solvent = 14% v/v water-propanol; *T* = 343 K. Chromatographic conditions are as given in Table 2.1.

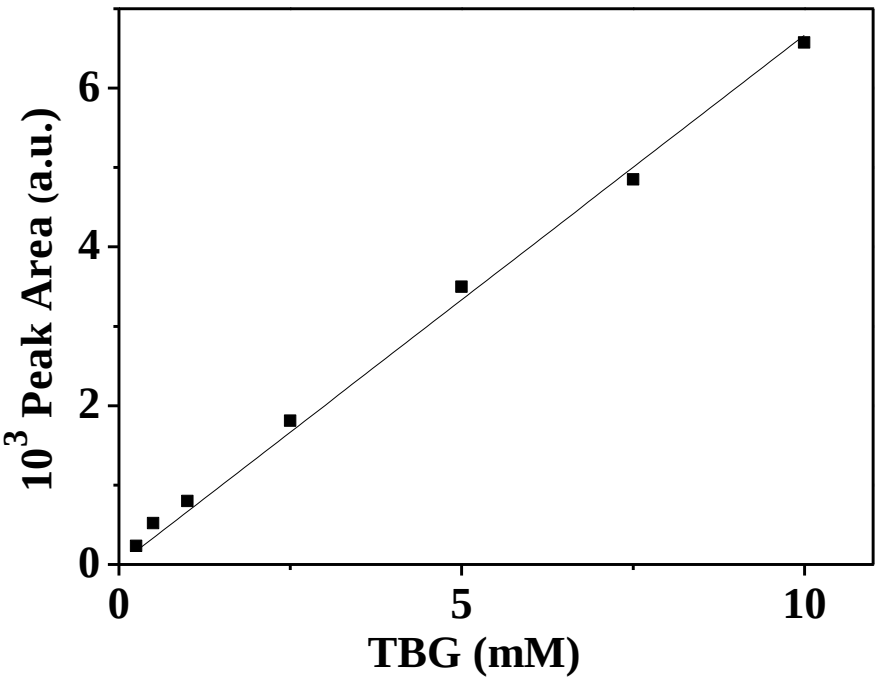

Figure 2.6: Calibration plot for TBG.

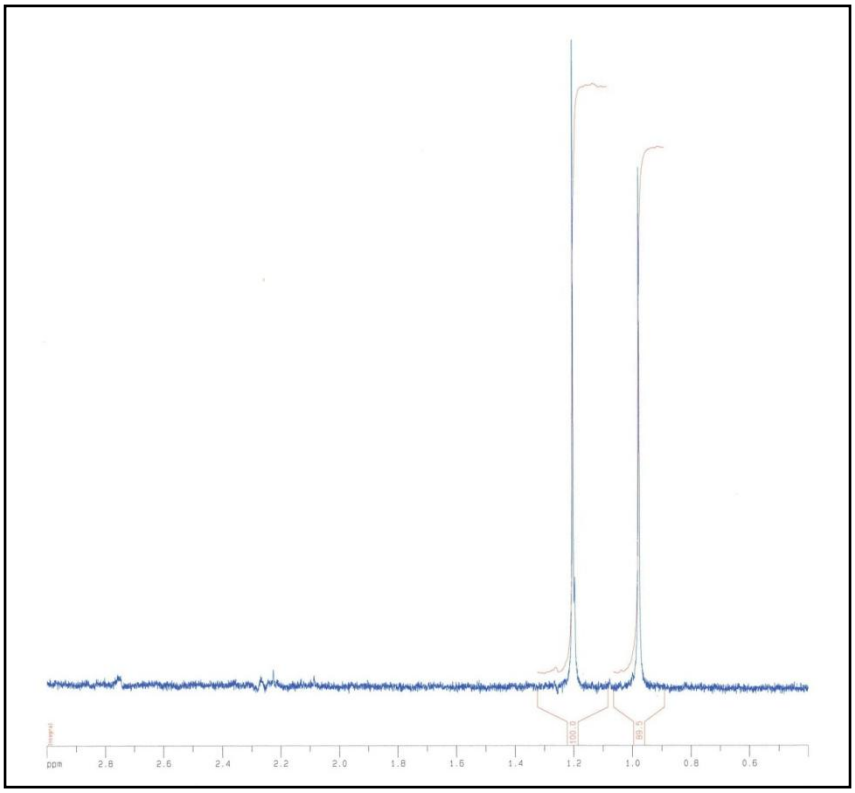

Figure 2.7: The 400 MHz proton spectrum of a sample at the end of the reaction (t = 50 min): NH_3/TMP = 0.5; TMP/Pd = 600; T = 343 K. HTBA and TMP appear as singlets centred at 0.95 and 1.2 ppm, respectively; signal due to TBG should appear as a singlet centred at 1.08 ppm.

Table 2.1: HPLC reversed phase gradient conditions for the analysis of TBG using OPA/BME at a flow rate of 1 cm^3 min^{-1}.

Time (min)	% Mobile phase B in eluent
0	5
4	25
6	80
8	80
12	25

2.5 Catalyst reuse

After the first reaction cycle, the reaction mixture was allowed to stand for 48 h and the liquid phase was extracted using a 50 cm^3 syringe. The catalyst was then reused directly in a second reaction with the addition of a fresh reactant charge. Alternatively, the catalyst was removed from the reactor and filtered (Whatman filter paper No. 1) on a Büchner sintered glass funnel (i.d. = 50 mm, porosity 3 (16-40 μm)). The catalyst was recovered, dried in air for 48 h and subjected to characterisation. Catalyst regeneration

post reaction involved two steps: (a) addition of 100 cm^3 distilled water, stirring at 1100 rpm for 50 min at ambient temperature, with syringe extraction of liquid; (b) second addition of 100 cm^3 distilled water with stirring at 1100 rpm and 343 K for 50 min with liquid extraction and introduction of a reactant charge followed by reaction with pH and product composition monitoring as above. Catalyst characterisation post reaction and after regeneration involved BET surface area, TPR, H_2 chemisorption and pH of zero charge measurements.

2.6 References

[2.1] G. Yuan, M. A. Keane; Catal. Today, 88, 27-36 (2003)

[2.2] A. Borodzinski, M. Bonarowska; Langmuir, 13, 5613-5620 (1997)

[2.3] T. Janiak, J. Okal; Appl. Catal. B: Environ., 92, 384-392 (2009)

[2.4] B. J. Kip, F. B. M. Duivenvoorden, D. C. Koningsberger, R. Prins; J. Catal., 105, 26-38 (1987)

[2.5] A. G. Shastri, A. K. Datye, J. Schwank; Appl. Catal., 14, 119-131 (1985)

[2.6] S. Gomez-Quero, F. Cardenas-Lizana, M. A. Keane; AIChE J., 56, 756-767 (2010)

[2.7] A. Dias, V. S. T. Ciminelli; Ferroelect., 241, 9-16 (2000)

[2.8] J. Vakros, C. Kordulis, A. Lycourghiotis; Chem. Commun., 17, 1980-1981 (2002)

[2.9] C. Amorim, M. A. Keane; J. Colloid Interf. Sci., 322, 196-208 (2008)

[2.10] C. Oprea, V. Ciupina, G. Prodan; Rom. J. Phys., 53, 223-230 (2008)

[2.11] Y.-S. Su, Y.-P. Lin, F.-C. Cheng, J.-F. Jen; J. Agric. Food Chem., 58, 120-126 (2010)

Chapter 3

Development of a Sustainable Catalytic Reductive Amination Process: Conversion of Trimethylpyruvic acid (TMP) to Tertbutylglycine (TBG)

In this Chapter, the catalytic reductive amination of trimethylpyruvic acid (TMP) was conducted in a three phase batch slurry reactor and an autoclave where an activated carbon supported Pd catalyst was used to promote the reaction to form tertbutylglycine (TBG). Mass transfer limitations have been evaluated by varying hydrogen flow rate, stirring speeds and catalyst loadings. Reaction conditions to achieve catalytic/kinetic control were determined and process optimisation addressed with respect to NH_3/TMP ratio, reaction temperature and solution pH. The role of the amination agent and the viability of catalyst reuse were also examined.

3.1 Introduction

Amines and their derivatives are essential precursors to a variety of active compounds such as pharmaceuticals, cosmetics, agrochemicals, dyes, adhesives and petroleum chemicals [1-5]. Reductive amination is viewed as a feasible means of preparing structurally diverse amines as it circumvents the problems associated with other synthesis methods as discussed in **Chapter 1**. This reaction has also been identified as a key green chemistry research topic [6]. It can be carried out under mild conditions and is compatible with substrates bearing carbonyl functions, *i.e*. aldehydes, ketones and carboxylic acids [7]. The carbonyl (C=O) group is converted in the presence of an aminating and reducing reagent. This proceeds via nucleophilic attack by the lone pair electrons on the aminating reagent with the formation of a carbinolamine (3) intermediate that releases H_2O to generate an imine (5) (a Schiff base) with subsequent reduction to the amine, as shown in **Figure 3.1** [8, 9]. Non-selective hydrogenation can generate the corresponding alcohol (7) [10], while the primary amine formed can react with the carbonyl substrate and/or imine to form undesired secondary amines [11]. Imine formation is under equilibrium control and is affected by the carbonyl substrate/ammonia molar ratio, solvent [12], temperature [13], pH [14], steric and electronic factors [9], acid/base additives and the nature of the catalyst.

Amination can be conducted using liquid or gas phase aminating agents, in batch or continuous mode. The use of aqueous NH_3 rather than NH_3 gas represents a more sustainable option in terms of lower energy requirements (associated with NH_3 storage and handling), and a safer system as the potential for release of ammonia gas as an environmental and toxic hazard is lessened [9, 15-19]. The aminating agent determines the nature of the amine products where the use of ammonia, a primary amine or a secondary amine generates primary, secondary or tertiary amines, respectively [10, 20, 21]. The choice of the reducing agent is critical to achieve selective imine reduction without attacking the carbonyl substrate. There are two possible approaches that can be taken in reductive chemical aminations [10]. The first employs molecular hydrogen, which is very effective in catalytic hydrogenation but is largely non-selective and may not be compatible with substrates containing carbon-carbon multiple bonds, reducible functionalities such as nitro and cyano groups, or halo-groups leading to hydrodehalogenation [22, 23]. A second methodology uses hydrides as reducing agents without catalyst, notably *N*-methylpyrrolidine zinc borohydride [24], $NaBH_3CN$ [25], $NaBH(OAc)_3$ [10], $NaBH_4$ [21], $B_{10}H_4$ [26] and Et_3SiH [27]. However, each of these exhibits limitations in terms of cost and show severe drawbacks in the context of green synthesis [22]. For example, $NaBH_3CN$ is highly toxic and generates by-products such as HCN and NaCN that can contaminate the target amine product [28]. $NaBH(OAc)_3$ is flammable, water-sensitive and poorly soluble in many organic solvents [29]. $NaBH_4$ requires the addition of toxic and corrosive acids such as H_2SO_4 and *p*-toluenesulfonic acid to facilitate imine formation and is non-selective [30, 31]. The use of organosilanes such as Et_3SiH as mild and environmentally friendly reducing agents overcomes the above disadvantages but these are not compatible with substrates that contain carbon-carbon double bonds [32, 33] and must be added to the reaction in excess amounts [34].

Depending on the nature of the catalyst employed, reductive amination can be classified as (i) homogeneous or (ii) heterogeneous. Heterogeneous reductive amination is typically promoted by supported or unsupported transition metals. Complexes such as $[Rh(cod)Cl]_2$ [35], $[Ir(cod)Cl]_2$ [36], Bu_2SnCl_2 [37], [(R,S)-BINAP]$PdBr_2$ [38], $(PhO)_2P(O)OH$ [39] and $InCl_3$ [34] have been used as catalysts in homogeneous catalytic systems. Homogeneous catalysts are generally more active but are less stable and necessitate separation/purification operations to extract the target product [40]. Such purification can be circumvented by using solid (heterogeneous) catalysts [41] but mass transfer limitations can lower the overall reaction rate with requisite higher energy

requirements (reaction temperatures up to 423 K and pressures up to 250 atm) [42]. Supporting the metal phase on a solid carrier provides enhanced dispersion and stabilisation of particles at the nano-scale [43]. Carbon has been widely used in this application to disperse ruthenium [44, 45], rhodium [46], palladium [11, 47], platinum [48], copper [49] and nickel [50-52]. A representative compilation of reductive amination studies using carbon supported metals is given in **Table 3.1**. The information presented serves to illustrate: (a) the nature of the supported metals that have been employed; (b) range of reactants; (c) operating temperatures and pressures; (d) catalytic performance with respect to conversion and selectivity. The use of heterogeneous systems facilitates catalyst separation and reuse. Catalyst recycling is critical in the application of green chemistry and process sustainability, as outlined in **Chapter 1**, allied to minimised by-product formation to reduce waste and ensure atom efficiency.

In this Chapter, the reaction of trimethylpyruvic acid (TMP) and aqueous ammonia to give tertbutylglycine (TBG) was promoted using palladium on carbon (Pd/C) as a model system to probe critical process variables. The target product, tertbutylglycine (TBG), is an industrially important amino acid building block for the pharmaceutical industry. Reductive amination of keto-carboxylic acids is viewed as a viable commercial route for the manufacture of amino acids [51]. The conversion of TMP represents a synthetic step in an industrial deracemisation to produce enantio-pure L-amino acids where the imine is converted to a racemic mixture and enantio-pure D-amino acid results from the action of an oxidase biocatalyst [53]. The target product (TBG) is used in the synthesis of peptide and other medicinal compounds for AIDS and cancer treatments [54]. In this study, a commercial Pd/C catalyst is used to promote the selective reductive amination of aqueous (as a clean solvent) solutions of TMP with hydrogen gas (rather than toxic hydrogen donors). The focus here is on the development of a cleaner sustainable process. As part of a comprehensive optimisation study, the conditions required for catalytic control are established with the goal of achieving 100% selectivity to TBG at an enhanced reaction rate.

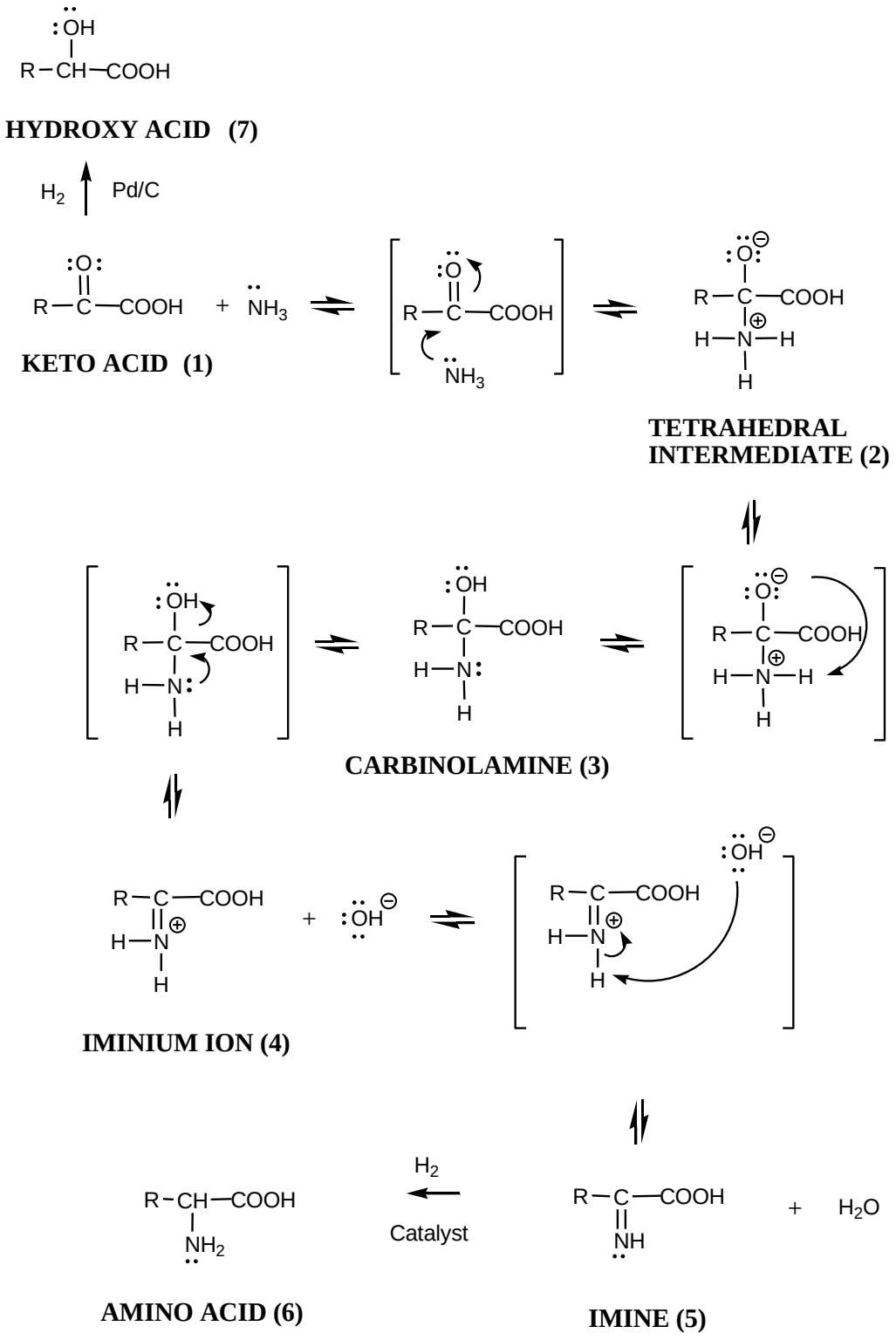

Figure 3.1: Reaction scheme for reductive amination: R = tert-butyl; (1) = TMP; (6) = TBG; (7) = 2-hydroxy-3,3-dimethylbutyric acid (HTBA).

Table 3.1: Compilation of published studies of reductive amination using carbon supported metal catalysts.

Reactant/ Amination Agent/ Solvent	Reactant: Amination Agent mol ratio	Catalyst	NH_3 phase	Nature of Support	BET Surface Area ($m^2 g^{-1}$)	Additive	Total Conversion (%)	Selectivity to amine (%)	Time (h)	*P* (bar)	*T* (K)	Ref.
Acetophenone/ Ammonia/ Ethanol	1:24	5% Ru/C	Gas	Carbon	924	NH_4Cl	97	45	5	80	323	[11]
		5% Pd/C			1035		98	7				
Butyraldehyde/ Ammonia/ Ethanol	1:16.5	5% Rh/C	Gas	Charcoal	818	-	100	85	0.7	50	353	[46]
		5% Rh/C		Graphite	95		100	80	1			
		5% Ru/C		Graphite	42		96	95	not given			
		5% Pt/C		Graphite	80		100	10	0.8			
		5% Pt/C		Graphite	57		99	15	0.8			
		5% Pd/C		Graphite	88		85	20	not given			

Reactant/ Amination Agent/ Solvent	**Reactant: Amination Agent Mol Ratio**	**Catalyst**	**NH_3 Phase**	**Nature of Carbon Support**	**BET Surface Area ($m^2\ g^{-1}$)**	**Additive**	**Total Conversion (%)**	**Selectivity to amine (%)**	**Time (h)**	***P* (bar)**	***T* (K)**	**Ref.**
Benzaldehyde/ Ammonia/ Methanol	1:16	5% Pd/C	Liquid	Peat	745	-	100	35	4.7	40	363	[44]
	1:2						100	7.5	5.3			
	1:16	5% Ru/C			858		100	98	4.2			
	1:2						100	77	4.5			
Methyl ethylketone/ Benzylamine/ Cyclohexane	1:1	5% Pd/C	Liquid	Carbon	800	L-alanine	87	89	24	60	298	[55]
Formadehyde/ Aniline/ Toluene	1.5:1	5% Pd/C	Liquid	Carbon	850	-	69	30	4	8.3	393	[56]
Formadehyde/ *o*-Toluidine/ Toluene	1.5:1	5% Pd/C	Liquid	Carbon	850	-	68	43	4	8.3	393	[56]
Formadehyde/ *m*-Toluidine/ Toluene							72	29				

Reactant/ Amination Agent/ Solvent	**Reactant: Amination Agent Mol Ratio**	**Catalyst**	**NH_3 Phase**	**Nature of Carbon Support**	**BET Surface Area ($m^2\ g^{-1}$)**	**Additive**	**Total Conversion (%)**	**Selectivity to amine (%)**	**Time (h)**	***P*** **(bar)**	***T*** **(K)**	**Ref.**
Formadehyde/ *p*-Toluidine/ Toluene	1.5:1	5% Pd/C	Liquid	Carbon	850	-	77	25	4	8.3	393	[56]
Acetone/ aniline/non solvent	15:1	5% Pd/C	Gas	Carbon	not given	-	87	77	1	27.6-41.4	378	[57]
							99	40	1		413	
		5% Pt/C					90	52	1		378	
		5% Rh/C					100	0	10		378	
		5% Ru/C					97	0	1.8		378	
Methyl isobutyl ketone/ *p*-Aminodiphenyl amine/non solvent	4:1	5% Pd/C 5% Pt/C	Gas	Carbon	not given	-	76	78	12.5	10.4-20.7	393	[57]
							92	93	10		373	

Reactant/ Amination Agent/ Solvent	**Reactant: Amination Agent Mol Ratio**	**Catalyst**	**NH_3 Phase**	**Nature of Carbon Support**	**BET Surface Area ($m^2\ g^{-1}$)**	**Additive**	**Total Conversion (%)**	**Selectivity to amine (%)**	**Time (h)**	***P*** **(bar)**	***T*** **(K)**	**Ref.**
Methyl isopropyl ketone/ Ethanolamine/ Water	1:1.2	5% Pt/C	Gas	Carbon	not given	-	100	99	1.25	23	373	[58]
Benzaldehyde/ Dimethylamine/ Water	1:1.2	5% Pd/C	Gas	Carbon	not given	-	96.1	96	4.5	24	403	[58]
							96	95		27	418	
Benzaldehyde/ Dimethylamine/ Water	1:1.2	5% Pt/C	Gas	Carbon	not given	-	99.7	92	4.5	27	403	[58]
							99.4	96	4.5	27	418	
Butyraldehyde/ Ethanolamine/ Water	1:2.6	5% Pt/C	Gas	Carbon	not given	-	98.1	96	5	24	353	[58]
		5% Pd/C					83.4	84	5.3			
		5% Ru/C					93.3	88	23			

3.2 Results and Discussion

3.2.1 Catalyst Characterisation

The physico-chemical characteristics of the commercial Pd/C catalyst used in this study are given in **Table 3.2**. The sample exhibited a BET surface area (850 m^2 g^{-1}) that is in keeping with areas quoted in the literature for commercial carbon based catalysts [59, 60]. The pore volume, with a mean pore size of 18 Å from BJH analysis, was found to be 0.48 cm^3 g^{-1}. The temperature program reduction (TPR) profile is shown in **Figure 3.2**. The profile is dominated by a negative peak (H_2 release) at 365 K that can be attributed to the decomposition of Pd hydride formed at room temperature [61]. The mol ratio of hydrogen absorbed relative to Pd content associated with the hydride (H_{abs}/Pd) is 0.12, significantly below the upper limit (0.67) for bulk Pd, indicating the presence of Pd particles at the nano-scale [62]. Mean Pd particle size, dispersion and specific surface area were calculated from H_2 chemisorption measurements. The H_2 uptake given in **Table 3.2** is based on the standard assumption of dissociative adsorption, *i.e.* H_2/Pd = 1/2 [63]. Representative high (I) and low (II) magnification TEM images are shown in **Figure 3.4a** where the number weighted mean diameter ($\bar{d}_n = \Sigma n_i d_i / \Sigma d_i$, see further details in **Chapter 2**) was equal to 4.6 nm on the basis of a measurement of over 600 particles. It can be seen that Pd particles exhibit a pseudo-spherical morphology with a relatively narrow size distribution (3-10 nm, see **Figure 3.4b**). XRD analysis (see **Figure 3.3**) reveals a response due to (cubic) Pd with peaks at 40.1º, 46.7º, 68.1º and 82.1º corresponding to (111), (200), (220) and (311) Pd planes, respectively (JCPDS-ICDD Card No. 05-0681). The peak at 33º can be indexed to a tetragonal PdO phase (JCPDS-ICDD Card No. 03-65-5261) formed during the passivation step and corresponding to the (100) plane [64]. Palladium size can be obtained from these three different approaches [65] and is compared in **Table 3.2**. XRD analysis generates a volume-weighted mean size [66] to give the highest value (6.0 nm). The accuracy of the XRD measurement can be affected if the instrumental contribution is greater than the broadening due to the crystallite size [67]. The surface area weighted particle size estimated from H_2 chemisorption (2.8 nm) is smaller than the TEM number-weighted size (4.6 nm), which may result from excess H_2 uptake, possibly due to spillover effects [68, 69]. TEM analysis has the drawback of presenting a two dimensional image of a three dimensional particle [70]. A general agreement of Pd size values for Pd/C catalysts calculated from H_2 chemisorption, TEM and XRD can be found in the literature [71-73].

The surface charge of the activated carbon support depends on the solution pH and determines ion exchange capacity [74]. The pH at the point of zero charge (pH_{pzc}) is the pH value at which there is no net surface charge. The pH_{pzc} value of Pd/C, determined using the potentiometric mass titration described in the **Chapter 2**, was 6.8, which falls within the range of values (6-8) quoted in the literature for carbon based catalysts [75-77]. Representative titration curves are shown in **Figure 3.5**. At pH < pH_{pzc}, the catalyst surface has a positive charge and its interaction with anionic species is favoured while at pH > pH_{pzc} cationic species are attracted to the catalyst surface. The pH_{pzc} determined suggests the presence of neutral or weakly acidic species such as phenolic, carbonyl, quinone and ether groups [78].

Table 3.2: Physico-chemical characteristics of the 5% w/w Pd/C catalyst.

BET surface area ($m^2\ g^{-1}$)	850
pH_{pzc}	6.8
H_2 uptake ($\mu mol\ g^{-1}$)	95
Mean Pd particle size[a] (nm)	2.8
Mean Pd particle size[b] (nm)	4.6
Mean Pd particle size[c] (nm)	6.0
Pd dispersion[a] (%)	40
Specific Pd surface area[a] ($m^2\ g_{Pd}^{-1}$)	180
Pore Volume ($cm^3\ g^{-1}$)	0.48
Pore Size (Å)	18

[a]from H_2 chemisorption
[b]from TEM analysis
[c]from XRD line broadening

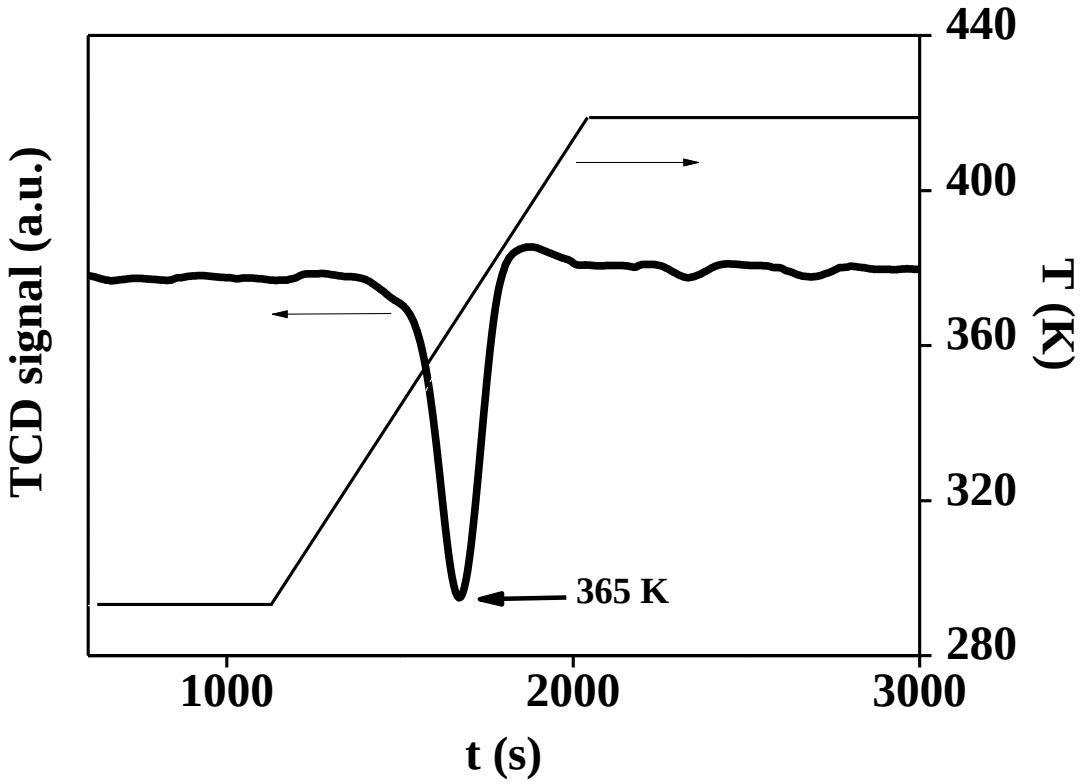

Figure 3.2: Temperature-programmed reduction (TPR) profile (to 423 K) for Pd/C.

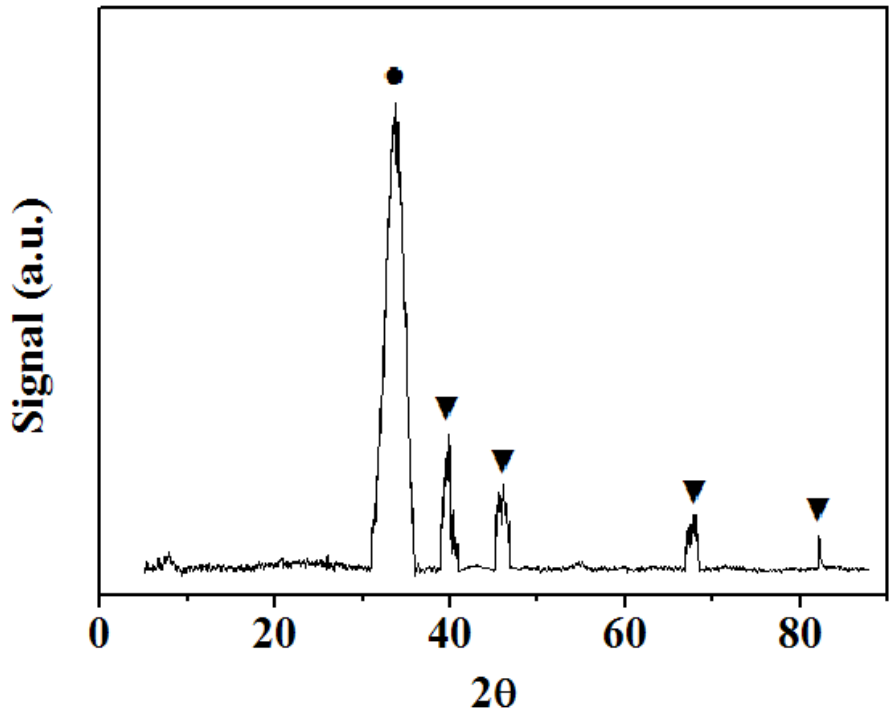

Figure 3.3: XRD pattern for Pd/C: peak assignment based on JCPDS-ICDD standards for (●) PdO (Card No. 75-584) and (▼) Pd (Card No. 06-0581).

(aI) **(aII)**

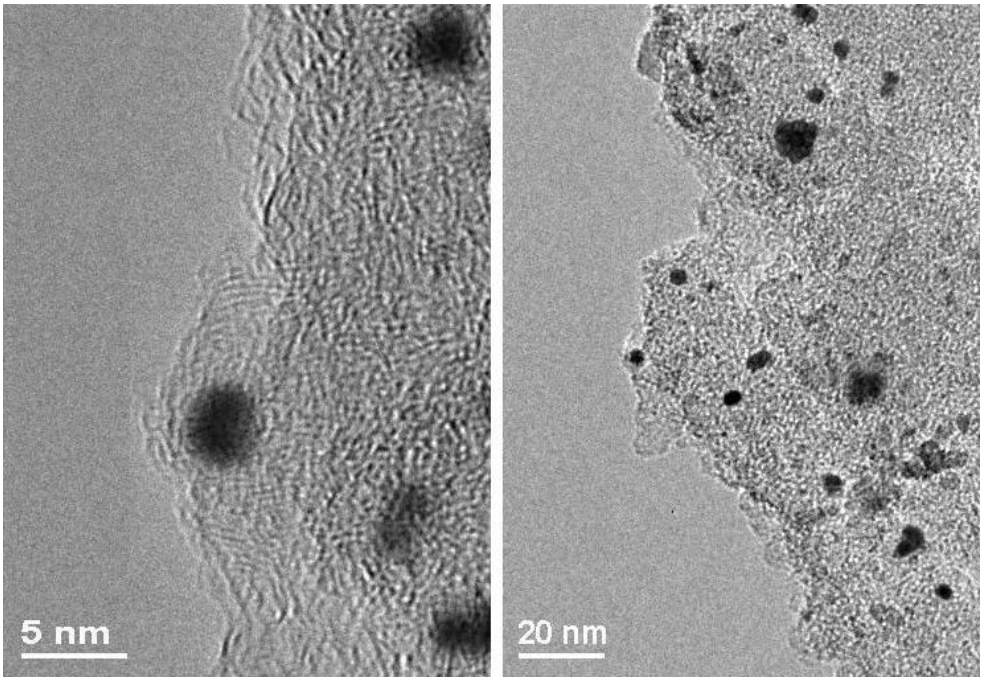

(b)

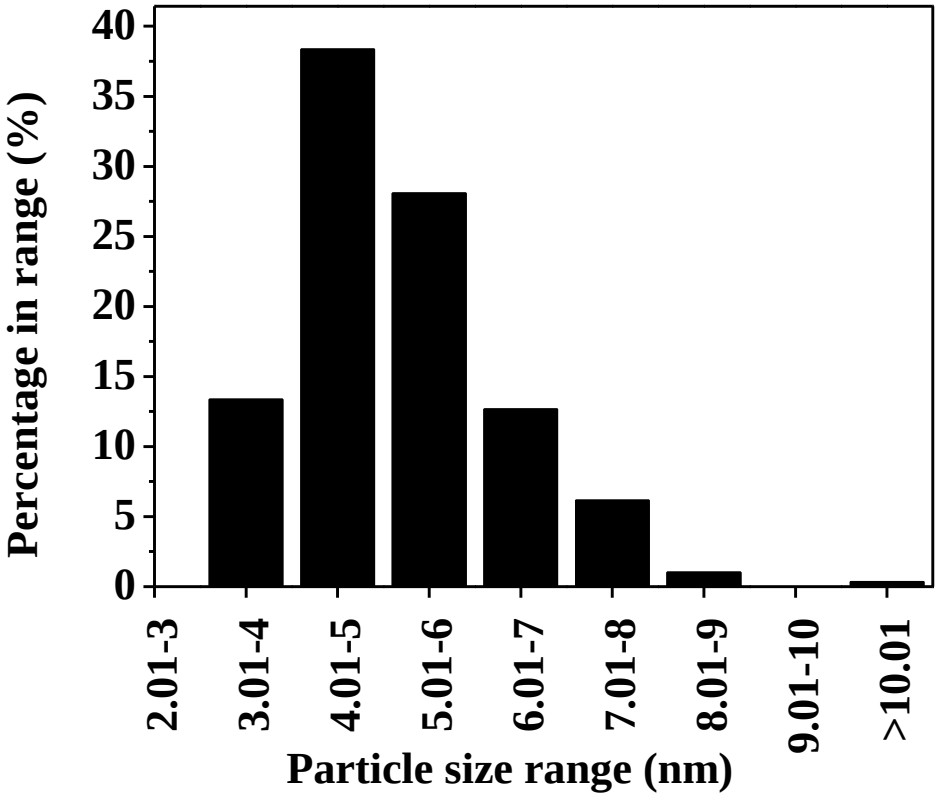

Figure 3.4: a) Representative (I) high and (II) low magnification TEM images and b) Pd particle size distribution for Pd/C.

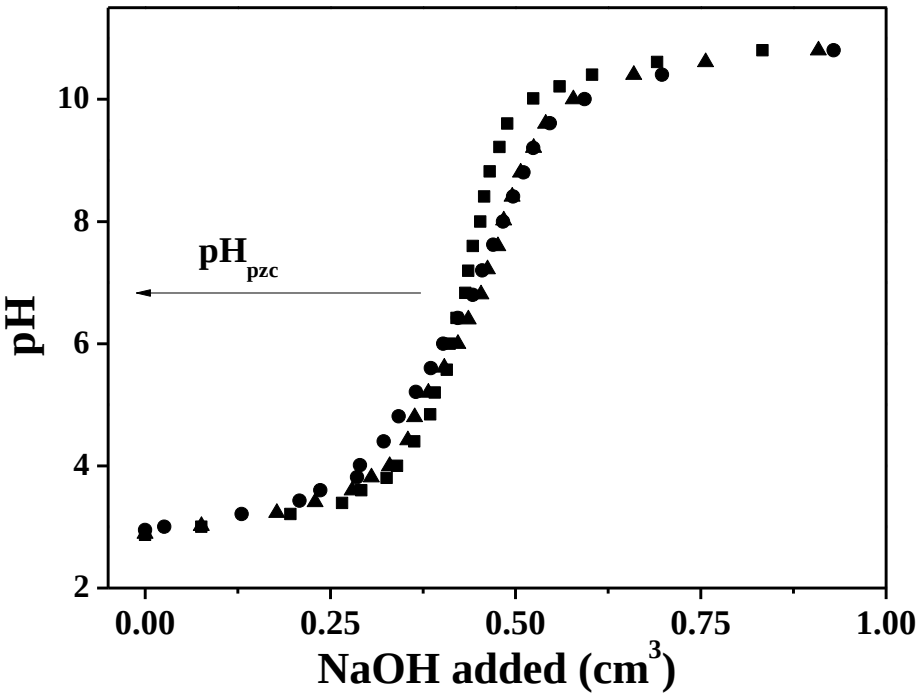

Figure 3.5: pH profiles associated with the pH of point of zero charge (pH_{pzc}) determined for 0.025 g (■), 0.050 g (▲) and 0.075 g (●) Pd/C.

3.2.2 Catalytic Activity and Selectivity

Reductive amination of TMP was monitored both in a slurry reactor and autoclave where the product composition coincided to within 4%. The time dependence of TBG production showed a linear response for reaction times ≤ 50 min, as illustrated in **Figure 3.6** for three representative reactions. The slope of these plots that relate the amount of TBG generated as a function of time has been used to measure the initial reaction rate (r_o). A similar approach has been applied to the measurement of benzaldehyde reductive amination (with gaseous ammonia) over Pd/C [44, 79]. The number of moles of TBG produced matched the H_2 and TMP consumption. Moreover, NMR analysis did not reveal the presence of 2-hydroxy-3,3-dimethylbutyric acid (HTBA, see **Figure 3.1**) in the product for a reaction time up to 24 h, indicating 100% selectivity to the target TBG product. The absence of secondary and tertiary amines (from NMR analysis) as a result of further reaction between TBG and TMP/imine points to low reactivity of TBG as observed in the literature for other primary amines [11, 60, 80]. Exclusive TBG production at atmospheric pressure using aqueous ammonia represents a significant advancement in the development of a sustainable reductive amination process. Indeed, such a high selectivity under mild conditions approaches that observed in enzymatic routes [81-84]. There was no significant variation in rate with increasing H_2 pressure (up to 20 bar at 343 K) in this study,

suggesting essentially a zero order dependence on H_2: initial rates at 1 and 20 bar are 0.30 and 0.24 mol dm^{-3} min^{-1} g_{Pd}^{-1}, respectively with a 100% selective to TBG. A zero order dependence was demonstrated by Freedman *et al.* [85] in the reaction of 12-aminostearic acid with gaseous ammonia over Raney nickel in the pressure 35-70 bar range. Moreover, Werkmeister *et al.* [86] did not observe any difference over 50-80 bar in the reaction of acetophenone with aniline over $Cu(OAc)_2$ and CuF_2. However, Bagal *et al.* [12] have recorded an increase in amine yield over the 25-35 bar interval in the conversion of benzaldehyde and aniline over a polymer supported Pd *N*-heterocyclic carbine (PS-Pd-NHC) catalyst. Hydrogen pressure effects have not been established for reductive amination over a supported transitional metal. We focus here on milder reaction conditions, with the overarching goal of sustainability. A requirement for high H_2 pressure (up to 40 bar) in general is noted in the literature for homogeneous [13, 87] and heterogeneous [9, 12, 46] reductive amination. The majority of studies have involved use of gaseous ammonia [11, 12, 44, 88]. A move away from elevated pressure to ambient pressure operation is an exemplar of "green chemistry" as defined by Anastas [89] and bridges a crucial sustainability gap in existing processes. A switch to aqueous ammonia, notably over Raney nickel, with high conversion and selectivity has been demonstrated as a critical improvement in cleaner amination processes [35, 50, 80, 90, 91]. It is worth flagging two cases that are particularly relevant to this work, involving α-keto-carboxylic acids, aqueous ammonia and H_2 as reactants. The first study, reported by Chan *et al.* [51], considered the reductive amination of pyruvic and phenylpyruvic acid over Raney Ni at 14 bar with selectivities of 97-98% at complete conversion (after 20 h). The second example also deals with pyruvic acid, catalysed by iridium hydride complexes where 96% selectivity was achieved at total substrate conversion (after 6 h) [92]. Use of aqueous ammonia, commercially available at concentrations of *ca.* 35% w/w, reduces safety risks and circumvents the requirement of pressurised storage for gaseous ammonia [93]. This is the first reported instance of reductive amination promoted using a supported metal catalyst with reaction exclusively in aqueous ammonia at atmospheric pressure.

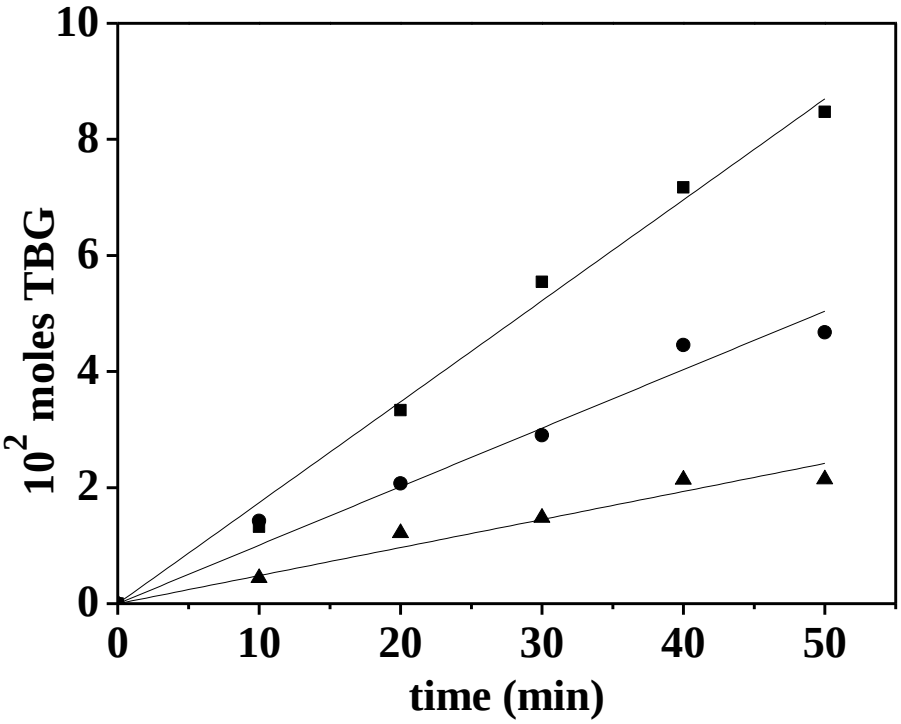

Figure 3.6: Temporal variation of TBG production where (■) TMP/Pd = 50 (r_o = 6.8×10^{-2} mol dm^{-3} min^{-1} g_{Pd}^{-1}), (●) TMP/Pd = 300 (r_o = 24×10^{-2} mol dm^{-3} min^{-1} g_{Pd}^{-1}) and (▲) TMP/Pd = 900 (r_o = 34×10^{-2} mol dm^{-3} min^{-1} g_{Pd}^{-1}); stirring speed = 1100 rpm; NH_3/TMP = 2.5; T = 343 K.

3.2.3 Transport limitations

It is well established that the rate of heterogeneous liquid/solid/gas reactions can be controlled by the external diffusion of reactant(s) and product(s) to and from the catalytically active sites [94-96]. In order to assess the intrinsic activity of the catalysts in the reductive amination of TMP, reaction conditions must first be established wherein the mass transfer limitations are negligible and the reactor is operated in the "reaction-limited" region. In terms of heat transfer effects, temperature gradients arising from heat transfer limitations are not as prevalent under liquid phase conditions when compared with gas phase operation. The relatively high thermal conductivity of the liquid phase, an order of magnitude higher when compared with the gas phase [97], coupled with the small heat of reaction per unit slurry volume means that there is a little temperature difference between particle and liquid. In the slurry type reactor used in this study, the overall rate of the TBG production can be governed by a series of reaction and mass-transfer steps that proceed simultaneously [98, 99]: (a) H_2 diffusion through the gas film at the gas/liquid interface; (b) H_2 diffusion through the liquid film at the gas/liquid interface; (c) TMP, NH_3 and H_2 diffusion through the liquid film at the

liquid/solid interface; (d) reaction and diffusion at the catalyst surface; (e) the reverse transport of TBG into bulk solution. The reactant TMP and product TBG are fully soluble in the reaction medium under the conditions employed in this study but H_2 transport can be conditioned by solubility and this must be addressed. Both chemical and physical processes occur simultaneously during a catalytic reaction and the overall rate of reaction is a composite of physical and chemical rates [100]. In order to evaluate the intrinsic catalytic activity, it is essential to ascertain the extent to which the physical processes control the overall conversion. Therefore, four experimental diagnostic criteria (agitation speed, H_2 flow rate, catalyst mass and temperature) have been employed. In every instance, TBG was detected as the sole product (*i.e.* 100% selective).

3.2.4 Effect of agitation speed

A more effective agitation of the reaction mixture can enhance the rate of mass transfer at both gas/liquid and liquid/solid interfaces but should not affect chemically or surface-controlled processes [99, 101]. Enhanced mixing serves to extend the liquid/gas/solid interface and limit transport constraints of H_2 from the gas phase to the bulk liquid phase and the TMP and NH_3 from the bulk liquid phase to the catalyst surface. The influence of stirring speed on initial rate (r_o) is shown in **Figure 3.7a**, where the rate exhibited a marked increase as the stirring speed was raised from 100 to 850 rpm, diagnostic of a transport contribution, but remained largely unchanged at stirring speed > 850 rpm. A stirring speed of 1100 rpm, taken to be the minimum required to avoid segregation of both fluid and solid catalyst while avoiding overly turbulent/vortex conditions and catalyst particle attrition, was accordingly used for subsequent reactions. In the literature on reductive amination, stirring speeds in the range of 1000-2000 rpm were chosen to minimise the mass transfer effects [20, 45, 60, 102].

3.2.5 Effect of hydrogen flow rate

Given the low H_2 solubility in water (0.84 mM at 100 kPa and 288 K [103]), H_2 transport constraints are inevitable. Hydrogen mass transfer limitations can be minimised by increasing the inlet H_2 flow rate, which enhances the gas holdup in the three phase slurry and therefore increases the total area of the gas/liquid interface [104]. The influence of H_2 flow rate on initial rate is shown in **Figure 3.7b**, where the rate was

essentially invariant over the range 18-150 cm^3 min^{-1}. Operating the reactor at a lower volumetric flow rate (18 cm^3 min^{-1}) represents the more sustainable option in terms of H_2 usage/atom efficiency. At an inlet flow of 150 cm^3 min^{-1}, H_2 is in excess (by a factor of 8) and unreacted H_2 in the exhaust stream must be recovered and recycled to the reactor. Invariant rates have also been observed as a function of gas flow rate for reductive amination conducted at atmospheric pressure [88, 105].

3.2.6 Effect of catalyst mass: TMP/Pd mol ratio

The effect of varying the mass of catalyst represents a third means of assessing the degree of transport control. Increasing the catalyst mass should be accompanied by a proportional increase in reaction rate where the supply of reactant(s) to the catalyst surface is not limited by mass transfer. The effect of altering the TMP/Pd mol ratio on r_o is shown in **Figure 3.8a**. Where TMP/Pd > 1750, there is a clear decrease in rate that can be attributed to insufficient catalyst present to promote the reaction. When TMP/Pd < 600, an increase in catalyst mass did not result in a corresponding increase in rate with the result that the system operates under transport retardation. The latter response has also been observed for the reductive amination of benzaldehyde [45, 79]. In our study, operation in the range TMP/Pd = 600-1750 can be taken as representing chemical catalytic control, which can be compared with studies using reactant/catalyst ratios of 700 for cyclopentanone over Raney Ni [50] and 900 for butyraldehyde over Pd/C [46]. In the literature, although the amount of catalyst has been varied and conversions recorded, an explicit correlation in terms of kinetic control has not been provided [88].

(a)

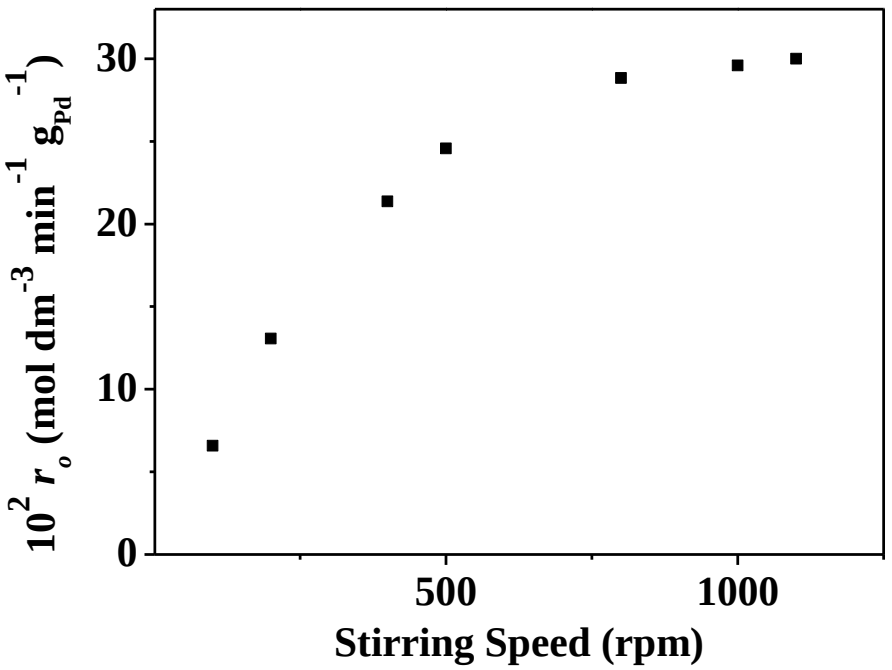

(b)

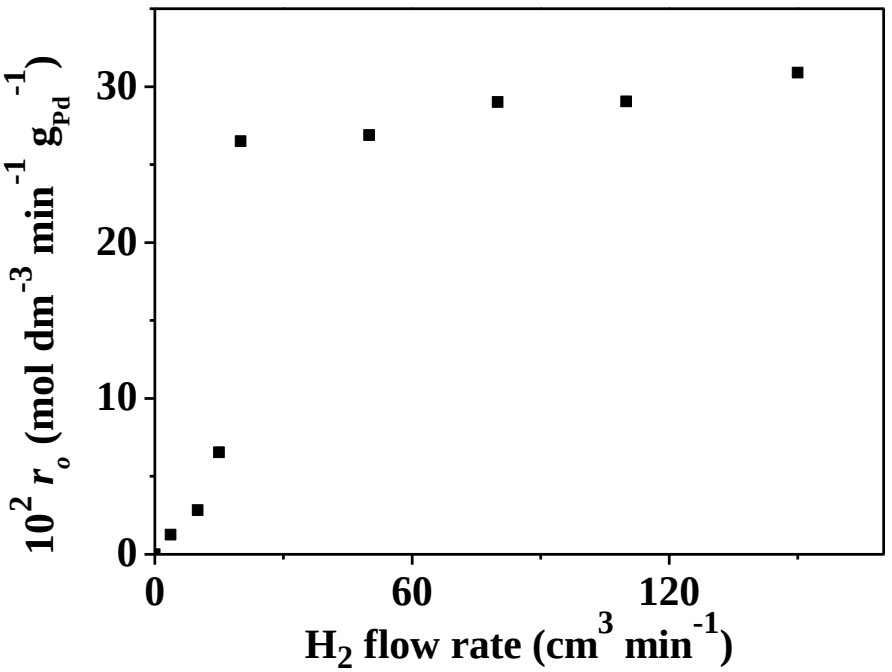

Figure 3.7: a) Initial rate of TBG production (r_o) as a function of stirring speed (NH_3/TMP = 2.2; TMP/Pd = 670; T = 343 K) and b) hydrogen flow rate (NH_3/TMP = 2.2; TMP/Pd = 670; T = 343 K; stirring speed = 1100 rpm).

(a)

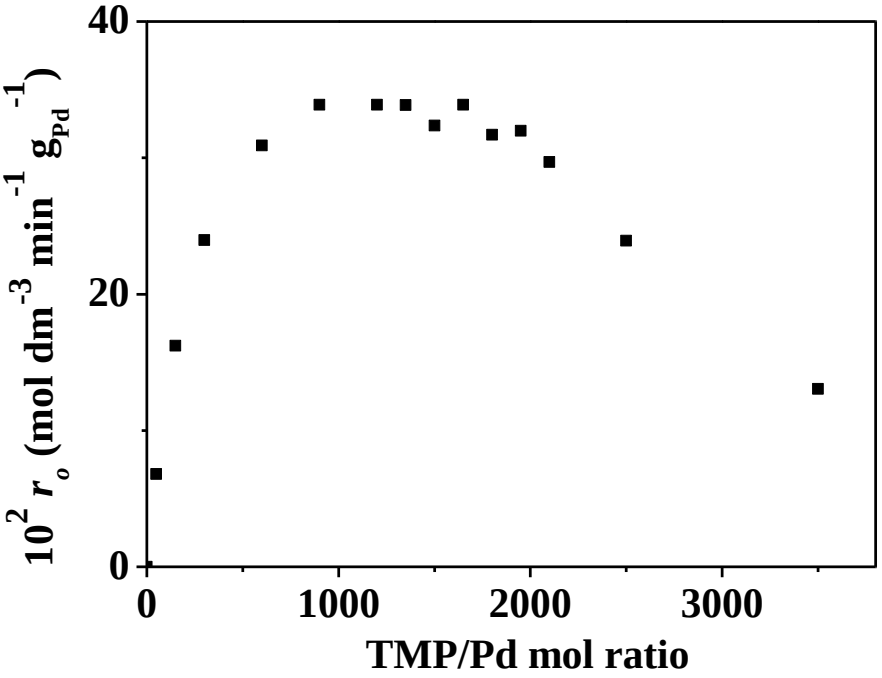

(b)

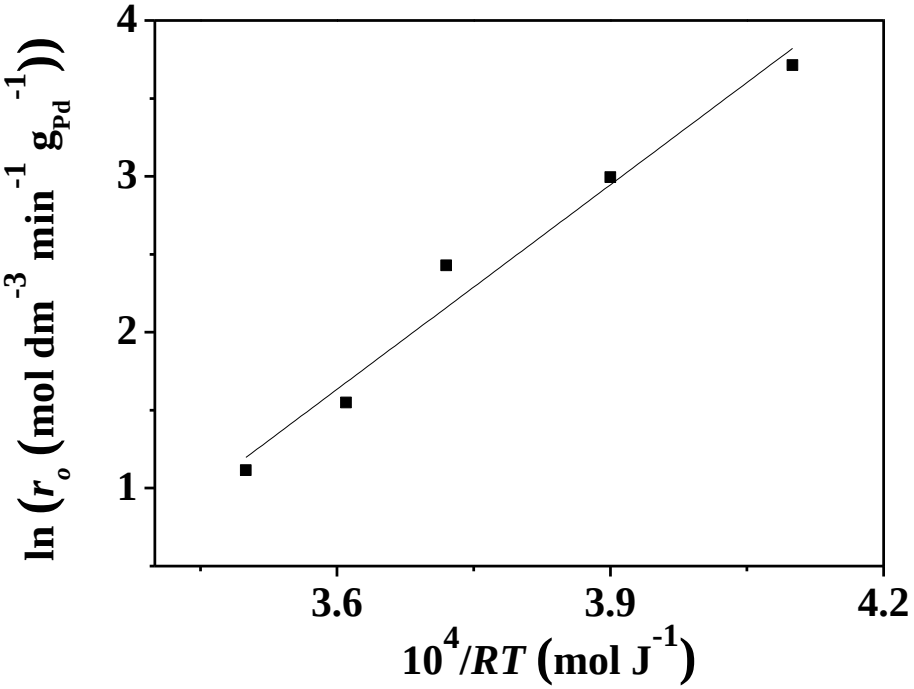

Figure 3.8: a) Initial rate of TBG production (r_o) as a function of TMP/Pd (NH_3/TMP = 2.5; T = 343 K; stirring speed = 1100 rpm) and b) reaction temperature as an Arrhenius plot (NH_3/TMP = 2.5; TMP/Pd = 600; stirring speed = 1100 rpm).

3.2.7 Effect of reaction temperature

The temperature dependence of reductive amination is presented as a conventional Arrhenius plot in **Figure 3.8b** where higher rates were achieved with increasing temperature. An increase in reductive amination rate with increasing temperature (293-343 K) has been reported previously [14, 58, 79, 106]. The activation energies of purely mass transfer controlled processes are typically in the range of 10-20 kJ mol^{-1} [107] while those that characterise reactions operating under chemical control exceed *ca*. 40 kJ mol^{-1} [94, 96, 108, 109]. The experimentally determined apparent activation energy can then be used to identify whether the reaction is a predominant chemical or physical controlled process. In this work, the reaction mixture can be taken as saturated with H_2 with no significant difference in solubility over the 293-343 K increment. The resultant apparent activation energy (ΔE_a) value for TBG production calculated from the slope of the Arrhenius plot (44 kJ mol^{-1}) is consistent with catalytic control. In the literature, a comparable activation energy (50 kJ mol^{-1}) was reported for an enzyme (alanine dehydrogenase) promoted conversion of pyruvic acid ($308 < T < 333$ K) [110] with higher values for the reaction of 3-nitrobenzaldehyde with methylamine (77 kJ mol^{-1}, 278-320 K) [111] and the reductive amination of ethanolamine over $NiCo/BPO_4.\gamma\text{-}Al_2O_3$ (116 kJ mol^{-1}, 550-660 K) [112]. As can be seen from entries in **Table 3.3**, the selectivity to TBG is 100% at T = 333-343 K but decreases at lower temperatures, with hydrogenation of TMP to form 2-hydroxy-3,3-dimethylbutyric acid (HTBA) as the predominant product at $T \leq 323$ K (see **Figure 3.1**). At these temperatures, a temporal increase in pH was observed, which can be accounted for by the higher pK_a (= 3.91) of HTBA relative to that of TMP (= 2.65) [14]. Indeed, there is evidence in the literature that alcohol formation is favoured at lower reaction temperatures [87, 113]. However, there are instances where the production of the alcohol by-product cannot be avoided even at higher temperatures (323-373 K) [22, 90].

Based on these results, reductive amination of TMP over Pd/C at a stirring speed = 1100 rpm, H_2 flow rate > 20 cm^3 min^{-1} and an initial TMP/Pd ratio in the range 600-1750 was conducted under conditions of minimal mass transfer limitation over the temperature range $293 \leq T \leq 343$ K. Under these conditions, the effects of varying critical process variables such as NH_3/TMP, solution pH and solvent on the intrinsic activity/selectivity can then be assessed.

Table 3.3: Variation of reaction selectivity (to TBG and HTBA) as a function of reaction temperature: TMP/Pd = 600; NH_3/TMP = 2.5; stirring speed = 1100 rpm.

T (K)	Selectivity to TBG (%)	Selectivity to HTBA (%)
293	13	87
308	20	80
323	32	68
333	100	0
343	100	0

3.2.8 Process parameters

3.2.8.1 Effect of NH_3/TMP mol ratio and pH

Efficient use of aqueous ammonia is critical in terms of sustainable processing and the effect of varying NH_3/TMP mol ratio (in the range 0.5-15) on reaction rate and selectivity was therefore studied under conditions of kinetic/catalytic control. The applicable range of ratios was limited in terms of TMP solubility in aqueous ammonia. The results are shown in **Figure 3.9** where a maximum initial rate was recorded at NH_3/TMP = 1.5 and the rate was invariant over NH_3/TMP = 5-15. Reductive amination should be favoured by excess ammonia in order to limit the competitive reduction of the C=O function (to HTBA) but the results have revealed that only a slight excess is required. Lower reaction rates at a higher ammonia content have been noted elsewhere [58, 114] and attributed to partial catalyst poisoning by NH_3, which reduced the available active metal surface area [59, 80]. A higher ammonia content leads to higher concentration of hydroxide ions and, according to **Figure 3.1**, this can inhibit formation of the iminium ion intermediate (4) with a reduction in reaction rate. At NH_3/TMP $\leq$ 1 (see **Table 3.4**), hydrogenation to HTBA predominated, as reported for reductive amination of aldehydes [9] and keto-carboxylic acids [92]. A temporal increase in pH at NH_3/TMP $\leq$ 1 was again indicative of HTBA formation. Generally, excess NH_3 is required for high reductive amination selectivities [60] with maximum rates and selectivities recorded at an NH_3 excess of 1.5 (acetophenone [11]), 1.9 (cyclopentanone [50]), 2 (benzaldehyde [9]) and 3.5 (cyclohexanone [49]).

Temporal variation (0-50 min) of solution pH as a function of NH_3/TMP mol ratio is recorded in **Table 3.4**. According to the Henderson-Basselbalch equation [115], the pH values are linked to the NH_3/TMP ratios through the pK_a of the amination agent:

$$pK_a = pH + \log\frac{[NH_4^+]}{[NH_3]} \quad \textbf{(3.1)}$$

If pH << pK_a the term (log $[NH_4^+]/[NH_3]$) >> 0 and NH_3 undergoes protonation to form NH_4^+ in the solution, which impedes nucleophilic attack of TMP, favouring HTBA formation by competitive TMP hydrogenation. This response was observed by Ogo *et al.* [92] with an optimum pH = 5 for the homogeneous reductive amination of pyruvic acid using aqueous ammonium formate at 353 K. If pH >> pK_a, (log $[NH_4^+]/[NH_3]$) << 0 and there is sufficient NH_3 for reaction to proceed but a high pH does not favour iminium ion formation. Consequently, the optimum pH value should be close to the pK_a of the amination agent, as reported by Huber *et al.* [14] in the reductive amination of α-keto acids. In this study, the optimum pH = 8.4 is close to the pK_a of ammonium hydroxide (9.2). This optimum exceeds the pH_{pzc} and the catalyst surface is negatively charged, facilitating stabilisation of the cationic intermediate generated from the nucleophilic substitution (see **Figure 3.1**). Titration with acetic acid was used to adjust the pH to 8.4 where the resultant initial rate was lower than that observed where pH was not adjusted (**Figure 3.9**). This may be due to a poisoning of surface sites by the acetic acid treatment and possible consumption of ammonia to form ammonium acetate. A decrease in rate with increasing ammonia content was also a feature of reaction with pH adjustment. There are examples in the literature where addition of acetic acid enhances homogenous reductive amination by suppressing reduction of the carbonyl function [10, 13, 106]. Gomez *et al.* [9] have also noted that acetic acid addition prevents reaction between the amine product and intermediate imine and/or reactant (benzaldehyde) through the formation of the corresponding ammonium salt.

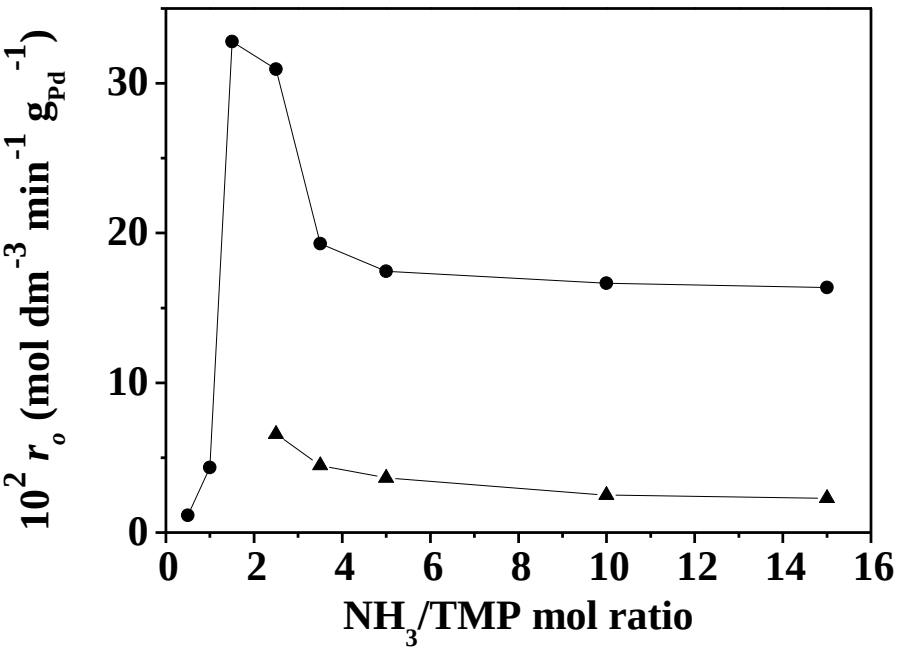

Figure 3.9: Initial rate of TBG production (r_o) as a function of NH_3/TMP mol ratio where pH varies with time (●) or is adjusted to 8.4 with acetic acid (▲): TMP/Pd = 600; *T* = 343 K; stirring speed = 1100 rpm.

Table 3.4: Variation of pH (*t* = 0-50 min) and reaction selectivity (to TBG and HTBA) as a function of NH_3/TMP mol ratio: TMP/Pd = 600; *T* = 343 K; stirring speed = 1100 rpm.

NH_3/TMP	Starting pH	Final pH	Selectivity to TBG (%)	Selectivity to HTBA (%)
0.5	1.3	2.3	0	100
1	1.8	2.9	6	94
1.5	8.4	8.2	100	0
2.5	9.3	9.1	100	0
5	10.6	10.3	100	0
10	11.1	10.6	100	0
15	11.8	11.2	100	0

3.2.8.2 Effect of Amination Reagent

Under the optimised reaction conditions, the scope of reductive amination was examined by reacting TMP with alternative amination reagents, *i.e.* ammonium acetate and ammonium nitrate. In both cases, TBG was generated but at a significantly lower rate relative to ammonium hydroxide (**Table 3.5**). According to **Figure 3.1**, low nucleophilicity with respect to the amination reagent will translate into a lower rate. Nucleophilicity is linked to basicity but is subject to the polarising influence of a protic solvent and steric effects [116, 117]. Solvated ions and bulky nucleophiles are less

nucleophilic than that resulting from basicity alone. Nevertheless, the observed increase in reaction rate (ammonium hydroxide > ammonium acetate > ammonium nitrate) does correlate with the basicity of the nucleophile; nitrate and acetate ions are poor nucleophiles [118, 119]. Abdel-Magid *et al.* [10] and Liu [120] have also reported lower rates using an amination agent with low nucleophilicity due to the involvement of electron-withdrawing substituents, *e.g.*, pK_a = 4.63 for aniline, 1.02 for 4-nitroaniline and -0.29 for 2-nitroaniline. The initial solution pH decreased in the order ammonium hydroxide > ammonium acetate > ammonium nitrate, indicting a shift in equilibrium with respect to the ammonium ion, which is unfavourable for nucleophilic attack.

Table 3.5: Initial rate of TBG production (r_o) obtained using different amination reagents (t = 0-50 min): TMP/Pd = 600; NH_3/TMP = 1 .5; T = 343 K; stirring speed = 1100 rpm.

Amination Reagent	r_o (mol min^{-1} dm^{-3} g_{Pd}^{-1})	Starting pH	Final pH
Ammonium Hydroxide	0.33	8.4	8.2
Ammonium Acetate	6.1×10^{-2}	3.6	4.5
Ammonium Nitrate	6.3×10^{-4}	1.9	2.1

3.3 Catalyst Reuse

The feasibility of catalyst reuse has also been considered in this study by employing the same catalyst sample in two reaction cycles. The catalytic activity in the subsequent run (given as a percentage) and critical catalyst characterisation values are presented in **Table 3.6**. Direct reuse of the catalyst resulted in a 50% loss of the initial activity. This can be attributed to: (i) occlusion of active sites by surface deposits (ii) modification of Pd electronic structure due to reactant(s) interaction [9, 121]; (iii) Pd particle growth; (iv) leaching of Pd into the solution [122]; (vi) alteration of surface chemistry. Washing the catalyst after use (see **Chapter 2**) did not recover the original level of activity and the degree of deactivation matched that recorded without the inclusion of a washing step. A significant degree of Pd sintering was observed with a larger mean Pd size (from H_2 chemisorption) after catalyst reuse. Palladium particle sintering during reaction (in H_2) has been observed at temperatures as low as 330 K [123]. Moreover, the appreciable decrease in BET surface area is indicative of pore blockage due to deposition. The pH_{pzc} value after the first run (= 4.7) was significantly

lower than that measured for the unused catalyst (= 6.8) and can be attributed to residual TMP on the carbon support. An increase in pH_{pzc} (= 8.0) was observed after catalyst washing. The results generated demonstrate that aqueous washing of the used catalysts is inadequate treatment for catalyst recycle. Removal of coke deposits is possible by temperature-programmed oxidation (TPO) but this can also result in gasification of the carbon support [124, 125]. Future work should focus on surface characterisation, notably the use of x-ray photoelectron spectroscopy (XPS) [126, 127], to establish possible alteration to the electronic state of the Pd particles (Pd^{2+}/Pd^{0} ratio) that can be linked to the observed deactivation.

Table 3.6: Initial activity decrease (%) and associated catalyst characteristics for reuse with and without treatment: TMP/Pd = 600; NH_3/TMP = 2.5; *T* = 343 K; stirring speed = 1100 rpm.

Catalyst use	Pd size (nm)	pH_{pzc}	BET Surface Area ($m^2\ g^{-1}$)	Starting pH	Final pH	Initial Rate Decrease (%)
1st	3	6.8	850	10.2	9.4	-
2nd without washing	11	4.7	8	9.7	9.4	50
2nd with washing	9	8.0	73	10.0	9.5	48

[a]from H_2 chemisorption

3.4 Conclusions

Taking the conversion of TMP to TBG promoted by (5% w/w) Pd/C (BET area = 850 $m^2\ g^{-1}$, Pd particle size range = 3-10 nm, Pd surface area = 188 $m^2\ g_{Pd}^{-1}$, pH_{pzc} = 6.8) as a model reaction, this study has set out to enhance sustainability in reductive amination processes. Pd/C promoted reductive amination using aqueous NH_3 at ambient pressure can be regarded as an energy efficient route to commercially important amines. Mass transfer limitations have been evaluated experimentally using the diagnostic criteria associated with varying hydrogen flow rate, stirring speed, catalyst concentration and temperature. These effects were at a minimum at a hydrogen flow > 20 $cm^3\ min^{-1}$, stirring speed = 1100 rpm, TMP/Pd ratio = 600-1750 and *T* = 293-343 K.

An equivalent reaction rate (to within 5%) was obtained for reactions operated in both batch slurry and autoclave reactors, where the rate was independent of pressure over the 1-20 bar range. By using ammonium hydroxide solution as the amination reagent, process optimisation focused on the impact of NH_3/TMP ratio, reaction temperature and solution pH on rate and selectivity to TBG. At $T \geq 333$ K, NH_3/TMP ≥ 1.5 and pH $\geq$ 8.4, the process was 100% selective, circumventing non-selective hydrogenation to 2-hydroxy-3,3-dimethylbutyric acid (HTBA). A maximum rate has been achieved where NH_3/TMP = 1.5 with an associated solution pH = 8.4 which exceeds the pH_{pzc} and the catalyst surface is negatively charged, stabilising the cationic intermediate. Catalyst reuse was accompanied by a 50% loss of activity that is linked to pore blockage/lower BET area and Pd sintering.

3.5 References

[3.1] G. R. Maxwell, Synthetic Nitrogen Products, Ethanolamines and Secondary Products, Kluwer Academic/Plenum Publishers, Springer, New York, pp. 317-324 (2005)

[3.2] G. T. Austin, Shreve's Chemical Process Industries, Industrial Gases, Mc Graw Hill, 5th ed., Singapore, pp. 111-112 (1984)

[3.3] A. Veawab, P. Tontiwachwuthikul; Ind. Eng. Chem. Res., 40, 4771-4777 (2001)

[3.4] L. Bu, T. Sawada, Y. Kuwahara, H. Shosenji, K. Yoshida; Dyes Pigm., 59, 43-52 (2003)

[3.5] F. Friedli, R. Keys, C. J. Toney, O. Portwood, D. Whittlinger, M. Doerr; J. Surfactac. Deterg., 4, 401-405 (2001)

[3.6] D. C. Constable, P. J. Dunn, J. D. Hayler; Green Chem., 9, 411-420 (2007)

[3.7] V. A. Tarasevich, N. G. Kozlov; Russ. Chem. Rev., 68, 55-72 (1999)

[3.8] F. A. Carey, Organic Chemistry, McGraw Hill, London, pp. 879-882 (2001)

[3.9] S. Gomez, J. A. Peters, T. Maschmeyer; Adv. Synth. Catal., 344, 1037-1057 (2002)

[3.10] A. F. Abdel-Magid, K. G. Carson, B. D. Harris, C. A. Maryanoff, R. D. Shah; J. Org. Chem., 61, 3849-3862 (1996)

[3.11] T. Ikenaga, K. Matsushita, J. Shinozawa, S. Yada, Y. Takagi; Tetrahedron, 61, 2105-2109 (2005)

[3.12] D. B. Bagal, R. A. Watile, M. V. Khedkar, K. P. Dhake, B. M. Bhanage; Catal. Sci. Technol., 2, 354-358 (2012)

[3.13] M. V. Klyuev, M. L. Khidekel; Transition Met. Chem., 5, 134-139 (1980)

[3.14] C. Huber, G. Wachtershauser; Tetrahedron Lett., 44, 1695-1697 (2003)

[3.15] S. Kobayashi, K. Hirano, M. Sugiura; Chem. Commun., 104-106 (2005)

[3.16] G. J. Kirmeyer, Optimizing Chloroamines Treatment, Implementation of Chloroamination, Awwa Research Foundation, 2nd ed., Denver, pp. 177-185 (2004)

[3.17] A. Kohl, R. Nielsen, Gas Purification, Control of Nitrogen Oxides, Gulf Publishing Company, 5th ed., Houston, pp. 923-925 (1997)

[3.18] L. F. Drbal, P. G. Boston, K. L. Westra, Power Plant Engineering, Power Plant Atmospheric Emissions Control, Black & Veatch, 1st ed., Overland Park, KS, pp. 432-433 (1996)

[3.19] F. Cavani, G. Centi, S. Perathoner, F. Trifirò, Sustainable Industrial Chemistry, Sustainable Chemistry and Inherently Safer Design, Wiley-VCH, 1st ed., Weinheim, pp. 51-55 (2009)

[3.20] I. V. Micovic, M. D. Ivanovic, G. M. Roglic, V. D. Kiricojevic, J. B. Popovic; J. Chem. Soc., Perkin Trans., 1, 265-269 (1996)

[3.21] N. Azizi, E. Akbari, A. K. Amiri, M. R. Saidi; Tetrahedron Lett., 49, 6682-6684 (2008)

[3.22] A. Robichaud, A. N. Ajjou; Tetrahedron Lett., 47, 3633-3636 (2006)

[3.23] B. Y. Nian, G. Xu, J. P. Wu, L. R. Yang; Chem. Res. Chin. Univ., 24, 120-122 (2008)

[3.24] H. Alinezhad, M. Tajbakhsh, F. Salehian, K. Fazli; Tetrahedron Lett., 50, 659-661 (2008)

[3.25] R. J. Mattson, K. M. Pham, D. J. Leuck, K. A. Cowen; J. Org. Chem., 55, 2552-2554 (1990)

[3.26] R. P. Tripathi, S. S. Verma, J. Pandey, V. K. Tiwari; Curr. Org. Chem., 12, 1093-1115 (2008)

[3.27] F. Nador, Y. Moglie, A. Ciolino, A. Pierini, V. Dorn, M. Yus, F. Alonso, G. Radivoy; Tetrahedron Lett., 53, 3156-3160 (2012)

[3.28] M. R. Saidi, R. S. Brown, A. Ziyaei-Halimjani; J. Iran. Chem. Soc., 4, 194-198 (2007)

[3.29] A. Heydari, S. Khaksar, M. Esfandyari, M. Tajbakhsh; Tetrahedron, 63, 3363-3366 (2007)

[3.30] P. S. Reddy, S. Kanjilal, S. Sunitha, R. B. N. Prasad; Tetrahedron Lett., 48, 8807-8810 (2007)

[3.31] A. F. Abdel-Magid, S. J. Mehrman; Org. Proc. Res. Dev., 10, 971-1031 (2006)

[3.32] T. Mizuta, S. Sakaguchi, Y. Ishii; J. Org. Chem., 70, 2195-2199 (2005)

[3.33] B.-C. Chen, J. E. Sundeen, P. Guo, M. S. Bednarz, R. Zhao; Tetrahedron Lett., 42, 1245-1246 (2001)

[3.34] O.-Y. Lee, K.-L. Law, C.-Y. Ho, D. Yang; J. Org. Chem., 73, 8829-8837 (2008)

[3.35] T. Gross, A. M. Seayad, M. Ahmad, M. Beller; Org. Lett., 4, 2055-2058 (2002)

[3.36] R.-Y. Lai, K. Surekha, A. Hayashi, F. Ozawa, Liu, Y-H., S.-M. Peng, S.-T. Liu; Organomet., 26, 1062-1068 (2007)

[3.37] R. Apodaca, W. Xiao; Org. Lett., 3, 1745-1748 (2001)

[3.38] L. Rubio-Perez, F. J. Perez-Flores, P. Sharma, L. Velasco, A. Cabrera; Org. Lett., 11, 265-268 (2009)

[3.39] T. Marcelli, P. Hammar, F. Himo; Chem. Eur. J., 14, 8562-8571 (2008)

[3.40] S. Koritala; JAOCS, 59, 309-312 (1982)

[3.41] F. Zhao, M. Shirai, Y. Ikushima, M. Arai; J. Mol. Catal. A: Chem., 180, 211-219 (2002)

[3.42] R. Aldea, H. Alper; J. Organomet. Chem., 593, 454-457 (2000)

[3.43] E. Auer, A. Freund, J. Pietsch, T. Tacke; Appl. Catal. A: Gen., 173, 259-271 (1998)

[3.44] S. Gomez, J. A. Peters, J. C. van der Waal, W. Z. Zhou, T. Maschmeyer; Catal. Lett., 84, 1-5 (2002)

[3.45] S. Gomez, J. A. Peters, J. C. van der Waal, T. Maschmeyer; Appl. Catal. A: Gen., 254, 77-84 (2003)

[3.46] J. Bodis, L. Lefferts, T. E. Muller, R. Pestman, J. A. Lercher; Catal. Lett., 104, 23-28 (2005)

[3.47] L. Xing, C. Cheng, R. Zhu, B. Zhang, X. Wang, Y. Hu; Tetrahedron, 64, 11783-11788 (2008)

[3.48] T. Harada, S. Ikeda, N. Okamoto, Y. H. Ng, S. Higashida, T. Torimoto, M. Matsumura; Chem. Lett., 37, 948-949 (2008)

[3.49] K. V. R. Chary, K. K. Seela, D. Naresh, P. Ramakanth; Catal. Commun., 9, 75-81 (2008)

[3.50] P. Dolezal, O. Machalicky, M. Pavelek, P. Kubec, K. Hradkova, R. Hrdina, R. Sulakova; Appl. Catal. A: Gen., 286, 202-210 (2005)

[3.51] A. S. C. Chan, C. C. Chen, Y. C. Lin; Appl. Catal. A: Gen., 119, L1-L5 (1994)

[3.52] S. Nishimura, Handbook of Heterogeneous Catalytic Hydrogenation for Organic Synthesis, Wiley-Interscience, New York, pp. 231-232 (2001)

[3.53] I. Fotheringham, I. Archer, R. Carr, R. Speight, N. J. Turner; Biochem. Soc. Trans., 34, 287-290 (2006)

[3.54] A. S. Bommarius, M. Schwarm, K. Stingl, M. Kottenhahn, K. Huthmacher, K. Drauz; Tetrahedron: Asymm., 6, 2851-2888 (1995)

[3.55] S. Gobolos, E. Tfirst, J. L. Margitfalvi, K. S. Hayes; J. Mol. Catal. A: Chem., 146, 129-138 (1999)

[3.56] A. P. Bonds, H. Greenfield, Catalysis of Organic Reactions, Marcel Dekker, New York, pp. 65-78 (1992)

[3.57] H. Greenfield, Catalysis in Organic Reactions, Marcel Dekker, New York, pp. 265-277 (1994)

[3.58] J. J. Birtill, M. Chamberlain, J. Hall, R. Wilson, I. Costello, Catalysis of Organic Reactions, Marcel Dekker, New York, pp. 255-272 (1998)

[3.59] A. W. Heinen, J. A. Peters, H. Van Bekkum; Appl. Catal. A: Gen., 194-195, 193-202 (2000)

[3.60] S. Gomez, J. A. Peters, J. C. van der Waal, P. J. van der Brink, T. Maschmeyer; Appl. Catal. A: Gen., 261, 119-125 (2004)

[3.61] K. N. Nab; J. Phys. Chem. B, 105, 5945-5949 (2001)

[3.62] V. A. Lomovskoi, B. F. Lyakhov, N. Y. Lomovskaya, A. Y. Tsivadze; Dokl. Phys. Chem., 411, 301-304 (2006)

[3.63] N. Krishnankutty, M. A. Vannice; J. Catal., 155, 312-326 (1995)

[3.64] S. Biniak, R. Diduszko, W. Gac, M. Pakula; React. Kinet. Mech. Catal. , 101, 331-342 (2010)

[3.65] M. A. Vannice, Kinetics of Catalytic Reactions, Metal Surface Area, Crystallite Size and Dispersion, Springer Science, New York, pp. 19-21 (2005)

[3.66] T. Hyde; Plat. Met. Rev., 52, 129-130 (2008)

[3.67] A. Rezvanifar, M. Zandrahimi; Iran. J. Materials Sci. Eng., 7, 32-38 (2010)

[3.68] J. H. Bitter, K. Seshan, J. A. Lercher; Top. Catal., 10, 295-305 (2000)

[3.69] A. J. Plomp, H. Vuori, A. O. I. Krause, K. P. de Jong, J. H. Bitter; Appl. Catal. A: Gen., 351, 9-15 (2008)

[3.70] D. B. Williams, C. B. Carter, Transmission Electron Microscopy, Limitations of TEM, Plenum, New York, pp. 9-11 (1996)

[3.71] N. Chen, R. M. Rioux, F. H. Ribeiro; J. Catal., 211, 192-197 (2002)

[3.72] W. Hui, W. J. Long; Sci. China Ser. B-Chem., 50, 692-699 (2007)

[3.73] O. Winjobi, Z. Zhang, C. Liang, W. Li; Electrochim. Acta, 55, 4217-4221 (2010)

[3.74] C. Moreno-Castilla, J. Rivera-Utrilla, M. V. Lopez-Ramon, F. Carrasco-Marin; Carbon, 33, 845-851 (1995)

[3.75] M. A. Ferro-Garcia, J. Rivera-Utrilla, I. Bautista-Toledo, C. Moreno-Castilla; Langmuir, 14, 1880-1886 (1998)

[3.76] A. Kumar, B. Prasad, I. M. Mishra; J. Hazard. Mater., 152, 589-600 (2008)

[3.77] M. Bjelopavlic, G. Newcombe, R. Hayes; J. Colloid Interf. Sci., 210, 271-280 (1999)

[3.78] S. Wang, G. Q. Lu, Activated Carbon Compendium, Effects of Acidic Treatments on the Pore and Surface Properties of Ni Catalyst Supported on Activated Carbon, Elsevier, Oxford, pp. 75-78 (2001)

[3.79] A. W. Heinen, J. A. Peters, H. van Bekkum; Eur. J. Org. Chem., 2000, 2501-2506 (2000)

[3.80] T. Nagano, S. Kobayashi; J. Am. Chem. Soc., 131, 4200-4201 (2009)

[3.81] A. L. Ahmad, P. C. Oh, S. R. Abd Shukor; Biotechnol. Adv., 27, 286-296 (2009)

[3.82] C. K. Savile; Science, 329, 305-309 (2010)

[3.83] H. Gröger, O. May, H. Werner, A. Menzel, J. Altenbuchner; Org. Proc. Res. Dev., 10, 666-669 (2006)

[3.84] A. Galkin, L. Kulakova, T. Yoshimura, K. Soda, N. Esaki; Appl. Environ. Microbiol., 63, 4651-4656 (1997)

[3.85] B. Freedman; J. Am. Oil Chem. Soc., 47, 311-312 (1970)

[3.86] S. Werkmeister, K. Junge, M. Beller; Green Chem., 14, 2371-2374 (2012)

[3.87] D. Imao, S. Fujihara, T. Yamamoto, T. Ohta, Y. Ito; Tetrahedron, 61, 6988-6992 (2005)

[3.88] S. R. Kirumakki, M. Papadaki, K. V. R. Chary, N. Nagaraju; J. Mol. Catal. A: Chem., 321, 15-21 (2010)

[3.89] P. T. Anastas, J. C. Warner, Green Chemistry: Theory and Practice, Oxford University Press, New York, pp. 19-28 (1998)

[3.90] R. Lai, C. Lee, S. Liu; Tetrahedron, 64, 1213-1217 (2008)

[3.91] R. Kadyrov, T. H. Riermeier; Angew. Chem., 42, 5472-5474 (2003)

[3.92] S. Ogo, K. Uehara, T. Abura, S. Fukuzumi; J. Am. Chem. Soc., 126, 3020-3021 (2004)

[3.93] Inherently Safer Chemical Processes: A Life Cycle Approach, Example of an Inherently Safer Study of a Steam Production Facility, John Wiley, 2nd ed., New Jersey, pp. 272-277 (2009)

[3.94] M. A. Keane; Zeolites, 13, 22-33 (1993)

[3.95] L. Forni; Catal. Today, 52, 147-152 (1999)

[3.96] M. Spiro, Comprehensive Chemical Kinetics, Reactions at the Liquid-Solid Interface, Elsevier, Amsterdam, pp. 69-92 (1989)

[3.97] U. K. Singh, M. A. Vannice; Appl. Catal. A: Gen, 213, 1-24 (2001)

[3.98] G. Yuan, M. A. Keane; Chem. Eng. Sci., 58, 257-267 (2003)

[3.99] S. Gomez-Quero, F. Cardenas-Lizana, M. A. Keane; AIChE J., 56, 756-767 (2010)

[3.100] J. M. Thomas, W. J. Thomas, Principles and Practice of Heterogenoeus Catalysis, Catalytic Process Engineering, VCH, Weinheim, pp. 455-458 (1997)

[3.101] Z. Junmei, D. Zhenya, X. Chunjian, Z. Ming; Chem. Eng. J., 136, 276-281 (2008)

[3.102] G. Siedlaczek, M. Schwickardi, U. Kolb, B. Bogdanovic, D. G. Blackmond; Catal. Lett, 55, 67-72 (1998)

[3.103] Y. Shindler, Y. Matatov-Meytal, M. Sheintuch; Ind. Eng. Chem. Res., 40, 3301-3308 (2001)

[3.104] J. B. Butt, Reaction Kinetics and Reactor Design, Marcel Dekker, 2nd ed., New York, pp. 592-607 (2000)

[3.105] J. Pasek, P. Kondelik, P. Richter; Ind. Eng. Chem. Prod. Res. Dev., 11, 333-37 (1977)

[3.106] T. C. Nugent, M. El-Shazly, V. N. Wakchaure; J. Org. Chem., 73, 1297-1305 (2008)

[3.107] R. M. Heck, R. J. Farrauto, Catalytic Air Pollution Control: Commercial Tecnnology, Catalyst Fundamentals, John Wiley, New Jersey, pp. 12-20 (2009)

[3.108] D. Horlait, N. Clavier, S. Szenknect, N. Dacheux, V. Dubois; Inorg. Chem., 51, 3868-3878 (2012)

[3.109] O. S. Pokrovsky, J. Schott; Geochim. Cosmochim. Acta, 68, 31-45 (2004)

[3.110] H. Laue, A. M. Cook; Arch. Microbiol., 174, 162-167 (2000)

[3.111] T. J. Connolly, A. Constantinescu, T. S. Lane, M. Matchett, P. McGarry, M. Paperna; Org. Proc. Res. Dev., 9, 837-842 (2005)

[3.112] Y. N. Litvishkov, Balaeva, D.R., Tairov, A.Z., Guseinova, A.M.; Theor. Found. Chem. Eng, 42, 305-313 (2008)

[3.113] M. Sun, X. Du, X. Kong, L. Lu, Y. Li, L. Chen; Catal. Commun., 20, 58-62 (2012)

[3.114] J. J. Birtill, Catalysis of Organic Reactions, Marcel Dekker, New York, pp. 249-262 (1995)

[3.115] D. J. de Ridder, M. McConville, A. R. D. Verliefde, L. T. J. van der Aa; Drink. Water Eng. Sci., 2, 57-62 (2009)

[3.116] E. V. Anslyn, D. A. Dougherty, Modern Physical Organic Chemistry, Experiments Related to Thermodynamics and Kinetics, Edwards Brothers, South Orange, NJ, pp. 458-466 (2006)

[3.117] H. K. Hall, R. B. Bates; Tetrahedron Lett., 53, 1830-1832 (2012)

[3.118] S. R. Hartshorn, Aliphatic Nucleophilic Substitution, The Mechanistic Borderline, Cambridge University Press, London, pp. 8-10 (1973)

[3.119] M. B. Smith, Organic Synthesis, Substitution Reactions, Elsevier, Amsterdam, pp. 117-128 (2010)

[3.120] Z. G. Liu, N. Li, L. Yang, Z. L. Liu, W. Yu; Chin. Chem. Lett., 18, 458-460 (2007)

[3.121] C. Xu, D. W. Goodman; J. Phys. Chem., 102, 4392-4400 (1998)

[3.122] H.-U. Blaser, A. Indolese, A. Schnyder, H. Steiner, M. Studer; J. Mol. Catal. A: Chem., 173, 3-18 (2001)

[3.123] P. Albers, J. Pietsch, S. F. Parker; J. Mol. Catal. A: Chem., 173, 275-286 (2001)

[3.124] S. Ordoñez, F. V. Diez, H. Sastre; Appl. Catal. B: Environ., 31, 113-122 (2001)

[3.125] S. Ordoñez, H. Sastre, F. V. Diez; Thermochim. Acta, 379, 25-34 (2001)

[3.126] R. F. Bueres, E. Asedegbega-Nieto, E. Diaz, S. Ordoñez, F. V. Diez; Catal. Commun., 9, 2080-2084 (2008)

[3.127] D. Teschner, Z. Révay, J. Borsodi, M. Hävecker, A. Knop-Gericke, R. Schlögl, D. Milroy, S. D. Jackson, D. Torres, P. Sautet; Angew. Chem., 120, 9414-9418 (2008)

Chapter 4

Role of the Catalyst (Metal and Support) in the Conversion of Trimethylpyruvic Acid (TMP) to Tertbutylglycine (TBG)

In this chapter, a set of activated carbon and alumina supported metal (Rh, Pd and Pt) catalysts have been employed to promote the reductive amination of trimethylpyruvic acid (TMP) to tert-butylglycine (TBG) in a triphasic batch slurry reactor. The supported metal catalysts have been characterised in terms of BET surface area, temperature programmed reduction, H_2 uptake and pH point of zero charge (pH_{pzc}). The role of the pH of the reaction media, identified as a critical parameter in Chapter 3, is also considered here. Furthermore, the effect of the dielectric constant of the solvent (water and water + alcohol mixtures) on the catalytic response is addressed.

4.1 Introduction

Precious metals, such as Pd, Pt, Rh and Ru, supported on carbon are frequently used as catalysts in reductive amination reactions [1-4]. At present, Pd/C has been the most widely studied catalyst because of its high selectivity to amine products [5, 6]. The rate of reaction has been found to be mainly governed by the intrinsic nature of the metal component although the support can also contribute to overall performance [3, 4, 7, 8]. Metal dispersion [9], loading [10] and surface area [8] are critical in determining catalytic activity. Selectivity has been found to depend primarily on the nature of the metal and the degree of dispersion [2, 4]. Regarding the support, the surface chemistry can impact on reactant adsorption and contribute to the catalytic step [9]. Activated carbon is the most common used support in reductive amination. The high associated total surface area and associated porosity can accommodate high metal loadings and ensure a well dispersed metal phase [2, 11]. Support porosity also influences diffusion of reactant(s) and product(s) to and from the catalytic active sites [12]. Surface acid-base character is influenced by basal planes (basic sites) and polar oxygen containing groups (acid sites) [13-15]. The oxygenated surface groups can be varied, allowing some tuning of acidity and hydrophilicity [7, 16].

Taking an overview of the relevant studies that have compared the catalytic activity of activated carbon supported precious metals, it is worth noting the work of Peters *et al.* [2, 3, 7, 17] and Heinen *et al.* [18] who examined the action of Pd, Pt and

Ru in the reductive amination of benzaldehyde using gaseous ammonia. They proposed structure sensitivity with rate dependence on metal particle size and support acidity. The authors established increasing rate with decreasing metal particle size, where smaller Pd particles (20-2 nm) [2] exhibited enhanced activity [7, 18]. Critical surface acidity effects have been attributed to contributions due to the carboxylic function [14, 19]. Bodis *et al*. [4] studied the reaction of butyraldehyde with ammonia over graphite supported Pd, Pt, Rh and Ru and carbon supported Rh and observed differences in performance associated with the range of metals but no obvious correlation between rate and metal particle size. Reductive amination rates are influenced by the pH of the reaction medium. Huber *et al.* [20] reported an optimum pH at the pK_a of the amination agent in the conversion of α-keto-carboxylic acids. This observation is consistent with the findings presented in **Chapter 3**. However, in the reductive amination of aldehydes and ketones, the effect of the pH on activity [7, 8, 18, 21, 22] and selectivity [7, 8, 22] remains unclear. While some studies report that the condensation step generating the imine is promoted in acidic media [7, 8, 18], other work [21, 22] suggests that acidic conditions results in protonation of the aminating reactant. In this Chapter the role of pH, adjusted by addition of acid and base, is examined.

A key consideration as part of the sustainability drive with respect to reductive amination is the use of greener solvents. The solvent serves three main functions in the reaction: (i) to dissolve reactants/products; (ii) to facilitate reactant transport to the reactive catalyst surface; (iii) to assist heat transfer due to reaction enthalpy [23, 24]. Water as a solvent is preferable to toxic organic solvents in terms of possible environmental impact [21, 25]. However, water is not suitable for reductive amination using hydrides as reducing agents as the generation of imines involves dehydration and is favoured by anhydrous conditions [26-28]. Solvent effects have been studied by correlating reaction rates with respect to solvation properties, notably in terms of dielectric constant [29, 30]. Reductive amination is typically conducted in polar media where water [21], methanol [2, 18, 31], ethanol [4, 7, 8] and aniline [32] have been employed. Nevertheless, the precise role of the solvent remains unclear and requires fundamental research to establish an optimum reaction medium.

The results in **Chapter 3** have served to indicate that reaction over Pd/C is a viable alternative to enzymatic amination routes to tert-butylglycine (TBG). Moreover, the use of H_2 at atmospheric pressure represents a critical improvement over high pressure (up to 50 bar) systems reported in the literature. In this Chapter the same model reaction was used to compare the performance of a range of supported metal

catalysts where catalytic activity is linked to critical characterisation measurements. Activated carbon has been chosen as the common carrier for Pd, Rh and Pt where the role of support was further probed by examining the action of Pd on alumina. Moreover, the effect of varying solvent (water, 1-propanol and 1-butanol and mixtures) has also been considered.

4.2 Results and Discussion

4.2.1 Catalyst Characterization

The catalysts were subjected to three main characterisation measurements: BET surface area; H_2 chemisorption; pH point of zero charge. The commercial (Degussa and Sigma-Aldrich) catalysts considered contain 1 or 5% w/w Pd, Pt or Rh (BET surface area in the range 497-850 m^2/g) and 1% w/w Pd/Al_2O_3 (BET surface area = 152 m^2/g), see **Table 4.1**. The BET area, obtained from the N_2 adsorption isotherm, comprises the sum of external and internal surface (pore wall) area [33]. Materials with higher BET surface area provide a greater surface on which to disperse the metal component, which has been shown to result in increased reductive amination activities [2, 7]. Generally in heterogeneous catalytic reactions over comparable catalysts the rate of reaction is directly proportional to the BET surface area if the whole surface area is accessible to the reactants but less than proportional if molecular transport to the active surface is impeded due to pore structure [34-36]. Activated carbon as a support is characterised by a large surface area with values falling within the range of 500-1200 m^2/g [2, 4, 18, 37]. The carbon source and treatment conditions can impact on area and surface chemistry [38-40]. Alumina supported Pd presents a markedly lower area, which is within the range of values reported in the literature for γ-Al_2O_3 supported metals (150-250 m^2/g) [41-43].

A measurement of the temperature programmed reduction (TPR) profile can inform catalyst activation procedure and gives some indication of the degree of oxidation of the metal component [44, 45]. Hydrogen consumption during treatment in flowing 5% v/v H_2/N_2 is illustrated in **Figure 4.1**. The TPR profiles associated with Pd on either carbon or alumina are characterised by a single negative peak at 363 ± 4 K, corresponding to H_2 release. This can be attributed to the decomposition of Pd hydride formed by the absorption of H_2 in the Pd crystal lattice, which is known to occur at ambient temperature [46]. Pd hydride decomposition has been reported over the range 323-373 K [47, 48]. The absence of any detectable H_2 consumption prior to the

observed hydrogen release suggests the presence of zero valent Pd prior to the temperature ramp. Hydrogen interaction with Pd involves absorption phenomena in the bulk metal (H_{abs}) and adsorption as a surface phenomenon (H_{ads}) [49]. The ratio of the number of moles of hydrogen absorbed to generate the hydride per total mol of Pd (H_{abs}:Pd) for all the Pd catalysts are given in **Table 4.2**. The hydride composition is sensitive to Pd particle size where Boudart *et al.* [50] established that a poorly dispersed Pd phase (larger Pd sizes) can accommodate more hydrogen (per mole Pd) due to an increase in the void space available for H_2 diffusion in the metal cluster. As a direct corollary, H_{abs}/Pd value approaches zero at high Pd dispersion. Taking the catalysts in this work, the recorded H_{abs}/Pd values (0.08 - 0.19) are significantly lower than that reported for bulk Pd (H_{abs}/Pd = 0.76), suggesting the presence of a dispersed Pd phase at the nano-scale. The values are consistent with those reported in the literature for related supported Pd systems [51, 52]. TPR of Pt/C (profile III in **Figure 4.1**) generated an ill-defined positive peak (H_2 consumption) during the temperature ramp (T_{max} = 350 K) with a second broad positive peak in the isothermal hold. According to the literature, PtO_2 is reduced to Pt^0 over the range of 323-550 K where difference in reduction temperature can reflect variation in precursor/support interaction and/or possible contribution due to desorption of spillover hydrogen from the support [53-57]. The TPR profile for Rh/C (IV) showed a single positive peak (profile IV in **Figure 4.1**) with associated T_{max} = 377 K, which can be ascribed to the reduction of Rh_2O_3 to Rh^0 [58-60]. There was no observed hydrogen release due to decomposition of Rh hydride, which is known to be unstable and may not be formed under the conditions of this study [61].

Ambient temperature H_2 chemisorption post-TPR is recorded in **Table 4.1** from which an average metal size and specific surface area was determined. These measurements derive from an assumption of: (i) spherical particle morphology; (ii) H:metal dissociative adsorption stoichiometry (= 1) [62, 63]. Metal particle sizes obtained by H_2 chemisorption using these assumptions have been validated in literature against other techniques, notably XRD and TEM [52, 64-69]. Hydrogen interaction is sensitive to metal particle size where Chou *et al.* [70] demonstrated that the heat of adsorption varied with the degree of Pd dispersion on SiO_2, Al_2O_3 and TiO_2, with significantly greater heats measured for Pd < 3 nm, a response that has been observed elsewhere [71]. Metal dispersion obtained from chemisorption measurements is given in **Table 4.2**. The metal particle sizes (**Table 4.1**) present a narrow range (1.6 - 3.3 nm)

and are within the interval (1-20 nm) reported in the literature as having an effect on reductive amination activity [2, 9, 18, 28].

Table 4.1: BET surface area, hydrogen chemisorption capacity, specific metal surface area, metal particle diameter and pH point of zero charge (pH_{pzc}).

Catalyst	BET surface area ($m^2\ g^{-1}$)	Hydrogen uptake ($\mu mol\ g^{-1}$)	Specific Metal Surface Area ($m^2\ g_{metal}^{-1}$)	Metal Particle Diameter (nm)	pH_{pzc}
Pd/C 5% w/w (Degussa)	850	95	180	2.8	6.8
Pd/C 5% w/w (Sigma-Aldrich)	810	79	150	3.3	8.3
Pt/C 5% w/w (Sigma-Aldrich)	505	68	131	2.1	5.1
Rh/C 5% w/w (Sigma-Aldrich)	538	142	257	1.9	9.0
Pd/C 1% w/w (Sigma-Aldrich)	497	32	308	1.6	8.2
Pd/Al_2O_3 1% w/w (Sigma-Aldrich)	152	24	231	2.2	8.0

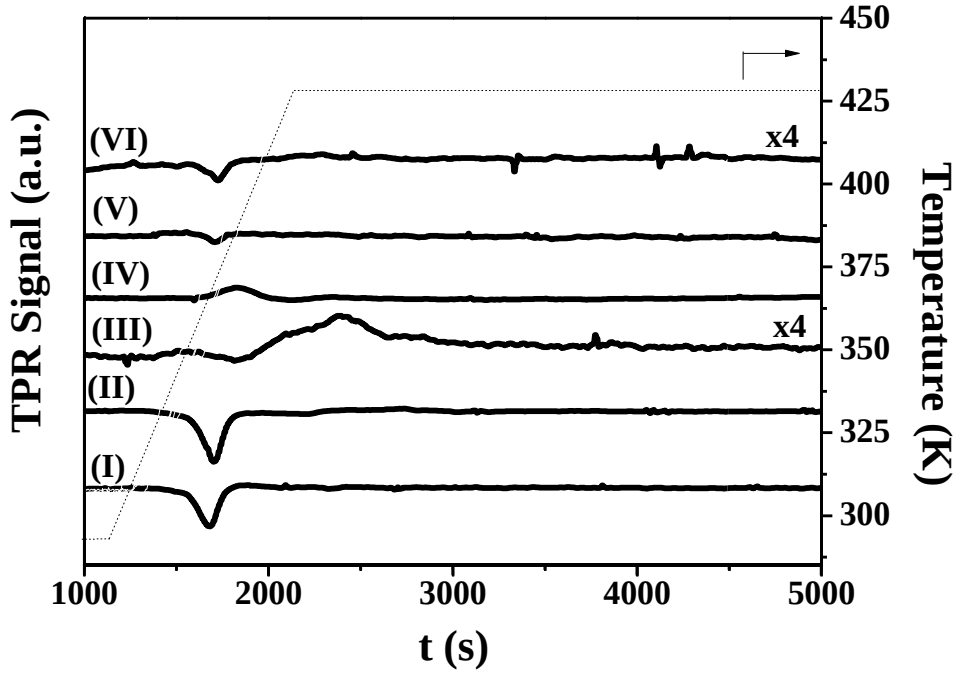

Figure 4.1: TPR profiles generated for 5% w/w Pd/C (Degussa, I), 5% w/w Pd/C (Sigma-Aldrich, II), 5% w/w Pt/C (Sigma-Aldrich, III), 5% w/w Rh/C (Sigma-Aldrich, IV), 1% w/w Pd/C (Sigma-Aldrich, V) and 1% w/w Pd/Al_2O_3 (Sigma-Aldrich, VI).

Table 4.2: Palladium dispersion, H_{abs}:Pd mol ratio (from TPR analysis), hydride decomposition temperature and H_{ads}:Pd mol ratio from chemisorption measurements.

Catalyst	Pd Dispersion (%)	H_{abs}:Pd ($\mu mol_H\ \mu mol_{Pd}^{-1}$)	Pd Hydride Decomposition Temperature (K)	H_{ads}:Pd ($\mu mol_H\ \mu mol_{Pd}^{-1}$)
Pd/C 5% w/w (Degussa)	40	0.12	365	0.20
Pd/C 5% w/w (Sigma-Aldrich)	34	0.19	367	0.17
Pd/C 1% w/w (Sigma-Aldrich)	69	0.08	364	0.35
Pd/Al_2O_3 1% w/w (Sigma-Aldrich)	52	0.09	359	0.26

Values of the pH point of zero charge (pH_{pzc}) associated with the catalysts are also shown in **Table 4.1**. Typical acid-base titration curves for a representative catalyst (Rh/C 5% w/w) are presented in **Figure 4.2**, where the catalyst exhibited the highest pH_{pzc} (= 9.0), indicating a weakly basic surface. The pH_{pzc} values obtained for Pd/Al_2O_3 (8.0) and the other carbon based catalysts (5.1-9.0) fit within the range reported for commercial γ-Al_2O_3 (7.0-10.0) [37, 72, 73] and activated carbon (3-10.5) [40, 74-76]. Variability of pH_{pzc} for activated carbon reflects the carbon source and nature of the pretreatment/activation [40, 77, 78]. The chemistry of the carbon surface is influenced by the presence of hetero atoms (H, O, N, S, P, etc) [16, 19, 79] and the pH_{pzc} provides a measure of overall basicity/acidity [80]. The observed acidity for 5% w/w Pt/C (pH_{pzc} = 5.1) can be ascribed to surface carboxylic (pK_a = 2-5 [81]) and/or quinonic (pK_a = 3-5 [82]) groups. Weak basicity (in the case of 5% w/w Pd/C (Sigma-Aldrich), 5% w/w Rh/C and 1% w/w Pd/C, pH_{pzc} = 8.2-9) can result from phenolic (pK_a = 7-10 [81]) groups and may reflect different (O and N) groups in tandem with π-electron density at the carbon basal planes [83]. These suggestions are only illustrative as the surface of carbon supports is very complex with the possible coexistence of a wide range of groups. Weak basicity of Pd/Al_2O_3 (pH_{pzc} = 8.0) can be attributed to the presence of Al-OH groups [84, 85]. The systems considered in this study show significant variability in surface chemistry. This is critical as the surface charge is dependent on the pH of the

reaction solution. Where the pH is above pH_{pzc}, the overall surface is negatively charged and adsorption of cationic species is favoured due to electrostatic attraction. Alternatively, when pH is below pH_{pzc} the overall surface bears a positive charge, facilitating interaction with anionic species.

The techniques considered in this study (BET area, TPR, H_2 chemisorption and pH of zero charge) to characterise the catalysts provide a measure of the critical properties of the catalysts that can contribute to overall reactivity. The pH point of zero charge is as a useful indicator of the surface groups that can contribute to the adsorption processes and to stabilise possible intermediates, impacting on activity and selectivity. BET analysis provides a measure of the available surface area for reaction, TPR data identify Pd hydride composition that can contribute to reaction while H_2 chemisorption provides an additional measure of the available surface hydrogen, also serving as a measure of metal particle size/dispersion.

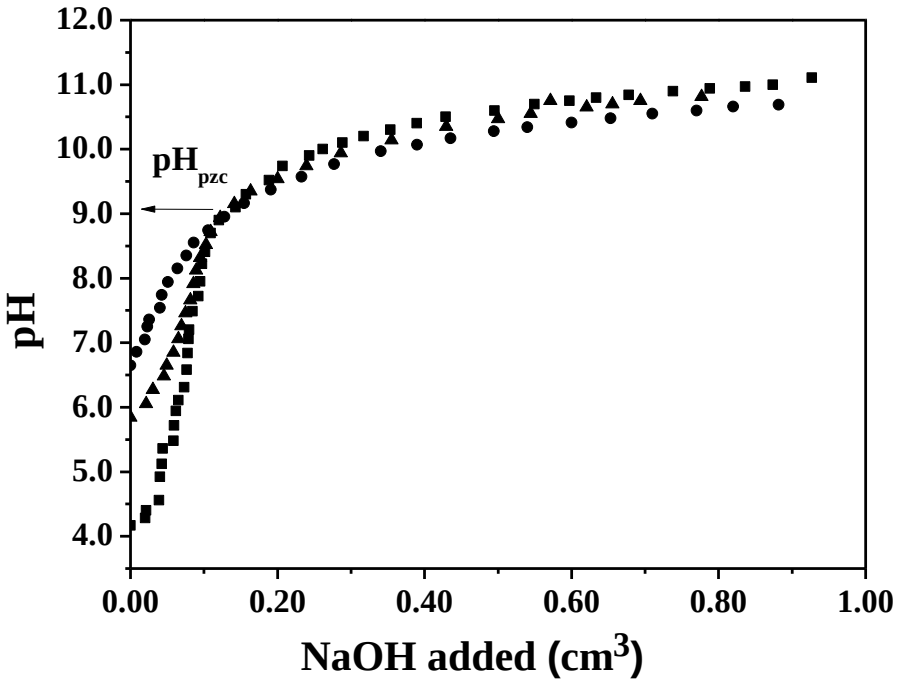

Figure 4.2: pH profiles associated with the pH of point of zero charge (pH_{pzc}) determination for 0.025 g (■), 0.075 g (▲) and 1.125 g (●) of 5% w/w Rh/C.

4.2.2 Catalytic Activity and Selectivity

Catalyst performance was assessed from a monitoring of the composition of the reaction mixture by HPLC and associated pH changes in the reaction medium. Conversion of TMP over all the supported catalysts generated TBG as the only product with an associated decrease in pH, identified in **Table 4.3**. The results from **Chapter 3**

establish that mass transfer limitations were overcome at the conditions applied (NH_3/TMP = 2.5, TMP/catalyst = 600, T = 343 K, P = 1 bar). The physico-chemical catalyst characteristics can be used to account for the reaction rate where reductive amination proceeds via the network of equilibrium and hydrogenation steps shown in **Chapter 3**. Taking an overview of the literature, the equilibrium for the generation of the imine can either apply to the catalyst surface, surface/liquid interface or bulk liquid phase, whereas imine hydrogenation is known to proceed on the catalyst surface [7, 86]. This involves reaction between surface hydrogen atoms generated via dissociative H_2 adsorption and the activated imine [7, 87]. Meaningful comparison of activity exhibited by catalysts with varying metal particles size requires a measure of specific initial rates (per m_{metal}^2), which are given in **Table 4.3**. Representative temporal variation of TBG in the reaction mixture is shown in **Figure 4.4**. Under identical reaction conditions, the following specific activity sequence was obtained: 5% w/w Rh/C > 5% w/w Pd/C (Sigma-Aldrich) > 5% w/w Pd/C (Degussa) ≈ 1% w/w Pd/C > 5% w/w Pt/C > 1% w/w Pd/Al_2O_3. As the carbon support, originating from different sources and possibly subjected to different pretreatment, exhibited different surface properties, this can complicate an explicit comparison of performance. The catalytic response suggests that activity is strongly influenced by the nature of the metal with Rh delivering the highest specific rate. The metal phase has been identified as a critical factor that determines reductive amination and attributed to electronic and geometric factors [3, 4, 8]. The d-character of the supported metal influences H_2 interactions where adsorption on Pd, Pt and Rh involves electron donation to the vacant metal d-orbitals [88]. For the metals used, the d-character increases in the order Pt (44%) < Pd (46%) < Rh (50%) [89]. In terms of geometric factors, metal atomic radius follows the order: Pt (1.38 Å) < Pd (1.37 Å) < Rh (1.34 Å) [90]. There is evidence in the literature that hydrogenation activity increases with d-character and decreases with decreasing metal radius. Beeck *et al.* [91] proposed the following activity sequence for the hydrogenation of ethylene to ethane: Pt < Pd < Rh. This was linked to increased efficiency for metals with greater d-character and lowest radius with associated lower heat of adsorption of H_2 (Pt = 113 > Pd = 109 > Rh = 107 kJ mol^{-1}) and greater reactivity. It should be noted that Rh has exhibited elevated activity in homogeneous catalytic applications [92-94]. A search through the literature did not reveal any studies that have compared use of carbon supported Rh with equivalent Pd and Pt catalysts under the same operating conditions. The closest study to this work was reported by Bodis *et al.* [4] who studied the reductive amination of butyraldehyde (with ammonia) over Pd, Pt and Rh on graphite. These

authors observed decreasing activity in the order Pt > Rh > Pd that they ascribed to the intrinsic nature of the metal. The higher activity delivered by the 5% w/w loaded Pd/C relative to Pt/C (**Table 4.3**) agrees with results reported by Peters *et al.* [2, 3] on the reductive amination of benzaldehyde. Lower activity recorded for Pt/C has also been ascribed in the literature to susceptibility for poisoning by generated amine product [5-7].

The effect of metal loading can be assessed from the entries in **Table 4.3** relating to Pd/C (supplied by Sigma-Aldrich) bearing 5 and 1% w/w loadings with a factor of two higher specific rate recorded for the former. Given the equivalency of the pH_{pzc} for both catalysts this suggests increased amination efficiency over larger Pd particles (3.3 nm vs. 1.6 nm, see **Table 4.1**). Peters *et al.* [2] obtained higher specific activities for smaller metal particles (20 → 2 nm) in the reductive amination of benzaldehyde over 5% Pd/C catalysts. Higher initial rates with smaller metal particle sizes (2.2-4.5 nm) were also reported by Harada *et al.* [28] in the reductive amination of acetone with aniline over Pt/C. A decrease in catalytic activity over smaller metal particles (< 3 nm) has been observed in liquid-phase hydrogenation of 1,3-butadiene over Pd/C [95, 96] and ascribed to the electron deficiency of small Pd particles (electronic effect) that leads to stronger interaction with the reactant, leading to catalyst deactivation [97]. Moreover, Teschner *et al.* [98], studying the hydrogenation of 1-pentyne over Pd/C catalysts, have proposed carbon occlusion of the active metal sites and the formation of a Pd-C_x phase that limits the available surface reactive Pd. The significantly higher rate (**Table 4.3**) measured for 5% w/w Pd/C supplied by Sigma-Aldrich relative to the Degussa sample cannot be explained on the basis of Pd particle size, which is essentially equivalent for both samples. Differences in pH_{pzc} (**Table 4.1**) may be significant in this regard as the Sigma-Aldrich sample is measurably more basic (pH_{pzc} = 8.3) than the Degussa sample (pH_{pzc} = 6.8). Although the acid-base character of the support has been related to activity in reductive amination [7-9, 18], there has been no explicit correlation with respect to pH_{pzc}. In contrast to the response observed here, Heinen [18] and Peters *et al.* [2] used a carbon support treated with strong acids ($(NH_4)_2S_2O_8$ and HNO_3) that served to increase activity that was linked to a shift in the equilibrium for iminium ion generation from carbinolamine (see **Figure 4.3**). These authors characterised surface acidity on the basis of titration measurements using NaOH (1.4 meq/g) and infrared (IR) analysis (focusing on the 1700 cm^{-1} band, characteristic of carboxylic acid groups). Solution pH during reaction decreased from 10.6 to 8.4-8.3 but did not fall below the pH_{pzc} of the two catalysts. Consequently, a net negative surface

charge prevails during reaction, which favours interaction with the intermediate iminium cationic species (**Figure 4.3**). The lower pH_{pzc} for the Degussa sample should if anything provide better stabilisation of iminium intermediate but this is not borne out by the catalytic data. Other factors must then be considered where interactions at the liquid/solid interface are critical in terms of hydrophobic/hydrophilic effects. It is tentatively proposed that the higher pH_{pzc} for the Sigma-Aldrich catalyst reflects surface functionalisation that renders the interface more hydrophilic, facilitating reactant/catalyst interaction that serves to increase the amination rate.

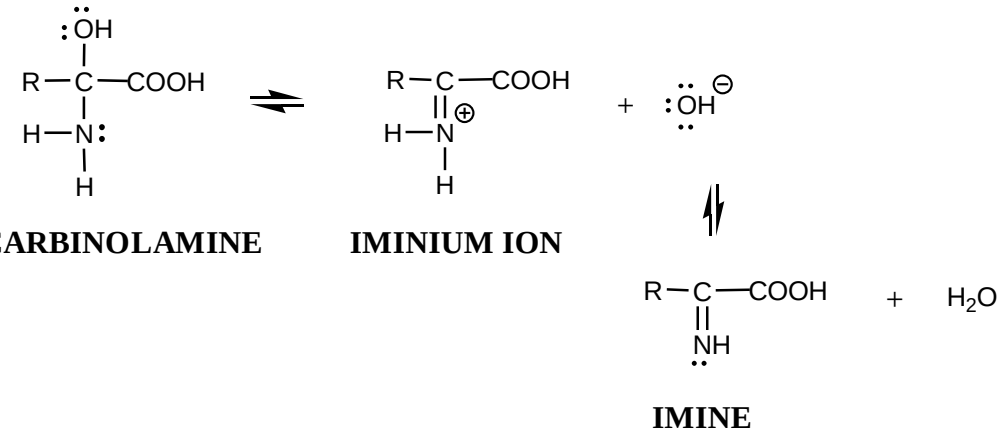

Figure 4.3: Formation of the imine from carbinolamine (see Figure 3.1).

Again, taking Pd as a common metal, it can be seen from the entries in **Table 4.1** that Pd/C delivered a specific rate that was a factor of 5 times greater than Pd/Al_2O_3 at a common 1% w/w loading. Support effects have been reported for reductive amination reactions [4, 7, 9, 18] and linked to differences in surface area, porosity and acid-base character. Our results agree with the study by Domine *et al*. [9] who achieved higher activities for commercial Pd and Pt supported on carbon relative to alumina supported systems in the reductive amination of cyclohexanone, 2-hexanone and 2-octanone with piperidine. The authors did not provide any explicit rationale to account for this effect but inferred a contribution due to the chemical (acid-base character) properties of the support. While H_2 chemisorption and pH_{pzc} values for Pd/Al_2O_3 and Pd/C are similar, the carbon support presents a much higher surface area (**Table 4.3**) that must serve to accommodate a greater number of reactant molecules that in turn facilitates a higher turnover rate. The data presented here points to contributions to reductive amination performance due to the nature of the supported metal, metal dispersion, support surface chemistry and area.

Table 4.3: Initial specific rate of TBG production (r'_o) and variation of pH (t = 0-50 min) for reaction over carbon and alumina supported Pd, Pt and Rh: initial pH = 10.6; TMP/catalyst = 600; stirring speed = 1100 rpm; NH_3/TMP = 2.5; T = 343 K.

Catalyst	$10^5\ r'_o$ (mol min^{-1} dm^{-3} m_{metal}^{-2})	Final pH	Selectivity to TBG (% molar)
Pd/C 5% w/w Degussa	1.5	8.4	100
Pd/C 5% w/w Sigma-Aldrich	3.2	8.3	100
Pt/C 5% w/w Sigma-Aldrich	1.4	8.5	100
Rh/C 5% w/w Sigma-Aldrich	3.6	8.2	100
Pd/C 1% w/w Sigma-Aldrich	1.5	9.2	100
Pd/Al_2O_3 1% w/w Sigma-Aldrich	0.3	9.1	100

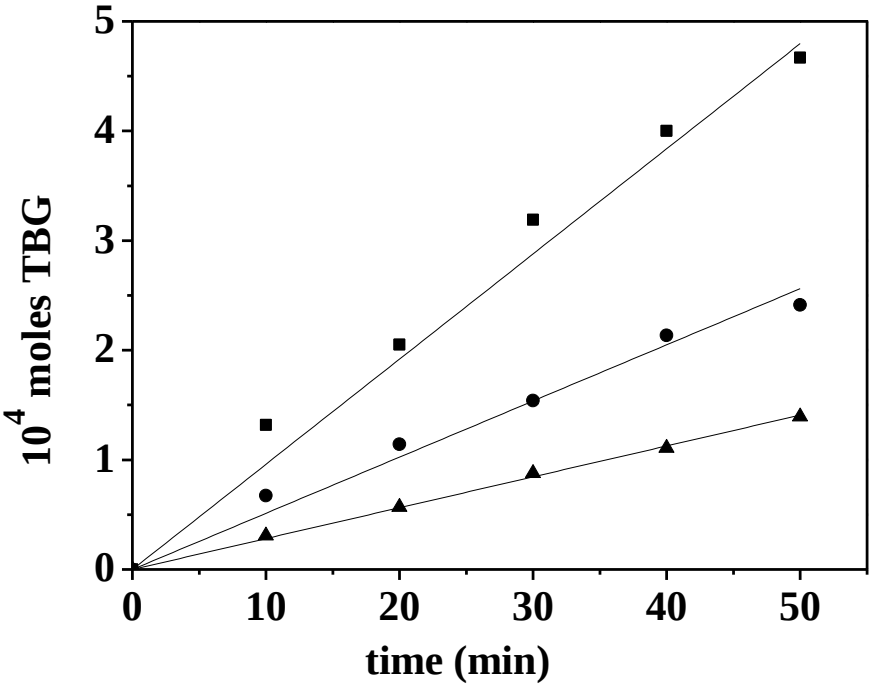

Figure 4.4: Temporal variation of moles TBG produced over (■) Rh/C 5% w/w (r'_o = 3.6×10^{-5} mol dm^{-3} min^{-1} m_{Rh}^{-2}), (●) Pd/C 5% w/w (Sigma-Aldrich, r'_o = 3.2×10^{-5} mol dm^{-3} min^{-1} m_{Pd}^{-2}) and (▲) Pd/C 5% w/w (Degussa, r'_o = 1.5×10^{-5} mol dm^{-3} min^{-1} m_{Pd}^{-2}); TMP/catalyst = 600; stirring speed = 1100 rpm; NH_3/TMP = 2.5; T = 343 K.

4.2.3 Effect of pH on initial rate

On the basis of the above catalytic results, Rh/C exhibited the best performance and was therefore chosen as the model catalyst in subsequent tests. Four sets of experiments with varying NH_3/TMP mol ratio were used to examine the effect of pH: (i) uncontrolled pH during the reaction; (ii) pH maintained under basic conditions by adding aqueous NaOH to reach pH = 11.2; (iii) pH under weakly basic conditions by adding CH_3COOH to reach pH = 8.4; (iv) pH = 4.7. The associated pH values at the start and end of each reaction presented in **Table 4.4** are indicative of the quantities of ammonia consumed. Rate dependence on NH_3/TMP is illustrated in **Figure 4.5**. The effect of pH on reductive amination rate has been explained in the literature according to the mechanism proposed in **Chapter 3** for neutral or basic solutions. According to this mechanism, Hine *et al*. [99] studied the reductive amination of isobutyraldehyde with diamines at various pH and demonstrated that the generation of the hydroxide ion with the formation of the iminium from carbinolamine (see **Figure 4.3**) is not favoured in strongly basic solution. An increase in solution acidity lowers the fraction of amination reactant in the unprotonated form. In more recent publications dealing with reductive amination of benzaldehyde and acetophenone with ammonia over carbon supported transition metals, iminium ion formation under acidic conditions has been proposed but the possible loss of aminating reactant in acidic conditions was not considered [3, 8, 18]. Under uncontrolled pH conditions, the rate increased with NH_3/TMP up to a limiting value (= 10), corresponding to an initial pH of 10.8 (point 4 in **Figure 4.5**). There is evidence in the literature that the optimum pH in heterogeneous catalysed reductive amination is close to the pK_a of the amine source [20, 100, 101]. This represents a compromise in terms of the iminium ion equilibrium step and possible ammonia inhibition. In our case the optimum pH (= 10.8) is higher than the pK_a of ammonia (9.2) and there is sufficient NH_3 for the nucleophilic attack to take place. Our results also demonstrate that reductive amination of TMP does not require excess NH_3, which represents a key factor in sustainable process design for liquid phase operation. Since solution pH during the reaction (= 10.8 – 9.0) was higher than pH_{pzc} of the catalyst (= 9.0), the carbon support surface was negatively charged and the interaction with the intermediate iminium cation species favoured.

Taking the reaction under controlled pH at 11.2, the rate was considerably higher than that achieved with uncontrolled pH at the same NH_3/TMP ratio. This can be explained, drawing on the observations in the previous chapter. In the proposed mechanism (**Figure 3.1**), NaOH serves only to modify solution pH and does not

influence the catalytic step or interact with the catalyst. At this pH, the unprotonated form of ammonia predominates in solution and nucleophilic addition to the carbonyl group occurs. It should be flagged that a higher rate is achieved by adding a small volume of strong base rather than using excessive quantities of aqueous ammonia, which is a significant sustainability consideration. There is no clear consensus in the literature regarding the effect of NaOH on reaction rate [7, 8, 21] but NaOH has been used to limit formation of secondary and tertiary amines [7]. Catalyst deactivation was observed under pH control by NaOH and can again be ascribed to poisoning of Pd by NH_3. The pH was also adjusted to 8.4 and 4.7 using acetic acid and the results are presented in **Figure 4.5**. In both cases, the initial rates were lower than in the uncontrolled experiments. This can be linked to solution pH lower than the pK_a of ammonia and consequently NH_4^+ is the predominant form in the solution, which impedes nucleophilic attack of TMP. This response is consistent with the observations of Scaros *et al*. [22] who demonstrated that the presence of acids (acetic, sulphuric or hydrochloric acid) resulted in incomplete reaction of carbonyl compounds but the authors did not provide any explanation for this. Rylander *et al*. [31] proposed that acid addition should increase rate by shifting the equilibrium in favour of iminium ion generation (see **Figure 4.3**), neutralising the inhibiting effect of the more basic amine product. This effect was not observed in this study where reaction at pH = 4.7 resulted in negligible TMP conversion. The lower availability of reactive ammonia due to the formation of ammonium acetate can account for rate inhibition. The literature on the effect of acid addition on reductive amination is inconclusive. The starting and final pH values recorded in **Table 4.4** are consistent with full reaction selectivity to TBG.

Table 4.4: Initial and final pH values during reaction at variable and fixed pH; the datum points are identified in Figure 4.5.

Datum Point	***Initial pH***	***Final pH***	***Datum Point***	***Initial pH***	***Final pH***	***Datum Point***	***Initial pH***	***Final pH***
1	*1.8*	*1.6*	*9*	*8.4*	*7.1*	*17*	*4.7*	*4.7*
2	*9.5*	*9.0*	*10*	*8.4*	*7.4*	*18*	*4.7*	*4.7*
3	*10.5*	*10.0*	*11*	*11.2*	*10.1*	*19*	*4.7*	*4.7*
4	*10.8*	*9.0*	*12*	*11.2*	*10.2*			
5	*11.2*	*10.4*	*13*	*11.2*	*10.4*			
6	*8.4*	*6.7*	*14*	*11.2*	*10.5*			
7	*8.4*	*6.8*	*15*	*4.7*	*4.5*			
8	*8.4*	*6.9*	*16*	*4.7*	*4.6*			

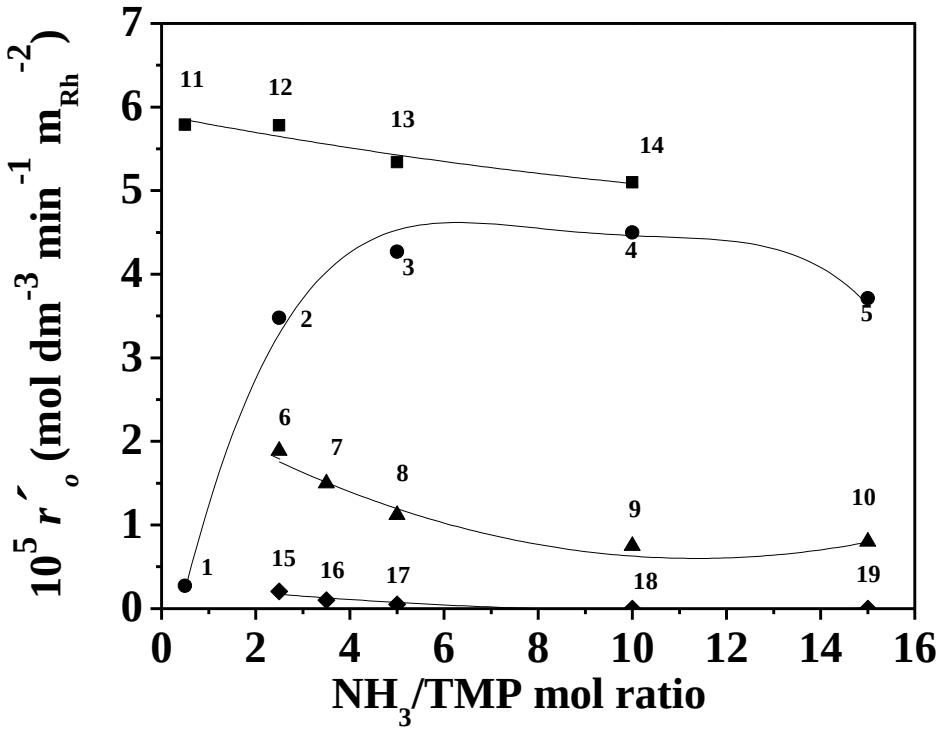

Figure 4.5: Initial rate of TBG production (r'_o) as a function of NH_3/TMP mol ratio where pH varies with time (●), pH is adjusted to 11.2 with NaOH (■), adjusted to 8.4 (▲) and adjusted to 4.7 with CH_3COOH (♦); TMP/Rh = 600; T = 343 K; stirring speed = 1100 rpm.

4.2.4 Effect of solvent on initial rate

Possible solvent effects were probed, again examining Rh/C as benchmark. Polar protic solvents, water and C_3-C_4 primary alcohols, were used to provide a range of dielectric constant values (ε = 20-80). The correlation of specific rate with dielectric constant is shown in **Figure 4.6**. Water, 1-propanol and 1-butanol (ε = 80.0, 20.1 and 17.8, respectively) [102] were chosen as their boiling points are higher than reaction temperature (343 K) [103] and they do not undergo unwanted side reactions (hydrogenation or amination) under these conditions. Use of longer-chain alcohols as solvents is limited due to the low solubility of TMP. The dielectric constant is a macroscopic property that measures the ability of a solvent to decrease the internal charge of a solute [104] and can serve as a quantitative measure of solvent polarity [105, 106]. A higher ε value indicates higher relative polarity and greater ability to stabilise charge. However, dielectric constant is a bulk property and does not take into account specific solvent/solute interactions that may occur at a molecular level, notably hydrogen bonding between the solvent molecule and TMP [107, 108]. Precise dielectric constant measurements can be found in the literature for mixed solvents that consider possible hydrogen-bonding interactions [109-111]. The dielectric constant of the mixed

solvent system (ε_m) was estimated according to an additive equation, assuming ideal mixing [112]:

$$\varepsilon_m = (\varepsilon_{water}\, x_{water}) + (\varepsilon_{organic}\,(1\text{-}x_{water})) \quad \textbf{(4.1)}$$

where x_{water} is the molar fraction of water in the mixture, ε_{water} and $\varepsilon_{organic}$ are the dielectric constants of water and the organic solvent, respectively. It can be seen from the entries in **Figure 4.6** that TMP reductive amination activity shows a dependence on the polarity of the reaction medium with a decrease in rate with increasing dielectric constant. The sequence of decreasing activity in polar protic solvents is: 1-butanol > 1-propanol > water. When the reaction was conducted in water+alcohol mixtures, the rate fell between the values observed in the individual solvents. It is known that binary mixtures of polar protic solvents exhibit different physico-chemical properties compared with single component systems [110, 113]. Use of alcohols as solvents increases TMP solubility and delivers higher TBG production rates. Water serves as a benign solvent [114] and is the preferred option in terms of green chemistry principles but delivers only a residual reaction rate. Use of water+alcohol mixtures represents a compromise in terms of sustainability while maintaining a significant level of reductive amination.

There is some evidence in the literature for variations in rate using different solvents in the reductive amination of aldehydes, ketones and carboxylic acids with higher conversions in less polar solvents [5, 27, 32]. The opposite effect has been reported by Klyuev *et al.* [115] who found that the rate of reductive amination of furfural with cyclohexylamine over Pd immobilised in a polymeric matrix was directly proportional to the dielectric constant but the authors did not provide any explanation for this response. Scaros *et al.* [22] observed an increase in rate with the water content in ethanolic-water mixtures for the reaction of benzaldehyde with ethanolamine over Pt/C. Omote *et al.* [116] did not find any explicit relationship between reaction rate and dielectric constant in Raney Ni promoted amination of cyclohexanone to cyclohexylamine and recorded the following sequence of decreasing rate: ethanol > water > methanol > isopropylalcohol. Peters *et al.* [7] established that, in the reductive amination of aldehydes and ketones, water has a positive effect on selectivity to the target amine that they attributed to solvation that lowers the reaction rate between imine and the amine to give a secondary amine. The negative effect of water on rate has been reported in studies using hydrides as reducing agents where imine formation is a

reversible reaction, requiring removal of water to shift the equilibrium to the right (see **Figure 4.3**) [1, 26, 117].

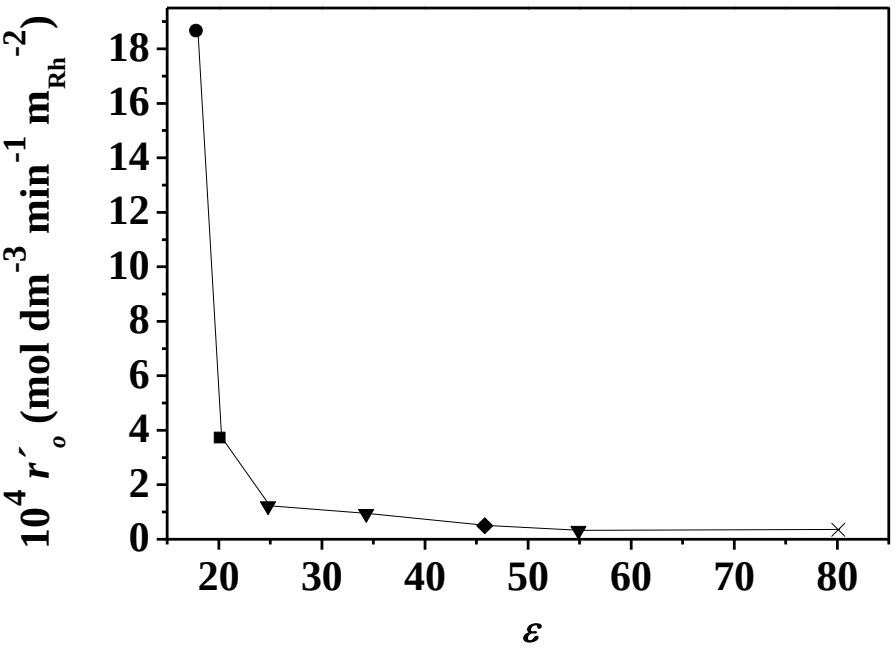

Figure 4.6: Initial rate of TBG production (r'_o) as a function of dielectric constant (ε) for reaction in 2-25% v/v water+1-propanol (▼), 14% v/v water+1-butanol (♦) mixtures and single component 1-propanol (■), 1-butanol (●) and water (×): NH_3/TMP = 2.5; TMP/Rh = 600; T = 343 K; stirring speed = 1100 rpm.

In liquid phase hydrogenation, solvents effects have been attributed to several factors: (i) reactant solubility [118]; (ii) solvent interaction with the reactants either in liquid phase or on the catalyst surface [119]; (iii) competitive adsorption of solvent and reactant on the catalyst surface [29, 120]; (iv) catalyst poisoning by the solvent [121]. Reactant solubility is a critical consideration in facilitating transport to (and from) the catalyst surface. Solvent interaction of TMP with the solvent can involve hydrogen bonding with the carboxyl and carbonyl groups and van der Waals interactions with the non-polar methyl groups. Solubility can be a contributing factor in this system, given that the order of decreasing TMP solubility (1-propanol > 1-butanol > water [122-124]) matches the order of decreasing reaction rate. A possible role in solvation of the nucleophile (ammonia) by more polar solvents may also serve to hinder reactivity with a resultant decrease in rate.

4.3 Conclusions

Carbon supported Pd, Pt and Rh and alumina supported Pd catalysts exhibited a range of activities in the reductive amination of TMP that can be linked to differences in

nature of the metal and support, where Rh/C delivered the highest specific rate. The latter can be attributed to higher intrinsic efficiency of Rh allied to surface basicity (reflected in the experimentally determined pH_{pzc}). All the catalysts exhibited 100% selectivity to TBG as the target product. As a general observation, the performance of activated carbon as Pd support exceeded that of alumina. This is the first report to show enhanced amination performance using Rh/C as catalyst (with molecular hydrogen and aqueous ammonia as reagents). The reaction was found to be pH-dependent where pH below the pK_a of ammonia delivered lower rates and the addition of base (NaOH) to increase the pH above the pK_a of ammonia enhanced rate to an upper limit with respect to NH_3/TMP. Effective reductive amination does not require excess ammonia, which is a critical sustainability consideration. Moreover, solvent selection also influenced the degree of amination that correlates with dielectric constant of the medium and increased in the order: water < 1-propanol < 1-butanol. This response can be attributed to the combined effects of TMP solubility and ammonia solvation.

4.4 References

[4.1] A. F. Abdel-Magid, K. G. Carson, B. D. Harris, C. A. Maryanoff, R. D. Shah; J. Org. Chem., 61, 3849-3862 (1996)

[4.2] S. Gomez, J. A. Peters, J. C. van der Waal, P. J. van der Brink, T. Maschmeyer; Appl. Catal. A: Gen., 261, 119-125 (2004)

[4.3] S. Gomez, J. A. Peters, J. C. van der Waal, T. Maschmeyer; Appl. Catal. A: Gen., 254, 77-84 (2003)

[4.4] J. Bodis, L. Lefferts, T. E. Muller, R. Pestman, J. A. Lercher; Catal. Lett., 104, 23-28 (2005)

[4.5] A. P. Bonds, H. Greenfield, Catalysis of Organic Reactions, Marcel Dekker, New York, pp. 65-78 (1992)

[4.6] H. Greenfield, Catalysis in Organic Reactions, Marcel Dekker, New York, pp. 265-277 (1994)

[4.7] S. Gomez, J. A. Peters, T. Maschmeyer; Adv. Synth. Catal., 344, 1037-1057 (2002)

[4.8] T. Ikenaga, K. Matsushita, J. Shinozawa, S. Yada, Y. Takagi; Tetrahedron, 61, 2105-2109 (2005)

[4.9] M. E. Domine, M. C. Hernandez-Soto, Y. Perez; Catal. Today, 159, 2-11 (2011)

[4.10] K. V. R. Chary, K. K. Seela, D. Naresh, P. Ramakanth; Catal. Commun., 9, 75-81 (2008)

[4.11] M. B. Dawidziuk, F. Carrasco-Marin, C. Moreno-Castilla; Carbon, 47, 2679-2687 (2009)

[4.12] B. K. Sharma, Industrial Chemistry, Catalysis, Goel Publishing House, Meerut, pp. 387-389 (1996)

[4.13] M. Franz, H. A. Arafat, N. G. Pinto; Carbon, 38, 1807-1819 (2000)

[4.14] M. V. Lopez-Ramon, F. Stoeckli, C. Moreno-Castilla, F. Carrasco-Marin; Carbon, 37, 1215-1221 (1999)

[4.15] M. A. Montes-Moran, J. A. Menendez, E. Fuente, D. Suarez; J. Phys. Chem. B, 102, 5595-5601 (1998)

[4.16] W. Shen, Z. Li, Y. Liu; Rec. Pat. Chem. Eng., 1, 27-40 (2008)

[4.17] S. Gomez, J. A. Peters, J. C. van der Waal, W. Z. Zhou, T. Maschmeyer; Catal. Lett., 84, 1-5 (2002)

[4.18] A. W. Heinen, J. A. Peters, H. van Bekkum; Eur. J. Org. Chem., 2000, 2501-2506 (2000)

[4.19] K. Laszlo, K. Josepovits, E. Tombacz; Anal. Sci., 17, 1741-1744 (2001)

[4.20] C. Huber, G. Wachtershauser; Tetrahedron Lett., 44, 1695-1697 (2003)

[4.21] G. B. Giovenzana, D. Imperio, A. Penoni, G. Palmisano; Beilstein J. Org. Chem., 7, 1095-1099 (2011)

[4.22] M. G. Scaros, M. L. Prunier, Catalysis of Organic Reactions, Marcel Dekker, New York, pp. 457-460 (1994)

[4.23] B. S. Akpa, C. D'Agostino, L. F. Gladden, K. Hindle, H. Manyar, J. McGregor, R. Li, M. Neurock; J. Catal., 289, 30-41 (2012)

[4.24] M. Lancaster, Green Chemistry An Introductory Text, Organic Solvents: Environmentally Benign Solutions, Royal Society of Chemistry, 2nd ed., Cambridge, pp. 139-141 (2010)

[4.25] D. B. Bagal, R. A. Watile, M. V. Khedkar, K. P. Dhake, B. M. Bhanage; Catal. Sci. Technol., 2, 354-358 (2012)

[4.26] S. Sato, T. Sakamoto, E. Miyazawa, Y. Kikugawa; Tetrahedron 60, 7899-7906 (2004)

[4.27] R. E. Malz, C.-Y. Lin, H. Greenfield, Catalysis of Organic Reactions, Marcel Dekker, New York, pp. 369-371 (1992)

[4.28] T. Harada, S. Ikeda, N. Okamoto, Y. H. Ng, S. Higashida, T. Torimoto, M. Matsumura; Chem. Lett., 37, 948-949 (2008)

[4.29] M. Khodadadi-Moghaddam, F. Sadeghzadeh-Darabi; J. Phys. Theor. Chem. IAU Iran, 8, 39-45 (2011)

[4.30] S. Mukherjee, M. A. Vannice; J. Catal., 243, 108-130 (2006)

[4.31] P. N. Rylander, Hydrogenation Methods, Academic Press, London, pp. 82-93 (1985)

[4.32] R. E. Malz, E. H. Jancis, M. P. Reynolds, S. T. O'Leary, Catalysis of Organic Reactions, Marcel Dekker, New York, pp. 263-271 (1994)

[4.33] M. A. Keane; J. Mater. Sci., 38, 4661-4675 (2003)

[4.34] S. K. Upadhyay, Chemical Kinetics and Reaction Dynamics, Kinetics of Catalyzed Reactions Springer, New Delhi, pp. 145-147 (2006)

[4.35] C. H. Bamford, C. F. H. Tipper, R. G. Compton, Kinetics and Chemical Technology, Catalytic and Non-catalytic Heterogeneous Reactions, Elsevier, Amsterdam, pp. 153-155 (1985)

[4.36] S. Özkar; Appl. Surf. Sci., 256, 1272-1277 (2009)

[4.37] M. J. Toebes, A. J. van Dillen, K. P. de Jong; J. Mol. Catal. A: Chem, 173, 75-98 (2001)

[4.38] R. Arriagada, R. Garcia, M. Molina-Sabio, F. Rodriguez-Reinoso; Micropor. Mat., 8, 123-130 (1997)

[4.39] Gonzalez, M. T., F. Rodriguez-Reinoso, A. N. Garcia, A. Marcilla; Carbon, 35, 159-165 (1997)

[4.40] J. R. Rangel-Mendez, F. S. Cannon; Carbon, 43, 467-479 (2005)

[4.41] G. V. Lowry, M. Reinhard; Environ. Sci. Technol., 33, 1905-1910 (1999)

[4.42] E. Seker, E. Gulari, H. Hammerle, C. Lambert, J. Leerat, S. Osuwan; Appl. Catal. A: Gen., 226, 183-192 (2002)

[4.43] A. Sayari, M. Jaroniec, Synthesis of Mesoporous Metal Oxides, Elsevier, Amsterdam, pp. 243-250 (2002)

[4.44] J. A. Moulijn, P. W. N. M. van Leeuwen, R. A. van Santen, Catalysis An Integrated Approach to Homogeneous, Heterogeneous and Industrial Catalysis, Temperature Programmed Reduction and Sulphiding, Elsevier, Amsterdam, pp. 401-404 (1993)

[4.45] J. Lynch, Physico-Chemical Analysis of Industrial Catalysts A Practical Guide to Characterization, Textural Characterization of Catalysts, Editions Technip, Paris, pp. 25-26 (2001)

[4.46] M. W. Tew, J. T. Miller, J. A. van Bokhoven; J. Phys. Chem. C, 113, 15140-15147 (2009)

[4.47] A. Cabiac, C. T., P. Trens, R. Durand; Appl. Catal. A: Gen., 340, 229-235 (2008)

[4.48] C.-B. Wang, H.-K. Lin, C.-M. Ho; J. Mol. Catal. A: Chem, 180, 285-291 (2002)

[4.49] E. W. Shin, S. Cho, J. H. Kang, W. J. Kim, J. D. Park, S. H. Moon; Korean J. Chem. Eng., 174, 468-472 (2000)

[4.50] M. Boudart, H. S. Hwang; J. Catal., 39, 44-52 (1975)

[4.51] P. W. Albers, K. Möbus, C. D. Frost, S. F. Parker; J. Phys. Chem. C, 115, 24485-24493 (2011)

[4.52] N. Krishnankutty, M. A. Vannice; J. Catal., 155, 312-326 (1995)

[4.53] D. Sebastian, E. G. Bordeje, L. Calvillo, M. J. Lazaro, R. Moliner; Int. J. Hydrogen Energy, 33, 1329-1334 (2008)

[4.54] M. C. Macias-Perez, C. Salinas-Martinez de Lecea, A. Linares-Solano; Appl. Catal. A: Gen., 151, 461-475 (1997)

[4.55] J. M. Garcia-Cortes, M. J. Illan-Gomez, A. Linares-Solano, C. Salinas-Martinez de Lecea; Appl. Catal. B: Environ., 25, 39-48 (2000)

[4.56] M. A. Fraga, E. Jordão, M. J. Mendes, M. M. A. Freitas, J. L. Faria, J. L. Figueiredo; J. Catal., 209, 355-364 (2002)

[4.57] A. Sepúlveda-Escribano, F. Coloma, F. Rodríguez-Reinoso; Appl. Catal. A: Gen., 173, 247-257 (1998)

[4.58] Q. He, S. Mukerjee, B. Shyam, D. Ramaker, S. Parres-Esclapez, M. J. Illan-Gomez, A. Bueno-Lopez; J. Power Sources, 193, 408-415 (2009)

[4.59] M. C. Aguirre, J. L. Fierro, P. Reyes; React. Kinet. Catal. Lett., 84, 351-358 (2005)

[4.60] T. A. Kainulainen, M. K. Niemelä, A. O. I. Krause; J. Mol. Catal. A: Chem, 140, 173-184 (1999)

[4.61] G. Pauer, A. Eichler, M. Sock, M. G. Ramsey, F. Netzer, A. Winkler; J. Chem. Phys., 119, 5253-5266 (2003)

[4.62] A. Cybulski, J. A. Moulijn, M. M. Sharma, R. A. Sheldon, Fine Chemicals Manufacture Technology and Engineering, Catalyst Characterization, Elsevier, Amsterdam, pp. 101-109 (2001)

[4.63] B. J. Kip, F. B. M. Duivenvoorden, D. C. Koningsberger, R. Prins; J. Catal., 105, 26-38 (1987)

[4.64] N. Krishnankutty, J. Li, M. A. Vannice; Appl. Catal. A: Gen., 173, 137-144 (1998)

[4.65] M. Bonarowska, B. Burda, W. Juszczyk, J. Pielaszek, Z. Kowalczyk, Z. Karpinski; Appl. Catal. B: Environ., 35, 13-20 (2001)

[4.66] M. Bonarowska, J. Pielaszek, V. A. Semikolenov, Z. Karpinski; J. Catal., 209, 528-538 (2002)

[4.67] A. Gampine, D. P. Eyman; J. Catal., 179, 315-325 (1998)

[4.68] G. M. Tonetto, D. E. Damiani; J. Mol. Catal. A: Chem., 202, 289-303 (2003)

[4.69] R. Wojcieszak, M. J. Genet, P. Eloy, P. Ruiz, M. Gaigneaux; J. Phys. Chem. C, 114, 16677-16684 (2010)

[4.70] P. Chou, M. A. Vannice; J. Catal., 104, 1-16 (1987)

[4.71] S. Shaikhutdinov, M. Heemeier, M. Bäumer, T. Lear, D. Lennon, R. J. Oldman, S. D. Jackson, H. J. Freund; J. Catal., 200, 330-339 (2001)

[4.72] B. Kasprzyk-Hordern; Adv. Colloid Interf. Sci., 110, 19-48 (2004)

[4.73] E. A. El-Katatny, S. A. Halawy, S. A. Mohamed, M. I. Zaki; Powder Technol., 132, 137-144 (2003)

[4.74] S. Kodama, H. Sekiguchi; Thin Solid Films, 506-507, 327-330 (2006)

[4.75] J. J. M. Orfao, A. I. M. Silva, J. C. V. Pereira, S. A. Barata, I. M. Fonseca, P. C. C. Faria, M. F. R. Pereira; J. Colloid Interf. Sci., 296, 480-489 (2006)

[4.76] L. R. Radovic, I. F. Silva, J. I. Ume, J. A. Menéndez, C. A. Leon y Leon, A. W. Scaroni; Carbon, 35, 1339-1348 (1997)

[4.77] A. Cabiac, G. Delahay, R. Durand, P. Trens, B. Coq, D. Plée; Chem. Sustain. Dev., 14, 553-558 (2006)

[4.78] I. I. Salame, T. J. Bandosz; J. Colloid Interf. Sci., 240, 252-258 (2001)

[4.79] C. Moreno-Castilla; Carbon, 42, 83-94 (2004)

[4.80] J. Vakros, C. Kordulis, A. Lycourghiotis; Chem. Commun., 17, 1980-1981 (2002)

[4.81] J. Barkauskas, M. Dervinyte; J. Serb. Chem. Soc., 69, 363-375 (2004)

[4.82] H. Nivinskas, S. Staškevičienė, J. Šarlauskas, R. L. Koder, A. F. Miller, N. Čėnas; Arch. Biochem. Biophys., 403, 249-258 (2002)

[4.83] F. Rodriguez-Reinoso; Carbon, 36, 159-175 (1998)

[4.84] D. Megias-Alguacil, E. Tervoort, C. Cattin, L. J. Gauckler; J. Colloid Interf. Sci., 353, 512-518 (2011)

[4.85] S. R. Tong, L. Y. Wu, M. F. Ge, W. G. Wang, Z. F. Pu; Atmos. Chem. Phys., 10, 7561-7574 (2010)

[4.86] J. Lehtonen, T. Salmi, A. Vuori, E. Tirronen; Org. Proc. Res. Dev., 2, 78-85 (1998)

[4.87] J. Li, R.-F. Li, G.-C. Wang; J. Phys. Chem. B, 110, 14300-14303 (2006)

[4.88] O. Johnson; J. Res. Inst. Catal. Hokkaido Univ., 21, 1-54 (1973)

[4.89] S. Srinivasan, Fuel Cells From Fundamentals to Applications, Electrocatalysis, Springer Science, New York, pp. 78-81 (2006)

[4.90] D. P. Woodruff, The Chemical Physics of Solid Surfaces, The Structure of Surface Alloy Phases on Metallic Substrates, Elsevier, Amsterdam, pp. 293-294 (2002)

[4.91] G. C. Bond; Plat. Met. Rev., 1, 87-93 (1957)

[4.92] V. I. Tararov, R. Kadyrov, T. Riermeier, A. Börner; Chem. Commun., 2000, 1867-1868 (2000)

[4.93] R. Kadyrov, T. H. Riermeier; Angew. Chem., 42, 5472-5474 (2003)

[4.94] R. P. Tripathi, S. S. Verma, J. Pandey, V. K. Tiwari; Curr. Org. Chem., 12, 1093-1115 (2008)

[4.95] J. Silvestre-Albero, G. Rupprechter, H. J. Freund; Chem. Commun., 80-82 (2006)

[4.96] J. Silvestre-Albero, G. Rupprechter, H. J. Freund; J. Catal., 235, 52-59 (2005)

[4.97] N. Semagina, A. Renken, D. Laub, L. Kiwi-Minsker; J. Catal., 246, 308-314 (2007)

[4.98] D. Teschner, E. Vass, M. Hävecker, S. Zafeiratos, P. Schnörch, H. Sauer, A. Knop-Gericke, R. Schlögl, M. Chamam, A. Wootsch, A. S. Canning, J. J. Gamman, S. D. Jackson, J. McGregor, L. F. Gladden; J. Catal., 242, 26-37 (2006)

[4.99] J. Hine, F. A. Via; J. Org. Chem., 42, 1972-1978 (1977)

[4.100] H. Xu, X. Hu; React. Funct. Polym., 42, 235-242 (1999)

[4.101] R. T. Lee, Y. C. Lee; Biochem., 19, 156-163 (1980)

[4.102] A. D'Aprano, D. I. Donato, E. Caponetti; J. Solut. Chem., 8, 135-146 (1978)

[4.103] G. Siedlaczek, M. Schwickardi, U. Kolb, B. Bogdanovic, D. G. Blackmond; Catal. Lett, 55, 67-72 (1998)

[4.104] F. A. Carey, R. J. Sundberg, Advanced Organic Chemistry, Study and Description of Organic Reaction Mechanisms, Kluwer Academic/Plenum Publishers, 4th ed., New York, pp. 237-239 (2000)

[4.105] E. Toukoniitty, P. Maki-Arvela, J. Kuusisto, V. Nieminen, J. Paivarinta, M. Hotokka, T. Salmi, D. Y. Murzin; J. Mol. Catal. A: Chem., 192, 135-151 (2003)

[4.106] U. K. Singh, M. A. Vannice; Appl. Catal. A: Gen, 213, 1-24 (2001)

[4.107] C. Reichardt, T. Welton, Solvents and Solvent Effects in Organic Chemistry, Classification of Solvents, Wiley-VCH, 3rd ed., New York, pp. 100-102 (2004)

[4.108] M. S. Zakerhamidi, A. Ghanadzadeh, M. Moghadam; Chem. Sci. Trans., 1, 1-8 (2012)

[4.109] R. J. Sengwa, V. Khatri, S. Sankhla; Indian J. Chem., 48A, 512-519 (2009)

[4.110] S. Sudo, N. Shinyashiki, Y. Kitsuki, S. Yagihara; J. Phys. Chem. A, 106, 458-464 (2002)

[4.111] H. Yilmaz; Turk. J. Phys., 26, 243-246 (2002)

[4.112] T. Sato, A. Chiba, R. Nozaki; J. Mol. Liq., 96-97, 327-339 (2002)

[4.113] A. Jouyban, S. Soltanpour, H. Chan; Int. J. Pharm., 269, 353-360 (2004)

[4.114] J. L. Young, D. E. Raynie, Challenges in Green Analytical Chemistry, Replacement of Hazardous Solvents and Reagents in Analytical Chemistry, Royal Society of Chemistry, Cambridge, pp. 51-55 (2011)

[4.115] V. A. Tarasevich, N. G. Kozlov; Russ. Chem. Rev., 68, 55-72 (1999)

[4.116] M. V. Klyuev, M. L. Khidekel; Transition Met. Chem., 5, 134-139 (1980)

[4.117] A. Heydari, S. Khaksar, M. Esfandyari, M. Tajbakhsh; Tetrahedron, 63, 3363-3366 (2007)

[4.118] C. K. Z. Andrade, L. M. Alves; Curr. Org. Chem., 9, 195-218 (2005)

[4.119] S. R. Reddy, Manikyamba; J. Chem. Sci., 119, 613-616 (2007)

[4.120] L. N. Protasova, E. V. Rebrov, K. L. Choy, S. Y. Pung, V. Engels, M. Cabaj, A. E. H. Wheatley, J. C. Schouten; Catal. Sci. Technol., 1, 768-777 (2011)

[4.121] U. K. Singh, S. W. Krska, Y. Sun; Org. Proc. Res. Dev., 10, 1153-1156 (2006)

[4.122] M. S. Wainwright, T. Ahn, D. L. Trimm; J. Chem. Eng. Data, 32, 22-24 (1987)

[4.123] Y. Shindler, Y. Matatov-Meytal, M. Sheintuch; Ind. Eng. Chem. Res., 40, 3301-3308 (2001)

[4.124] M. Safamirzaei, H. Modarress, M. Mohsen-Nia; Fluid Phase Equilib., 289, 32-39 (2010)

Chapter 5

Further Developments, Conclusion and Future Work

The results presented in Chapter 3 and 4 have demonstrated the feasibility of catalytic reductive amination, in terms of green chemistry principles. In this chapter, some further work that has been carried out is introduced with guidelines for future research direction to build on this work.

5.1 Further Developments

The catalytic reductive amination of TMP to generate TBG over commercially available Pd/C, Pt/C, Rh/C and Pd/Al_2O_3 catalysts at atmospheric pressure and 343 K has been demonstrated. The system with 5% w/w Pd/C catalyst (BET area = 850 $m^2 g^{-1}$, pore volume = 0.48 $cm^3 g^{-1}$, mean Pd particle size = 4.6 nm, pH_{pzc} = 6.8) was found to be free from mass transfer resistance over a range of inlet H_2 flow rates (20-150 $cm^3 min^{-1}$), stirring speeds (1100-1500 rpm), catalyst concentrations (TMP/Pd ratio = 600-1750) and temperatures (293-343 K). The rate did not show an appreciable dependence on H_2 pressure (1-20 bar) but was affected by NH_3/TMP ratio and solution pH (maximum rate at NH_3/TMP = 1.5, pH = 8.4). More importantly the system showed 100% selectivity to TBG with no evidence of direct TMP hydrogenation to HTBA at $T \geq 333$ K, $NH_3/TMP \geq 1.5$ and pH ≥ 8.4. The nature of the aminating agent has been probed and the rate was found to increase in the order: ammonium nitrate < ammonium acetate < ammonium hydroxide. The catalyst has also been reused for a second run but a *ca.* 50% decline in activity was recorded. Among the tested catalysts, 5% w/w Rh/C (BET area = 538 $m^2 g^{-1}$, mean Rh particle size = 1.9 nm and pH_{pzc} = 9.0) delivered the highest specific activity under the same reaction conditions. Solution pH values above the pK_a of ammonia (= 9.2) led to an enhancement of reaction rate to an upper limit with respect to NH_3/TMP (= 10). A lower dielectric constant of the solvent (ε = 17.8, 100% 1-butanol) has also been found to increase the initial rate of reaction.

5.1.1 Effect of Substrate Substitution

The effect of substituents on the reactant was studied in order to assess the potential of this reductive amination route as a viable synthesis pathway for a variety of

amino acids. Two α-keto-carboxylic acids, pyruvic (**Table 5.1**, **2a**) and phenylpyruvic acid (**Table 5.1**, **3a**) were tested and compared with TMP (**Table 5.1**, **1a**) where the pH values at the start/end of reaction are given. Alanine (**Table 5.1**, **2b**) and phenylalanine (**Table 5.1**, **3b**) were produced from the reductive amination of pyruvic and phenylpyruvic acid, respectively. The reactions were carried out at room temperature to minimise thermal decomposition of reactants. From the literature it is known that the decomposition/dimerisation of pyruvic acid in aqueous solution occurs at pH > 8 and increases with temperature at $T > 318$ K [1-3]. Based on the results shown in **Table 5.1**, the rate increased in the following sequence of substituents: methyl > benzyl > *t*-butyl. This trend can be related to substituent steric and electronic effects. The dual parameter Taft equation has been used to quantify polar and steric effects of R substituent groups in methyl esters ($RCOOCH_3$) for hydrolysis reactions [4-6]:

$$log\frac{k}{k_o} = \sigma^* \times \rho^* + \delta \times E_S \qquad \textbf{(5.1)}$$

where k/k_o is the rate ratio of a methyl ester having a given R substituent relative to $-CH_3$, ρ^* and δ are the sensitivity factors for the reaction to polar and steric effects, respectively, σ^* and E_s are the polar and steric hindrance substituent constants, respectively, associated with the R substituent (relative to $-CH_3$). Values for σ^* and E_s are shown in **Table 5.1** [7, 8] and they have also been used to evaluate reactivity and properties of other aliphatic compounds such as carboxylic acids [7, 9]. It can be noted that the measured reaction rates decreased with the steric effect of the substituent (lower E_s). This response is consistent with reports in the literature [10-17]. Malz and Greenfield [12] carried out the reductive amination of ketones with dibutylamine and H_2 over 5% Pd/C and found the following sequence of reaction rates: acetone > methylethyl ketone > methylisobutyl ketone. Birtill [13] observed the sequence, cyclohexanone > methylisopropyl ketone > 2-methylcyclohexanone, for the reaction of monoethanolamine with H_2 over 5% Pd/C. An electron-donating inductive effect of the carboxylic acid substituent should increase the electron density of the carbonyl carbon and consequently disfavour nucleophilic attack by the ammonia molecule [18]. The σ^* values of the substituents increase in the order: *t*-butyl < methyl < benzyl, but the rate did not show any correlation with σ^*. Therefore, the steric effect must have a stronger influence on rate than the polarity of substituents. To investigate further whether steric effect predominate over electronic effect, it is proposed here to use benzoylformic acid

(σ* = 0.60, E_s = -2.55) with a phenyl group substituent with the highest σ* value respect to pyruvic acid. If steric effects are primarily rate controlling, a more negative value of E_s should give a lower rate. On the contrary, if electronic effects are predominating, a higher value of σ* diminishes the electron density of the carbonyl carbon leading to a higher rate. A study of steric and electronic effects with additional substituents on the aromatic ring is seen as a valuable extension to this work. For example, reductive amination of 4-hydroxyphenylpyruvic acid with an OH group in the *para*- position should represent a suitable case study. Taft constants for 4-hydroxybenzyl group are not reported in literature. However, steric and electronic effects for benzyl and 4-hydroxybenzyl substituents have been quantified using different parameters and found to be equivalent so similar reaction rates are expected [19]. Differences in activities/selectivities using these substrates (under conditions of catalytic control), notably as a function of solution pH and temperature can follow the procedures adopted in this work. The protocol established using Rh/C is of wider potential application for different substituted α-keto-carboxylic acids to produce a variety of high-value amino acids, such as phenylglycine (from benzoylformic acid) and tyrosine from (4-hydroxyphenylpyruvic acid).

Table 5.1: Reductive amination of α-keto-carboxylic acids with aqueous ammonia over 5% carbon supported Rh: TMP/Rh = 600; stirring speed = 1100 rpm; NH_3/TMP = 2.5; *T* = 298 K; *t* = 50 min.

Entry	Substrate	Product	10^3 Initial Rate[a]	Initial pH	Final pH
1	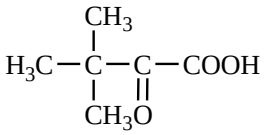 **1a** (σ^* = -0.30, E_s = -1.54)	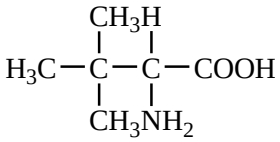 **1b**	1.8	9.5	9.8
2	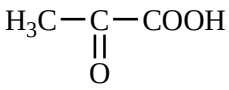 **2a** (σ^* = 0.0, E_s = 0.0)	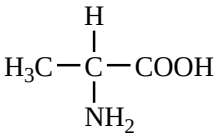 **2b**	39.7	9.5	9.6
3	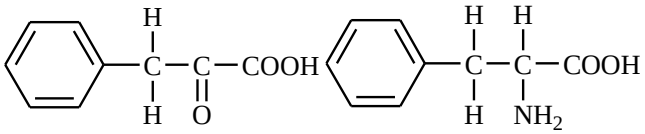 **3a** (σ^* = 0.22, E_s = -0.38)	**3b**	12.8	9.7	9.6

[a] units = mol min^{-1} dm^{-3} g_{Rh}^{-1}

5.2 Conclusions

In **Chapter 3**, the reductive amination of TMP catalysed by 5% w/w Pd/C is presented as a sustainable process where TMP was converted to TBG with 100% selectivity under temperature, NH_3/TMP ratio and solution pH control. Reaction conditions (H_2 flow rate, stirring speed, catalyst concentration and temperature) were determined wherein mass transport constraints were minimised. The rate did not show a dependence on H_2 flow rate but passed through a maximum as NH_3/TMP ratio was increased corresponding to a solution pH close to the pK_a of NH_3. This optimal reaction pH exceeded the pH_{pzc} of catalyst, facilitating the adsorption of the cationic intermediate and representing a compromise between low (formation of NH_4^+) and high (unfavoured iminium ion formation) pH values. The rate was also found to increase with the basic

character of the aminating agent. Catalyst characterisation pre- and post- reaction suggested deactivation due to occluded species in the pores and Pd sintering.

In **Chapter 4**, the performance of a set of catalysts including 5% w/w Pd/C from two sources, 5% w/w Pt/C, 5% w/w Rh/C, 1% w/w Pd/C and 1% w/w Pd/Al_2O_3 was compared. The Rh/C catalyst delivered the highest specific activity and differences in initial rates were attributed to the intrinsic nature of metal and support. The solution pH dependency was also examined using 5% w/w Rh/C as a model catalyst; NaOH addition served to increase the reaction rate by keeping pH constant and above both catalyst pH_{pzc} and the pK_a of NH_3. However, CH_3COOH addition led to lower rates due to the formation of NH_4^+ that limits NH_3 availability. The combined effect of lower TMP solubility and ammonia solvation explains the decreasing reaction rates at higher dielectric constant of solvent. Steric effects due to the α-keto-carboxylic substituent contributed to lower rates.

The studies presented here contribute to the understanding of this reaction over metals supported on carbon and alumina carriers. This reductive amination route allows the use of H_2 at atmospheric pressure, water/alcohol as solvents and minimum amounts of aqueous ammonia compared with less efficient heterogeneous catalytic systems reported in the literature (using higher pressures, gaseous ammonia and hydrides as reducing agents). The research findings can provide a platform for future studies directed at catalytic activity enhancement.

5.3 Future Work

The findings from this work and those in the existing literature still leave gaps in heterogeneous reductive amination studies that must be considered. The following studies are proposed for further investigation in order to close critical gaps in our understanding of the reductive amination of α-keto-carboxylic acids.

5.3.1 Catalyst Deactivation

A feasibility study of the reuse of 5% w/w Pd/C (Degussa) is presented in **Chapter 3**. Catalyst characterisation has revealed possible causes of deactivation: (i) Pd sintering; (ii) pore blockage due to reactants/products/coke deposition. TEM and XRD characterisation pre and post-reaction are necessary to fully probe Pd sintering and possible carbon structural changes. TEM analysis will show changes in Pd particle size

and morphology. XRD analysis pre- and post- reaction can also confirm Pd particle sizes, which should be complimented by H_2 chemisorption. Occluded reactants and products in the pores could be decomposed and reversibly removed by subjecting the samples to a high temperature reductive or oxidative treatment. Catalyst testing following this regeneration can then determine the efficacy of this treatment. Further experimental research on the exact source and mechanism of catalyst deactivation is necessary to improve the sustainability of this process by effective recycling the catalyst. Applying these tests to the range of catalysts screened in **Chapter 4** should reveal generic and specific features of catalyst deactivation, which can inform applicable regeneration strategies.

5.3.2 Effect of base addition

NaOH was added to the bulk solution (see **Chapter 4**) to maintain a constant basic pH (= 11.2) while varying the NH_3/TMP ratio. This test revealed a dependence of rate on pH where values above the pK_a of ammonia resulted in a more effective reductive amination over Rh/C. The possible effect of base addition on catalyst performance should be examined further by varying the nature of the alkali metal cation (*e.g.* KOH and LiOH) and using metal oxides (*e.g.* CaO)/carbonates (*e.g.* Na_2CO_3, $NaHCO_3$) [10, 15]. Results generated across the hydroxide series can be compared with those generated for NaOH addition to further probe the role of solution pH on process efficiency. An increase of rate in the order LiOH < NaOH < KOH is expected, in accordance with increasing basicity [20] to enhance NH_3 availability. This work should be coupled with an assessment of the effect of base on carbon support surface acid-base character [21, 22] and the supported metal site [23].

5.3.3 Effect of Catalyst Support

It has been established in **Chapter 4** that catalyst surface pH_{pzc} is a crucial parameter in determining deamination rate over supported Pd catalysts. An explicit link between metal support and TMP reaction performance has yet to be established. With respect to carbon supports, a higher (basic) pH_{pzc} has been found to deliver a higher rate, an effect that is tentatively ascribed to a more favourable reactant/catalyst interaction. Future work should examine the link between surface hydrophilicity and rate with a consideration of the mode of reactant adsorption. A systematic study is proposed of

support modification to alter pH_{pzc} and obtain a range of hydrophilicity. It is reported in the literature that thermal treatment of carbon based catalysts at high temperature (973-1273 K) under H_2 removes surface acidic groups and lowers hydrophilicity [24, 25]. Stronger acidic groups (carboxylic acids) decompose over the temperature range 373-900 K while weakly acidic functionalities (phenols) degrade at higher temperature ranges (873-1253 K) [26]. The carbon supported Pd catalysts used in this study can be subjected to a controlled TPR treatment (final temperature in the range 600-1000 K) to alter surface chemistry, which can be inferred from the pH_{pzc} measurement used in this study. Catalyst testing following the approach presented to ensure chemical control will provide a correlation of rate with acidity. Total acidity and acid strength distribution can be characterised by NH_3 chemisorption coupled with temperature programmed desorption (TPD). Other possible catalyst structural changes resulting from this thermal treatment should be analysed by BET surface area/porosity, H_2 chemisorption, XRD and TEM measurements. Variation in surface chemistry can impact on spillover hydrogen which, in turn, can influence reductive amination, a response that should be the subject of future research.

5.3.4 Effect of the Reductant

The feasibility of an alternative reductant to gaseous hydrogen used in this work should be considered as part of an overall approach to enhancing sustainability. Ammonium formate is proposed as a candidate for testing as it has been reported as an indirect non-toxic and environmentally safe source of hydrogen for reductive amination of ketones and a replacement for hydrides such as $NaBH_3CN$, $NaBH(OAc)_3$ and $NaBH_4$ [27, 28]. Carbon supported Pd has exhibited activity under moderate reaction conditions with ammonium formate as a hydrogen and nitrogen source [29-31]. Formic acid as a renewable biomass based chemical readily undergoes decomposition with hydrogen release. Application of ammonium formate and formic acid in TMP conversion is proposed where the results presented in this thesis can serve as a benchmark.

5.4 References

[5.1] O. Forsberg, B. Gelland, P. Ulmgren, O. Wahlberg; Acta Chem. Scan., 32, 345-352 (1978)

[5.2] J. Luedtke, A. McCoy; J. Phys. Chem. Lab., 10, 23-28 (2006)

[5.3] D. Jin, S. Liu, L. Xu, H. Ye; Afr. J. Biotechnol., 10, 14083-14089 (2011)

[5.4] A. Sangal, Advanced Organic Chemistry Vol. 1, Quantitative Treatment of the Effect of Structure on Reactivity, Krishna Prakashan Media, Meerut, pp. 237-238 (2010)

[5.5] D. Murzin, T. Salmi, Catalytic Kinetics, Relationship between Thermodynamics and Kinetics, Elsevier, Amsterdam, pp. 90-91 (2005)

[5.6] C. Hansch, A. Leo, R. W. Taft; Chem. Rev., 91, 165-195 (1991)

[5.7] J. Zhang, T. Kleinöder, J. Gasteiger; J. Chem. Inf. Model., 46, 2256-2266 (2006)

[5.8] R. A. Larson, E. J. Weber, Reaction Mechanisms in Environmental Organic Chemistry, Organic Chemicals in the Environment, Lewis, Florida, pp. 22-23 (1994)

[5.9] Y. Liu, E. Lotero, J. G. Goodwin Jr.; J. Catal., 243, 221-228 (2006)

[5.10] S. Gomez, J. A. Peters, T. Maschmeyer; Adv. Synth. Catal., 344, 1037-1057 (2002)

[5.11] P. N. Rylander, Hydrogenation Methods, Academic Press, London, pp. 82-93 (1985)

[5.12] R. E. Malz, H. Greenfield, Heterogeneous Catalysis and Fine Chemicals II, Elsevier, Amsterdam, pp. 351-358 (1991)

[5.13] J. J. Birtill, Catalysis of Organic Reactions, Marcel Dekker, New York, pp. 249-262 (1995)

[5.14] J. J. Birtill, M. Chamberlain, J. Hall, R. Wilson, I. Costello, Catalysis of Organic Reactions, Marcel Dekker, New York, pp. 255-272 (1998)

[5.15] G. B. Giovenzana, D. Imperio, A. Penoni, G. Palmisano; Beilstein J. Org. Chem., 7, 1095-1099 (2011)

[5.16] M. V. Klyuev, M. L. Khidekel; Transition Met. Chem., 5, 134-139 (1980)

[5.17] B. Chen, U. Dingerdissen, J. G. E. Krauter, H. G. J. Lansink Rotgerink, K. Möbus, D. J. Ostgard, P. Panster, T. H. Riermeier, S. Seebald, T. Tacke, H. Trauthwein; App. Catal. A: Gen., 280, 17-46 (2005)

[5.18] O. P. Agrawal, Organic Chemistry Reactions and Reagents, Addition Reactions (Unsaturation and Conjugation), Krishna Prakashan Media, Meerut, pp. 426-430 (2009)

[5.19] T. Fujita, Qsar and Drug Design: New Developments and Applications, Hydrophobicities of Di- to Pentapeptides having Unionizable Side Chains and

Correlation with Substituent and Structural Parameters, Elsevier Science, Amsterdam, pp. 186-188 (1995)

[5.20] D. N. Singh, Basic Concepts of Inorganic Chemistry, Acids and Bases, Dorling Kindersley, New Delhi, pp. 114-116 (2010)

[5.21] V. Felis, C. De Bellefon, P. Fouilloux, D. Schweich; App. Catal. B: Environ., 20, 91-100 (1999)

[5.22] S. Gomez, J. A. Peters, J. C. van der Waal, T. Maschmeyer; Appl. Catal. A: Gen., 254, 77-84 (2003)

[5.23] L. Cerveny, Catalytic Hydrogenation, Promoting Effects, Elsevier Science, Amsterdam, pp. 447-457 (1986)

[5.24] M. S. Shafeeyan, W. M. A. W. Daud, A. Houshmand, A. Shamiri; J. Anal. Appl. Pyrol., 89, 143-151 (2010)

[5.25] A. Dandekar, R. T. K. Baker, M. A. Vannice; Carbon, 36, 1821-1831 (1998)

[5.26] J. L. Figueiredo, M. F. R. Pereira, M. M. A. Freitas, J. J. M. Orfao; Carbon, 37, 1379-1389 (1999)

[5.27] E. Byun, B. Hong, K. A. De Castro, M. Lim, H. Rhee; J. Org. Chem., 72, 9815-9817 (2007)

[5.28] R. Kadyrov, T. H. Riermeier; Angew. Chem., 42, 5472-5474 (2003)

[5.29] M. Allegretti, V. Berdini, M. Cesta, R. Curti, L. Nicolini, A. Topai; Tetrahedron Lett., 42, 4257-4259 (2001)

[5.30] P. Falus, Z. Boros, G. Hornyanszky, J. Nagy, F. Darvas, L. Urge, L. Poppe; Tetrahedron Lett., 52, 1310-1312 (2011)

[5.31] V. Berdini, M. Cesta, R. Curti; Tetrahedron, 58, 5669-5674 (2002)